Peak to Average Power Ratio Reduction and Error Control in MIMO-OFDM HARQ System

by

Francisco Alberto SANDOVAL NOREÑA

MANUSCRIPT-BASED THESIS PRESENTED TO ÉCOLE DE TECHNOLOGIE SUPÉRIEURE IN PARTIAL FULFILLMENT FOR THE DEGREE OF DOCTOR OF PHILOSOPHY
Ph.D.

MONTREAL, JULY 03, 2019

ÉCOLE DE TECHNOLOGIE SUPÉRIEURE
UNIVERSITÉ DU QUÉBEC

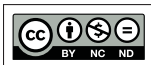

BOARD OF EXAMINERS

THIS THESIS HAS BEEN EVALUATED

BY THE FOLLOWING BOARD OF EXAMINERS

Pr. François Gagnon, Thesis Supervisor
Department of Electrical Engineering, École de technologie supérieure

Dr. Gwenael Poitau, Co-supervisor
Chief Technology Officer, Ultra Electronics

Pr. Ismail Ben Ayed, President of the Board of Examiners
Artificial Intelligence in Medical Imaging, École de technologie supérieure

Pr. Georges Kaddoum, Member of the jury
Department of Electrical Engineering, École de technologie supérieure

Pr. Tayeb A. Denidni, External Examiner
Énergie Matériaux Télécommunications Research Centre, Institut national de la recherche scientifique

THIS THESIS WAS PRESENTED AND DEFENDED

IN THE PRESENCE OF A BOARD OF EXAMINERS AND THE PUBLIC

ON "DEFENSE DATE"

AT ÉCOLE DE TECHNOLOGIE SUPÉRIEURE

ACKNOWLEDGEMENTS

A would like to express my sincere gratitude to my advisor Prof. Francois Gagnon for the continuous support and help of my Ph.D. study and related research. From the beginning he has trusted me. Thanks for your guidance and especially for your friendship. I also want to thank my co-asvisor Dr. Gwenael Poitau, and through him Ultra Electronic, for the opportunity provided to work together, and I acknowledge Eric Kwati who helped me improve my English writing.

I am grateful to the Natural Sciences and Engineering Research Council of Canada, and the Ultra Electronics TCS through the Industrial Research Chair in High Performance Wireless Emergency and Tactical Communications for funding, in part, this work.

I want to thank my committee members, Professor Ismail Ben Ayed (President of the Board of Examiners), Professor Georges Kaddoum (Member of the jury), Professor Tayeb A. Denidni. (External Examiner) for serving as my committee members and I also want to thank you for your interesting comments and suggestions, thanks to you.

I thank the UTPL for the support provided, especially the colleagues of the Electronics and Telecommunications Section, and the Department of Computer Science and Electronics.

Un profundo agradecimiento para Glenda, mi esposa, quien desde un principio ha apoyado mis sueños a pesar de los sacrificios que traen consigo, quien ha sufrido, se ha alegrado y me ha acompañado de muchas maneras durante este camino, con mucho amor y dedicación. Gracias de todo corazón.

Gratitud inmensa para mis padres Lubín y Fabiola, mis hermanos José y María Fabiola, y toda mi familia ya que siempre han creído en mí y me han brindado sus oraciones, su apoyo, su ánimo y alegría para superar los obstáculos y lograr las metas propuestas.

Agradezco también a todas las amigas y los amigos que de una u otra manera han apoyado este caminar y me han animado a seguir adelante.

I also place on record, my sense of gratitude to one and all, who directly or indirectly, have helped and supported me during my work in the ÉTS and my life in Canada, especially the friends with whom we have shared this process: Byron and family, Tuesman, Katty, Alex, Gabriel and family, Ruth, and Verónica.

Réduction du rapport de puissance crête à moyenne et contrôle des erreurs dans le système HARQ MIMO-OFDM

Francisco Alberto SANDOVAL NOREÑA

RÉSUMÉ

Actuellement, les systèmes MIMO-OFDM constituent la base d'importants systèmes de communication sans fil tels que les réseaux commerciaux 4G et 5G, les communications tactiques et les communications interopérables pour la sécurité publique. Cependant, un inconvénient de la modulation OFDM est le haut rapport puissance crête à puissance moyenne (PAPR). Ce problème augmente lorsque le nombre d'antennes d'émission augmente.

Ce travail consiste à proposer une nouvelle technique de réduction de PAPR hybride pour les systèmes MIMO-OFDM de codage de bloc espace-temps (STBC). Cette technique combine les capacités de codage aux méthodes de réduction des PAPR tout en exploitant le nouveau degré de liberté offert par la présence de plusieurs chaînes de transmission (MIMO).

Dans la première partie, nous présentons une revue de littérature approfondie des techniques de réduction de PAPR pour les systèmes OFDM et MIMO-OFDM. Ces travaux ont permis de mettre au point une taxonomie de technique de réduction de PAPR, d'analyser les motivations de réduction de PAPR dans les systèmes de communication actuels tenant compte du gain de couverture, de comparer par simulation les caractéristiques de chaque catégorie et conclure par l'importance des techniques de réduction de PAPR hybride.

Dans la deuxième partie, nous étudions l'effet des codes de correction d'erreurs en aval (FEC), tels que les codes de bloc linéaires et les codes de convolution sur le PAPR du système OFDM codé (COFDM). Nous avons simulé et comparé la fonction de distribution cumulative complémentaire (FDCC) du PAPR et sa relation avec l'autocorrélation du signal COFDM avant de transiter par le bloc de transformée de Fourier rapide inverse (IFFT). Cela permet de conclure sur les caractéristiques principales des codes qui génèrent des pics élevés dans le signal COFDM, et donc sur les paramètres optimaux afin de réduire le PAPR.

Enfin, nous proposons une nouvelle technique de réduction de PAPR hybride pour le système STBC MIMO-OFDM, dans laquelle le code de convolution est optimisé pour éviter la dégradation de PAPR, et combine les schémas successifs de rotation, d'inversion (SS-CARI), de composition modifiée itérative et de filtrage sous-optimal. La nouvelle méthode permet d'obtenir un gain net considérable pour le système, c'est-à-dire une réduction considérable du PAPR, un gain de taux d'erreur sur les bits (BER) par rapport au système MIMO-OFDM de base, une faible complexité et une empreinte spectrale réduite. La nouvelle technique hybride a été largement évaluée par simulation et la fonction de distribution cumulative complémentaire (CCDF), le BER et la densité spectrale de puissance (PSD) ont été comparés au signal STBC MIMO-OFDM d'origine.

Mots-clés: Compression, codes convolutifs, amplificateur de puissance élevée, entrées multiples sorties multiples (MIMO), multiplexage par répartition orthogonale de la fréquence (OFDM), rapport de puissance pic à moyenne (PAPR), codage de bloc espace-temps (STBC), communication tactique

Peak to Average Power Ratio Reduction and Error Control in MIMO-OFDM HARQ System

Francisco Alberto SANDOVAL NOREÑA

ABSTRACT

Currently, multiple-input multiple-output orthogonal frequency division multiplexing (MIMO-OFDM) systems underlie crucial wireless communication systems such as commercial 4G and 5G networks, tactical communication, and interoperable Public Safety communications. However, one drawback arising from OFDM modulation is its resulting high peak-to-average power ratio (PAPR). This problem increases with an increase in the number of transmit antennas.

In this work, a new hybrid PAPR reduction technique is proposed for space-time block coding (STBC) MIMO-OFDM systems that combine the coding capabilities to PAPR reduction methods, while leveraging the new degree of freedom provided by the presence of multiple transmit chairs (MIMO).

In the first part, we presented an extensive literature review of PAPR reduction techniques for OFDM and MIMO-OFDM systems. The work developed a PAPR reduction technique taxonomy, and analyzed the motivations for reducing the PAPR in current communication systems, emphasizing two important motivations such as power savings and coverage gain. In the tax onomy presented here, we include a new category, namely, hybrid techniques. Additionally, we drew a conclusion regarding the importance of hybrid PAPR reduction techniques.

In the second part, we studied the effect of forward error correction (FEC) codes on the PAPR for the coded OFDM (COFDM) system. We simulated and compared the CCDF of the PAPR and its relationship with the autocorrelation of the COFDM signal before the inverse fast Fourier transform (IFFT) block. This allows to conclude on the main characteristics of the codes that generate high peaks in the COFDM signal, and therefore, the optimal parameters in order to reduce PAPR. We emphasize our study in FEC codes as linear block codes, and convolutional codes.

Finally, we proposed a new hybrid PAPR reduction technique for an STBC MIMO-OFDM system, in which the convolutional code is optimized to avoid PAPR degradation, which also combines successive suboptimal cross-antenna rotation and inversion (SS-CARI) and iterative modified companding and filtering schemes. The new method permits to obtain a significant net gain for the system, i.e., considerable PAPR reduction, bit error rate (BER) gain as compared to the basic MIMO-OFDM system, low complexity, and reduced spectral splatter. The new hybrid technique was extensively evaluated by simulation, and the complementary cumulative distribution function (CCDF), the BER, and the power spectral density (PSD) were compared to the original STBC MIMO-OFDM signal.

Keywords: Compression, convolutional codes, high power amplifier, multiple-input multiple-output (MIMO), orthogonal frequency division multiplexing (OFDM), peak-to-average power ratio (PAPR), space-time block coding (STBC), tactical communication

TABLE OF CONTENTS

LIST OF TABLES

LIST OF FIGURES

LIST OF ABREVIATIONS

ACE	Active constellation extension
AWGN	Additive white Gaussian noise
BER	Bit error rate
BLAST	Bell Laboratories layered space-time
BS	Base station
CARI	Cross-antenna rotation and inversion
CBC	Complement block coding
CDF	Cumulative distribution function
CCDF	Complementary cumulative distribution function
C+MSP	Coding plus Multiple Signaling and Probabilistic techniques
C+MSP+SD	Coding plus Multiple Signaling and Probabilistic techniques plus Signal Distortion techniques
CP	Cyclic prefix
COFDM	Coded orthogonal frequency division multiplexing
C+SD	Coding plus Signal Distortion techniques
DAB	Digital Audio Broadcasting
DAC	Digital to analog converter
D-BLAST	Diagonal Bell Laboratories layered space-time
dSLM	Directed selected mapping
DSI	Dummy sequence insertion

DVB-S	Digital Video Broadcasting-Satellite
DVB-T	Digital Video Broadcasting-Terrestrial
eNB	Node-B
ECC	Error-correcting codes
EC-SLM	Error control selected mapping
EC-SLM-CP	Error control selected mapping with clipping
FEC	Forward error correction
HARQ	Hybrid automatic repeat request
H-BLAST	Horizontal Bell Laboratories layered space-time
HPA	High power amplifier
IBO	Input back-off
IFFT	Inverse fast Fourier transform
iSLM	Individual selected mapping
ITU	International Telecommunication Union
JTRS	Joint Tactical Radio System
LDPC	Low-density parity-check codes
LST	Less significant bit
LTE	Long-Term Evolution
MCR	Modified code repetition
MCR-SLM-CP	Modified code repetition, selected mapping and clipping

MGSTC	Multi-group space time coding
MIMO	Multiple-input multiple-output
MME/GT	Mobility management entity/gateway
MSP	Multiple signaling and probabilistic
MSP+SD	Multiple signaling and probabilistic plus Signal Distortion techniques
MuCT	Modified μ-law compander transform
MU-MIMO	Multiple-user multiple input multiple output
NCT	Nonlinear companding transform
NOSTBC	Non-orthogonal space-time block codes
OFDM	Orthogonal frequency division multiplexing
OFDMA	Orthogonal frequency division multiplexing access
oSLM	Ordinary selected mapping
OSTBC	Orthogonal space-time block codes
PA	Power amplifier
PAPR	Peak-to-average power ratio
PMEPR	Peak-to-mean envelope power ratio
PSD	Power spectral density
PR	Peak ratio
PRT	Peak reduction tones
P/S	Parallel-to-serial

PTS	Partial transmit sequence
PTS-ECC	Partial transmit sequence Using Error-Correcting Code
QPSK	Quadrature phase-shift keying
QAM	Quadrature amplitude modulation
QoS	Quality of service
RA	Repeat accumulate codes
RC	Repetition codes
RM	Reed-Muller
SBCC	Sub-block complementary coding
SC-FDMA	Single Carrier Frequency Division Multiple Access
SD	Signal distortion
SISO	Single-input single-output
SLM	Selected mapping
S/P	Serial-to-parallel
SRW	Soldier radio waveform
SS-CARI	Successive suboptimal cross-antenna rotation and inversion
SSPA	Solid state power amplifier
SOPC	Simple odd parity code
STBC	Space-time block codes
STC	Space-time coding

STTC	Space-time trellis codes
SU-MIMO	single-user multiple input multiple output
TI	Tone injection
TR	Tone reservation
TSTC	Threaded space-time coding
uCT	μ-law compander transform
UE	User equipment
UNW	Universal Networking Waveform
V-BLAST	Vertical Bell Laboratories layered space-time
WEA	Wavelet entropy algorithm
WNW	Wideband Network Waveform
WiMAX	Worldwide Interoperability for Microwave Access
4G	4th generation
5G	5th generation

LISTE OF SYMBOLS AND UNITS OF MEASUREMENTS

c	Speed of light
$\mathbf{c}_i$	Code word vector
$E[\cdot]$	Expected value
E_s	Symbol energy
E_{s_c}	Symbol energy of the companded signal
f	Frequency
$\mathbf{G}$	Generation matrix
G_R	Receiver antenna gain
G_T	Transmitter antenna gain
$\mathbf{h}_{ij}$	Channel from the ith transmit antenna to the jth receive antenna
$H_{ij}[k]$	Channel frequency response of the (i, j)th channel
$\mathbf{I}_k$	$k \times k$ Identity matrix
j	Imaginary unit
K	Number of subcarriers (OFDM) (Chapter 2)
K	Number of states (Chapter 3)
K	Normalization constant (Chapter 4)
L	Maximum length of channel
N	Number of subcarriers (OFDM)
N_{cp}	Length of the cyclic prefix

N_R	Number of receive antennas
N_t	Number of transmit antennas
$\mathbf{P}$	Parity matrix
P_R	Received power
P_T	Radiated power
$\mathrm{PAPR}(\cdot)$	peak-to-average power ratio
PL_{FS}	Path loss in free space
PR	Peak ratio
$\Pr(\cdot)$	Probability distribution function
R	Code rate
$\mathbf{R}(k)$	State correlation matrix
t_s	sampling period
U	Number of phase sequences (SLM)
V	Number of subsequences (PTS) (Chapter 2)
V	Peak amplitude of compressor (Chapter 4)
$x_i(n)$	Discrete-time baseband OFDM signal from the *i*th transmit antenna
$x(n)$	Discrete-time baseband OFDM signal
$x(t)$	continuous-time baseband OFDM signal
$X(k)$	Data symbol (OFDM)
$\mathbf{X}$	Data block (OFDM)

$\{X_i[k]\}_{k=0}^{N-1}$	Frequency-domain signal from the ith transmit antenna
x_{peak}	Peak of the actual signal
$Y_j[k]$	Received frequency-domain signal at the jth receive antenna
ΔA	Gain in coverage area
ΔR	Incremental range extension
η	Power amplifier efficiency
π	Number pi
λ	Wavelength
α	Path loss exponent
$\mathbf{\Pi}$	Transition probability matrix
dB	DeciBels
max	maximum

INTRODUCTION

Increased range and coverage are essential to improve tactical communication networks because the network density in it is lower than in commercial communications and thus increased range is key to maximize the coverage.

Multiple tactical waveforms, such as the Universal Networking Waveform (UNW) and the Wideband Network Waveform (WNW), are based on orthogonal frequency division multiplexing (OFDM) for inherent mobility robustness. OFDM is present in all 4G wireless communication systems, including the IEEE 802.16 Worldwide Interoperability for Microwave Access (WiMAX) and Long Term Evolution (LTE) standards. Furthermore, OFDM is a popular modulation for other communication systems; for example, it is included in IEEE 802.11 a/g/n/ac wireless LANs, Digital Audio Broadcasting (DAB), Digital Video Broadcasting-Terrestrial (DVB-T), and Digital Video Broadcasting by Satellite (DVB-S). Additionally, OFDM is part of the 5G waveforms proposal.

Multi-carrier modulation OFDM has multiples advantages, such as high spectral efficiency, high data rate transmission over a multipath fading channel, simple implementation by the Fast Fourier transformation (FFT), and low receiver complexity (Yang, 2005). However, a critical drawback of OFDM is the high peak-to-average power ratio (PAPR) it produces, which can impact the performance of the non-linear elements in the system, such as the high power amplifier (HPA) and the digital-to-analog converter (DAC). Besides, the high picks in the multi-carrier signal can indirectly influence the system's range and coverage or power consumption (Sandoval *et al.*, 2017).

The problem of PAPR in OFDM modulation has been widely analyzed in the literature, as presented in Chapters 1 and 2, where PAPR reduction techniques are organized into four categories, namely, Coding, Multiple Signaling and Probabilistic (MSP), Signal Distortion (SD), and Hybrid. In Coding schemes, codewords that minimize the PAPR are selected, while mul-

tiple permutation of the multi-carrier signal is generated in Multiple Signal techniques, and the signal with the minimum PAPR is chosen for transmission. For their part, the probabilistic methods modify different parameters in the multi-carrier signal and optimize them to minimize the PAPR. Finally, the hybrid schemes combine two or more techniques for PAPR reduction in a bid to take advantage of different techniques that can result in greater PAPR reduction, better performance, and stronger control of parameters such as computational complexity, additional transmission power requirements, and data rate drops.

Combining OFDM with multiple-input multiple-output (MIMO) wireless communication systems results in MIMO-OFDM, one of the most used techniques in current systems, and the most promising. On the other hand, MIMO-OFDM presents the problem of a high PAPR, results in a higher PAPR than OFDM alone since the PAPR increases as the number of transmit antennas increases as well.

Research Objectives

The main contribution of this thesis is to combine coding capabilities with PAPR reduction methods while leveraging the new degree of freedom provided by the presence of multiple transmit chains (MIMO). The research objectives include:

1. Analyze the main performance improvements for PAPR reduction in current communications systems with an emphasis on tactical communications systems.
2. Explore OFDM PAPR reduction techniques proposed in the literature, their classification, their characteristics and their possibilities of being combined with hybrid techniques.
3. Study, model, and compare the PAPR reduction capabilities of forward error correction codes.
4. Examine the proposed PAPR reduction techniques for MIMO-OFDM systems and check which of the systems have better characteristics that can be combined with coding techniques.

5. Propose a novel hybrid peak-to-average power ratio reduction scheme that combines a code-based technique with signal distortion or multiple signaling and a probabilistic method in a tactical MIMO-OFDM system to reduce the PAPR and to achieve BER reduction without increasing the saturation point of a power amplifier.

Methodology

This research begins with an extensive review of the literature on OFDM systems and PAPR reduction techniques. The work develops a systematic approach for PAPR reduction under different propagation, topology or traffic conditions, and presents a detailed analysis of the motivations for reducing the PAPR in current communication systems, emphasizing the resulting coverage gain. The thesis summarizes the recent literature on hybrid PAPR reduction techniques, compares the important parameters it incorporates, and concludes on its usability in current commercial, public safety, and tactical communications systems.

An OFDM communication system with different PAPR reduction techniques, including multiple signals and probabilistic (MSP) and signal distortion (SD) methods, was simulated over an additive white Gaussian noise (AWGN) channel. The results compared the net gain performance based on the complementary cumulative distribution function (CCDF) and the bit error rate (BER). Additionally, other parameters were taken into account for the final analysis as the need for side information, the technique computational complexity, the in-band or out-of-band radiation, or increased power requirements at the transmitter.

The effects of forward error correction (FEC) on the PAPR for the coded orthogonal frequency division multiplexing (COFDM) system, are explored. We conducted an analysis comparing the CCDF of PAPR to the autocorrelation of the COFDM signal before the inverse fast Fourier transform (IFFT) block. This allowed us to deduce the principal coding characteristics that

generate the peak factor after the IFFT block, following which we could then choose the parameters of the coded structure in order to reduce the peak power.

A space-time block coding (STBC) MIMO-OFDM system over a Rayleigh channel was simulated based on commercial communication parameters. The most outstanding PAPR reduction techniques available in the literature were compared, and a selection of the best methods to combine in the new hybrid technique was made based on the work objectives.

We proposed a new hybrid PAPR reduction technique for an STBC MIMO-OFDM system, in which the convolutional code is optimized to avoid PAPR degradation, and combined the SS-CARI and an iteratively modified companding and filtering methods. The new technique aimed to achieve a significant net gain for the system, i.e., considerable PAPR reduction, BER gain as compared to the basic MIMO-OFDM system, low complexity, and reduced spectral splatter. The new hybrid technique was extensively evaluated, and the CCDF, the BER, and the PSD were compared with the original STBC MIMO-OFDM signal.

Thesis Organization

This thesis is composed of four themed chapters, set out as follows:

The first chapter presents a systematic literature review of the PAPR reduction techniques available to MIMO-OFDM systems aiming to classify, analyze, and compare the documented methods. First, the MIMO-OFDM system model and the PAPR formulation are introduced. We then go on to describe the systematic literature review methodology, present and analyze the results, and finally, present a conclusion on the literature review. The study classifies the techniques according to the following criteria: the MIMO system, the strategy applied in reducing the PAPR in the OFDM signal, and whether or not the method is an extension of a proposed scheme for OFDM or takes advantage of the MIMO structure in designing the new technique.

Chapter 2 presents our first paper, *"Hybrid Peak-to-Average Power Ratio Reduction Techniques: Review and Performance Comparison"*. This paper, which was published in IEEE Access, describes the PAPR problem and summarizes the best known OFDM signal reduction techniques. It analyzes the main motivations for reducing the PAPR in current communication systems, and then highlights two of them: power savings and coverage gain. Additionally, we present a completed taxonomy for PAPR reduction techniques broken down into four categories, namely, coding, signal distortion, multiple signaling and probabilistic, and hybrid techniques. To conclude, the paper compares one scheme under each category in an OFDM binary phase shift keying (BPSK) modulation system over an AWGN channel, evaluates the CCDF of the PAPR and the BER performance, and summarizes the results based on the introduction of the net gain concept.

Chapter 3 presents the second paper, *Optimizing Forward Error Correction Codes for COFDM with Reduced PAPR*. It has been submitted to IEEE Transactions on Communications. This work studies the impact of FEC on the PAPR for the COFDM system. An analysis is done based on a study of the distribution of the PAPR for the COFDM signal, and the relation between the autocorrelation before the IFFT block in an uncoded and in a coded OFDM system, as well as the maximum PAPR of the COFDM. For this, a Markov Chain model for autocorrelation of the coded OFDM is suggested and related with the upper bound of the peak factor of the coded OFDM signal. The theory is tested by simulation over linear block and convolutional codes. In the case of convolutional codes, four parameters that can impact the PAPR degradation and the BER performance were studied in detail: the code rate, the code structure, the maximum free distance, and the constraint length. The results in this paper will contribute to correctly selecting the codes to be used in conjunction with an OFDM system to avoid increasing the PAPR.

The third paper, *On Optimizing the PAPR of OFDM Signals with Coding, Companding, and MIMO*, published in IEEE Access, is presented in Chapter 4. We proposed a new hybrid PAPR reduction method for the STBC MIMO-OFDM system, in which the convolutional code is optimized to avoid PAPR degradation, and combine the SS-CARI and the iteratively modified companding and filtering schemes. The new hybrid PAPR reduction technique is evaluated by simulation in STBC MIMO-OFDM QPSK modulation over the Rayleigh channel, and the main results and contribution are presented at the end of the chapter.

The final chapter brings together the different strands of the thesis, summarizes the main findings of this work, and identifies areas for further research.

List of contributions

The majority of these works have been published or submitted to international journals. They are listed as follows:

Journal papers

- *"Hybrid Peak-to-Average Power Ratio Reduction Techniques: Review and Performance Comparison"* in IEEE Access (published) (Sandoval *et al.*, 2017);
- *"Optimizing Forward Error Correction Codes for COFDM with Reduced PAPR"* in IEEE Transactions on Communications (published) (Sandoval *et al.*, 2019a);
- *"On Optimizing the PAPR of OFDM Signals with Coding, Companding, and MIMO"* in IEEE Access (published) (Sandoval *et al.*, 2019b).

CHAPTER 1

MIMO-OFDM PAPR REDUCTION TECHNIQUES: DESCRIPTION AND SYSTEMATIC REVIEW

1.1 Introduction

The use of multiple antennas at both the transmitter and the receiver is a standard method for improving the performance and increasing the capacity of wireless communications systems. A multiple-input multiple-output (MIMO) system in a wireless network provides, spatial diversity and array and multiplexing gains (Gesbert *et al.*, 2003). When a MIMO is used, the system capacity can be improved as compared to a single-input single-output (SISO) system with flat Rayleigh fading or narrowband channels (Foschini, 1996). However, when MIMO is used in wideband channels, the intersymbol interference (ISI) problem is compounded that is solved by using orthogonal frequency division multiplexing (OFDM) which is combined with MIMO to improve the capacity and achieve ISI mitigation.

One of the main implementation drawbacks of OFDM is the high peak-to-average power ratio (PAPR) it entails, in addition to which it also affects the MIMO-OFDM system. Currently, numerous works propose techniques to reduce the PAPR in MIMO-OFDM. The first ideas in this regard were in the form extensions of existing techniques for OFDM systems. Then, new proposals emerged aimed at taking advantage of the MIMO architecture. However, the sheer number of proposed techniques makes it difficult to compare, classify and discern the choice of PAPR reduction schemes for MIMO-OFDM systems. Furthermore, it should be recalled that there may be various MIMO applications and ways in which it can be implemented, and so appropriate technique for a specific situation must be determined.

Through a systematic literature review, this chapter reports the state of the art on the PAPR reduction techniques available to the MIMO-OFDM system. More than 100 papers were reviewed, with the following being the main findings: more and more techniques are being proposed for reduce peaks in MIMO systems, and the favorite approach consists in taking ad-

vantage of the structure of the systems based on multiple signalling and probabilistic schemes such as selected mapping, partial transmit sequence, precoding, and more recently, hybrid techniques. Additionally, most of the schemes found in the literature are directed at generic and spatially diverse MIMO systems, although there are some contributions aimed at other types of implementations, such as spatial multiplexing, multi-user MIMO or massive MIMO.

The chapter is organized as follows. Section 1.2 begins by laying out the theoretical dimensions of the research and looks at how the PAPR problem affects the MIMO-OFDM system, and describes a simplified model. The third section is concerned with the systematic literature review methodology used for this study. The results are presented and analyzed in Section 1.4, and the final section concludes the literature review.

1.2 Background

1.2.1 MIMO-OFDM system

In general, OFDM modulation and the MIMO system allow easy integration and increase of the spectral efficiency. Let us consider a MIMO-OFDM system with N_t transmit antennas, N_r receive antennas, and N subcarriers. At each transmit antenna, the conventional OFDM modulator is employed, i.e., to generate the OFDM symbol, the input signal is serial-to-parallel (S/P) converter followed by an inverse fast Fourier transform (IFFT). Each OFDM symbol is parallel-to-serial (P/S) converted and a cyclic prefix (CP) of length N_{cp} is added. As expected, the OFDM demodulator structure is used at each receiver antenna, as can be seen in Fig. 1.1.

Let us assume that the discrete-time baseband equivalent channel between each transmit-to-receive antenna link has a frequency impulse response of maximum length L, and is quasi-static. Hence, the channel from the ith transmit antenna to the jth receive antenna is:

$$\mathbf{h}_{ij} = \left[h_{ij}[0], h_{ij}[1], \cdots, h_{ij}[L-1]\right]^T. \tag{1.1}$$

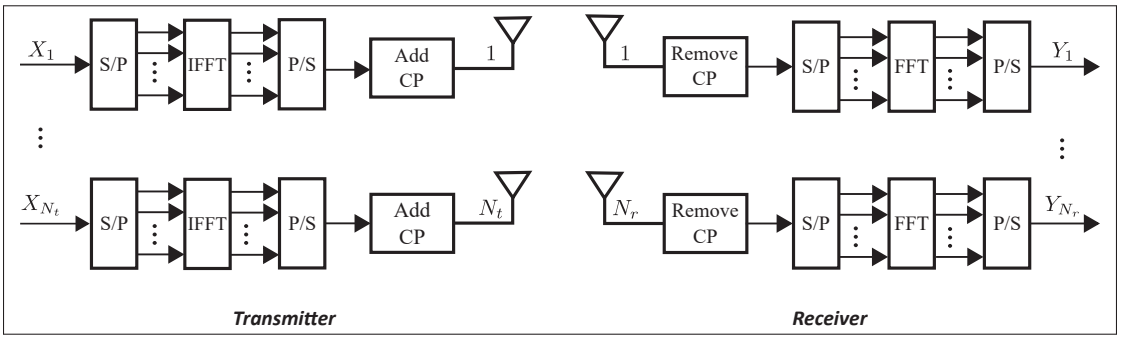

Figure 1.1 MMO-OFDM generic model

If we consider N IFFT points from the ith transmit antenna, $\{X_i[k]\}_{k=0}^{N-1}$ represents the frequency-domain signal, where k is the frequency index, and the discrete-time baseband OFDM signal $x_i[n]$ after applying IFFT is given by:

$$x_i[n] = \frac{1}{\sqrt{N}} \sum_{k=0}^{N-1} X_i[k] e^{\mathrm{j}2\pi \frac{kn}{N}},\ n = 0, 1, \ldots, N-1, \tag{1.2}$$

where n denotes the discrete-time index, and j is the imaginary unit.

Let us assume perfect time synchronization and that there is no inter-symbol interference (ISI) between OFDM symbols, i.e., $N_{\mathrm{cp}} \geq L$. The received frequency-domain signal at the jth receive antenna can be expressed as:

$$Y_j[k] = \sum_{i=1}^{N_t} H_{ij}[k] X_i[k] + W_j, \tag{1.3}$$

where $H_{ij}[k]$ is the channel frequency response of the (i, j)th channel, and is equal to:

$$H_{ij}[k] = \sum_{l=0}^{L-1} h_{ij}[l] e^{\mathrm{j}2\pi \frac{kl}{N}}, \tag{1.4}$$

and $W_j[k]$ is the fast Fourier transform (FFT) of the Gaussian noise with variance σ_w^2.

1.2.2 PAPR problem

Large peaks can be present in the instantaneous output of an OFDM signal at each transmit antenna, known as a PAPR. The PAPR of a discrete-time baseband OFDM signal is defined as the ratio between the maximum instantaneous power and its average power (Jiang & Wu, 2008), and from the *i*th transmit antenna, it is:

$$\mathrm{PAPR}(x_i[n]) \triangleq \frac{\max\limits_{0\leq n\leq N-1} |x_i[n]|^2}{\frac{1}{N}\sum\limits_{n=0}^{N-1} |x_i[n]|^2}. \tag{1.5}$$

In the MIMO-OFDM system, the PAPR is defined as the maximum of all N_t PAPR values evaluated in each MIMO path (Manasseh *et al.*, 2012), that is:

$$\mathrm{PAPR}_{\mathrm{MIMO}} = \max_{1\leq i\leq N_t} \mathrm{PAPR}(x_i[n]). \tag{1.6}$$

In the literature, the complementary cumulative distribution function (CCDF) is an important metric for comparing the performance of different systems related to the PAPR. It should be recalled that the PAPR is a random variable, and so the CCDF is the probability that the PAPR of the MIMO-OFDM signal exceeds a given threshold γ (also represented by PAPR0 in this thesis), i.e.:

$$\mathrm{CCDF} = \Pr(\mathrm{PAPR} > \gamma). \tag{1.7}$$

1.2.3 PAPR reduction techniques

The best alternative for reducing the high PAPR in the MIMO-OFDM system is to try to decrease the wide variations in the OFDM signal before tackling the nonlinear devices. Section 2.3 explain and demonstrates how to do this. There are many techniques proposed in the literature for reduction the PAPR in OFDM system, and some of these techniques have been adapted for use in MIMO-OFDM systems. The PAPR reduction techniques for OFDM systems can be classified into four categories, according to our taxonomy (Sandoval *et al.*, 2017),

namely: Coding (C), Multiple Signaling & Probabilistic (MSP), Signal Distortion (SD), and Hybrid (H).

For the PAPR Coding reduction technique, the idea is to select the code words that minimize the PAPR. Sandoval *et al.* (2017) classified the coding technique based on the coded scheme used, including block coding, convolutional codes, and concatenate coding schemes. Examples of Coding methods are: Simple Odd Parity code (SOPC) (Wilkinson & Jones, 1995), Modified Code Repetition (MCR) (Ngajikin *et al.*, 2003), Complement Block Coding (CBC) (Jiang & Zhu, 2005), Sub-block Complementary Coding (SBCC) (Jiang & Zhu, 2004b), and Golay Complementary Sequences (Wilkinson & Jones, 1995; Jiang *et al.*, 2004b).

Multiple Signaling techniques create multiple permutations of the signal and calculate the PAPR to select the signal with the minimum value for transmission. Meanwhile, Probabilistic techniques reduce the high peaks by changing and optimizing different parameters of the OFDM signal. The best-known Probabilistic techniques include: Selected Mapping (SLM) (Bäuml *et al.*, 1996; Muller & Huber, 1997b), Partial Transmit Sequence (PTS) (Muller & Huber, 1997b), Interleaving (Jayalath & Tellambura, 2000), DFT-Spreading or Single Carrier-FDMA (SD-FDMA), Tone Reservation (TR) (Tellado-Mourelo, 1999), Tone Injection (TI) (Tellado-Mourelo, 1999), and Dummy Sequence Insertion (Ryu *et al.*, 2004).

On the other hand, in Signal Distortion techniques, the signal is distorted before the power amplifier, in order to reduce the PAPR. For instance, Amplitude Clipping (O'Neill & Lopes, 1995), Peak Windowing (Nee & de Wild, 1998), Companding (Wang *et al.*, 1999a), are methods which distort the signal.

Hybrid methods combine two or more PAPR reduction schemes. Examples of such techniques are: Partial Transmit Sequence using Error-Correction Code (PTS-ECC) (Ghassemi & Gulliver, 2010), Error Control Selected Mapping (EC-SLM) (Xin & Fair, 2004), and Error Control Selected Mapping with Clipping (EC-SLM-CP) (Carson & Gulliver, 2002).

A summary of the taxonomy for PAPR reduction techniques is shown in Fig. 1.2. Most of these PAPR reduction techniques for OFDM systems are presented in detail in Chapter 2, Section 2.4. The techniques used in MIMO-OFDM systems are discussed in Subsections 1.4.4, 1.4.5, and 1.4.6 of this chapter.

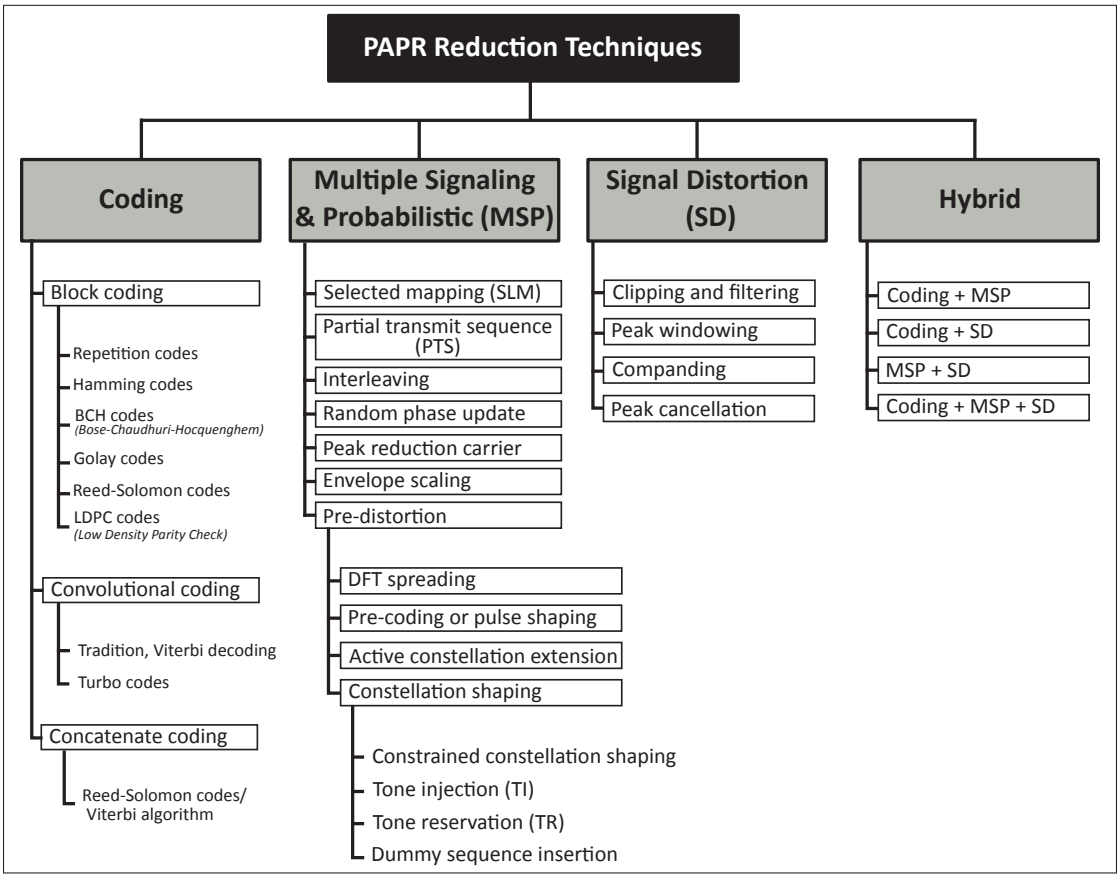

Figure 1.2 Taxonomy for PAPR reduction techniques

1.3 Research methodology

The systematic literature review is a strict method that facilitates the identification, extraction, classification, and synthesis of available information in the literature regarding a specific research topic (Britto & Usman, 2015; Dyba *et al.*, 2007). The systematic literature review is selected in this work to specify how research methodology and its implementation is based on

the guide proposed by Petersen et al. (Petersen *et al.*, 2015). The process used to conduct this systematic literature review is detailed below.

1.3.1 Research questions

The objective of this mapping study is to understand the state of the art on PAPR reduction techniques in a MIMO-OFDM systems and to determine the most commonly suggested of these techniques in the literature, as well as their performance. Consequently, we propose the following research questions:

- *Question 1 (RQ1)*: How many studies were published over the years?
- *Question 2 (RQ2)*: What kind of MIMO system is analyzed?
- *Question 3 (RQ3)*: Which technique is suggesting for reducing the PAPR in a MIMO-OFDM system?
- *Question 4 (RQ4)*: Is the suggested technique adapted from OFDM or takes advantage of the structure of MIMO?

1.3.2 Search strategy

The search is based on the strategy suggested by Wohlin *et al.* (2012), which includes PICOC (population, intervention, comparison, outcomes, and context). These help determine keywords and formulate search strings according to the research questions (Petersen *et al.*, 2015).

- *Population*: Solutions that implement a MIMO-OFDM PAPR reduction technique.
- *Intervention*: We do not have an explicit intervention to be investigated.
- *Comparison*: In this study, we compare different methods used to reduce the PAPR in the MIMO-OFDM system, in terms of the CCDF of PAPR, BER and other performance measures available.
- *Outcomes*: Improve the CCDF of PAPR in a MIMO-OFDM system.
- *Context*: Commercial, public safety, and tactical communication systems.

The keywords are extracted from the population, comparison, outcomes, and context. After determining all relevant keywords, we relate them with synonyms. The result of this work can

be seen in Table 1.1, where we list all the keywords, synonyms and its relation with PICOC elements.

Table 1.1 Keywords and Synonyms

Keyword	Synonyms	Related to
BER	Bit error rate	Comparison
CCDF	Complementary cumulative distribution function	Comparison, Outcomes
MIMO-OFDM	Multiple antennas OFDM	Population
PARP	PAR Peak-to-average power ratio Peak-to-mean envelope power ratio PMEPR	Population
Reduction		Population
Technique	Method Scheme	Population

Based on the research questions, the PICOC criteria and the keywords found, we obtained the following search strings:

("MIMO-OFDM" **OR** "multiple antennas OFDM") **AND** ("PAPR" **OR** "Peak-to-average power ratio" **OR** "PAR" **OR** "PMEPR" **OR** "peak-to-mean envelope power ratio") **AND** ("reduction " **OR** "technique" **OR** "method" **OR** "scheme")

The primary sources were selected based on the recommendation made by Dyba *et al.* (2007): IEEE Xplore[1], ISI Web of Science[2], Scopus[3], and Inspec/Compendex[4] (Engineering village). These sources cover most of the important electrical engineering databases, such as IEEE, Springer, Elsevier, and the Wiley Online Library.

The search string was optimized for each database. The values used in each case are presented in Table 1.2. The search process was limited to the English language. In addition, in the case

[1] http://ieeexplore.ieee.org

[2] http://www.isiknowledge.com

[3] http://www.scopus.com

[4] http://www.engineeringvillage.com

of the Scopus source, the initial search gave a large number of documents, and so a new search was carried out, limiting the keywords to just the title and the abstract. The search summary is presented in Table 1.3.

Table 1.2 Searches in databases

Database	Search
IEEE Digital Library	(MIMO-OFDM **OR** multiple antennas OFDM) **AND** (PAPR **OR** Peak-to-average power ratio **OR** PAR **OR** PMEPR **OR** peak-to-mean envelope power ratio) **AND** (reduction **OR** technique **OR** method **OR** scheme)
ISI Web of Science	(**TS=**(("MIMO-OFDM" **OR** "multiple antennas OFDM") **AND** ("PAPR" **OR** "Peak-to-average power ratio" **OR** "PAR" **OR** "PMEPR" **OR** "peak-to-mean envelope power ratio") **AND** ("reduction " **OR** "technique" **OR** "method" **OR** "scheme"))) **AND** Idioma: (English)
Scopus	**TITLE-ABS-KEY** (("MIMO-OFDM" **OR** "multiple antennas OFDM") **AND** ("PAPR" **OR** "Peak-to-average power ratio" **OR** "PAR" **OR** "PMEPR" **OR** "peak-to-mean envelope power ratio") **AND** ("reduction " **OR** "technique" **OR** "method" **OR** "scheme")) **AND** (**LIMIT-TO** (LANGUAGE , "English"))
El Compendex	((("MIMO-OFDM" **OR** "multiple antennas OFDM") **AND** ("PAPR" **OR** "Peak-to-average power ratio" **OR** "PAR" **OR** "PMEPR" OR "peak-to-mean envelope power ratio") AND ("reduction " **OR** "technique" **OR** "method" **OR** "scheme"))) **AND** (english WN LA))

Table 1.3 Summary of search results

Source	**Extraction date**	**All languages**	**Only English**
El Compendex	25-July-2017	511	481
Scopus (All)	25-July-2017	1366	1306
Scopus (TITLE-ALL-KEY)	25-July-2017	303	289
ISI	26-July-2017	204	204
IEEE	25-July-2017	91	90
Total (with Scopus (all))		**2172**	**2081**
Total (with Scopus (TITLE-ALL-KEY))		**1109**	**1064**

1.3.3 Study selection and quality assessment

The Parsifal[5], an online tool for systematic literature reviews within the context of Software Engineering, was used to remove duplicates and to execute the systematic literature review.

[5] https://parsif.al/

The study selection was conducted on title and abstracts by applying the following inclusion and exclusion criteria:

- Inclusion criteria:
  1. The papers are reported in peer-reviewed workshop conference, journal or technical reports.
  2. The papers are written in English.
  3. The papers improve the PAPR of the MIMO-OFDM system. However, they do not use a specific PAPR reduction technique.
  4. The papers proposed a PAPR reduction solution for a MIMO-OFDM system.
- Exclusion criteria:
  1. Full text of studies is not accessible.
  2. Studies that are duplicates of other studies.
  3. The papers are not described in English.
  4. The papers have not been published in a peer-reviewed conference or journal.
  5. The papers do not propose a PAPR reduction solution for a MIMO-OFDM system.

The number of included, excluded, and duplicated articles is shown in Table 1.4 for each source. It should be noted that apparently, the exclusion list was updated during the full-text reading process for the given criteria.

Table 1.4 Number of studies per study selection

Source	**Accepted**	**Rejected**	**Duplicated**	**Total**
Compendex	136	45	300	481
IEEE Digital Library	10	2	78	90
ISI Web of Science	15	18	171	204
Scopus	56	59	174	289
All Sources	**217**	**124**	**723**	**1064**

The quality assessment was conducted on the set of selected articles. Four questions were evaluated at this point:

1. Is the research objective a PAPR reduction technique in a MIMO-OFDM system?
2. Is the PAPR reduction technique in the MIMO-OFDM system clearly defined?

3. Does the article compare the performance of the technique presented with the conventional MIMO-OFDM system? (Yes = CCDF and BER, Partial = CCDF or BER, No = none)
4. Has the article been cited (Google scholar)? (Before 2015: N_c = number of citations, if $N_c \geq 10$ then Yes, if $10 < N_c \leq 3$ then Partial, if $3 < N_c \leq 0$ then No. For 2015 to 2017: if $N_c \leq 5$ then Yes, if $5 < N_c \leq 1$ then Partial, if $N_c = 0$ then No)

The possible answers for all quality questions were the same, and are presented with their weights assigned in Table 1.5. The maximum score for the quality assessment was 4, and the cutoff scores, 2. The result after executing the quality assessment for all selected articles is summarized in Table 1.6.

Table 1.5 Quality Assessment: Answers

Description	**Weight**
Yes	1.0
Partial	0.5
No	0.0

Table 1.6 Quality Assessment Score

Quality score	**Number of articles**
4	26
3.5	43
2.5	36
Subtotal (accepted)	**163**
2	33
1.5	10
0.5	3
0	4
Subtotal (rejected)	**54**
Total	**217**

1.3.4 Data extraction

The data extractions from primary studies were conducted according to the form in Table 1.7.

Table 1.7 Data extraction form

Description	Kind	RQ
1a. Study ID	String Field	
1b. Article Title	String Field	
1c. Author name	String Field	
1d. Year of Publication	Integer Field	RQ1
1e. Download Database	String Field	
2a. Kind of MIMO-OFDM system used	String Field	RQ2
2b. Number of antennas for simulation	String Field	RQ2
3a. PAPR reduction technique used	String Field	RQ3
3b. Classification of the PAPR reduction technique: i Coding (C) ii Hybrid (H) iii Multiple Signalling & Probabilistic (MSP) iv Signal Distortion (SD)	Select One Field	RQ3
3c. The PAPR reduction technique is: i adapted from OFDM ii takes advantage of the structure of MIMO system	Select One Field	RQ4
3d. PAPR reduction technique description	String Field	RQ3
4a. How much improve the PAPR (CCDF $= 10^{-3}$)?	String Field	RQ5
4b. Does the technique cause BER degradation? i No ii There is no information iii Yes	Select One Field	RQ5

1.3.5 Data analysis

The information collected from the data extraction form for each primary study was tabulated. Tables and illustrations were developed to present the extracted data efficiently (see Section 1.4).

1.4 Results of systematic literature review

1.4.1 Frequency of publication (RQ1)

The analysis of the number of articles per year is shown in Fig. 1.3. We find articles that refer to PAPR reduction techniques in MIMO-OFDM, starting in 2003. The number of articles per

year has increased significantly since 2007, with likely reason being the growing interest in MIMO systems and their combination with OFDM, the inclusion of MIMO-OFDM in all 4th generation (4G) and next generation (5G) wireless communications systems. Note that for the year 2017, the mapping covers only the period before July 25.

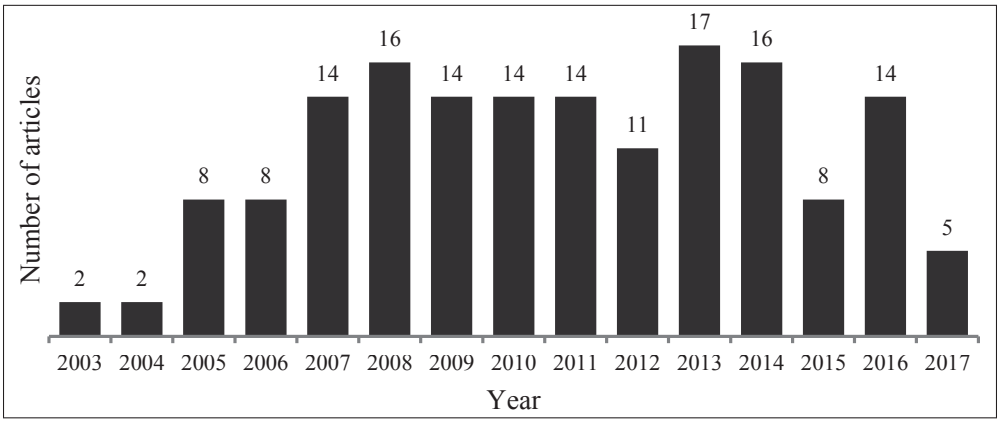

Figure 1.3 Final articles per year (2017, before of 25 July)

1.4.2 Download Database

Fig. 1.4 presets the number of articles per download database. It can be seen here that 75% of the articles were downloaded from IEEE explore. On the other hand, the Springer Link, Elsevier, and Wiley online libraries respectively saw a total of 6%, 4%, and 3% of all downloads. All of the articles were from conference papers, journal papers or letters.

1.4.3 MIMO-OFDM system applied (RQ2)

Next, we clarify the taxonomy employed in this work. First, in the MIMO literature, we can see a classification of MIMO systems based on antenna configurations. Four categories are recognized, namely, single-input single-output (SISO), single-input multiple-output (SIMO), multiple-input single-output (MISO), and multiple-input multiple-output (MIMO). However, note that, strictly speaking, a MIMO system should be one with multiples antennas at both the transmitter and receiver (Hampton, 2013).

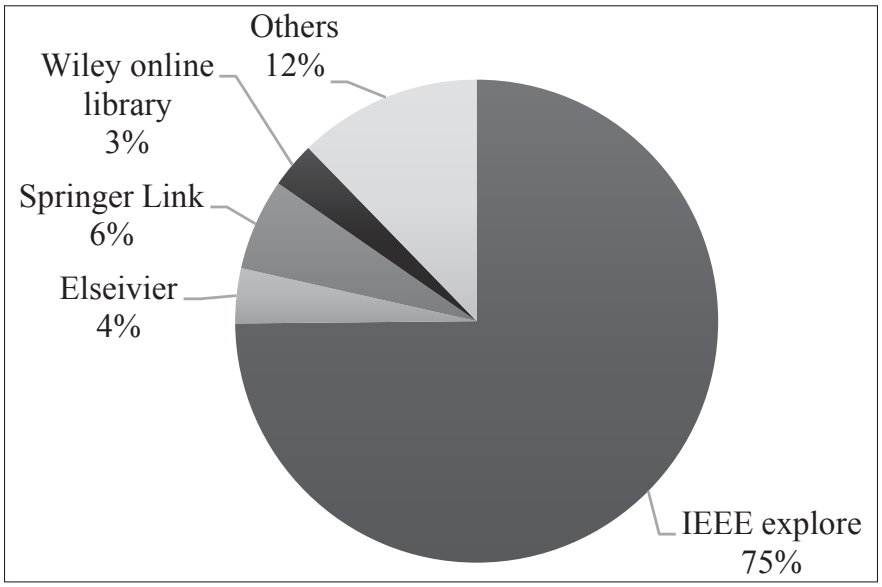

Figure 1.4 Articles per download database

On the other hand, MIMO techniques can be divided into two categories according to the target objective, namely, spatial diversity or spatial multiplexing (see Fig. 1.5). Spatial diversity techniques aim to combat fading, and are used to improve reliability and provide diversity gain. With spatial diversity, we send information across the different propagation paths using the space-time coding (STC) schemes. The STC include two major categories: space-time block codes (STBCs) and space-time trellis codes (STTCs). Meanwhile, STBCs are divided into two subclasses, namely, orthogonal space-time block codes (OSTBCs) and non-orthogonal space time block codes (NOSTBCs). Unlike spatial diversity, in spatial multiplexing techniques, we send different portions of information along different propagation paths. Spatial multiplexing is used to increase throughput and provides degrees of freedom (multiplexing gain). There are some schemes that are used to implement spatial multiplexing (see Fig. 1.5), and that are based on layered space-time (LST) coding, such as the Bell Laboratories layered space-time (BLAST) family: horizontal BLAST (H-BLAST), vertical BLAST (V-BLAST), and diagonal BLAST (D-BLAST), multi-group space-time coding (MGSTC), and threaded space-time coding (TSTC) (Hampton, 2013). Additionally, spatial multiplexing can be implemented using Eigen-beamforming (Hampton, 2013).

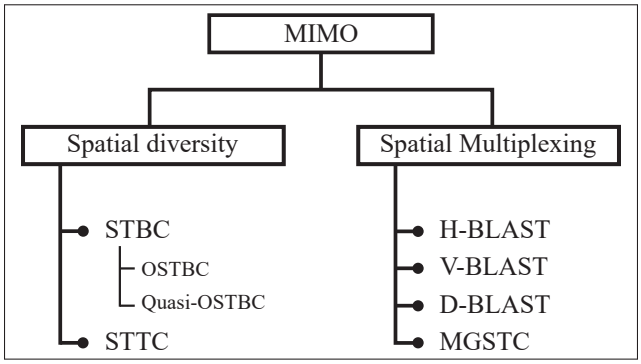

Figure 1.5 Purpose MIMO taxonomy
Hampton (2013)

Another classification is possible, based on the number of users, and in that the MIMO techniques can be categorized as single-user MIMO (SU-MIMO) or multi-user MIMO (MU-MIMO). SU-MIMO involves one transmitting node with multiple antennas, and one receiving node (Hampton, 2013). In MU-MIMO, depending on the mobile cellular system, each piece of user equipment (UE) with a single antenna transmits to a Node-B (eNB), and the eNB processes the signals of each UE as if they were coming from multiple transmit antennas (Hampton, 2013).

Additionally, we can classify MIMO techniques according to what is know about the transmitter and receiver of the channel characteristics. In this case, we know two categories: open-loop and closed-loop. MIMO techniques, in which only the receiver requires knowledge of the channel are open-loop. In contrast, in closed-loop techniques, the receiver must send the channel information back to the transmitter.

Finally, we introduce the term massive MIMO, which refers to a MIMO system with a large number of antennas, which can go into the hundreds or thousands, for example, and that can multiply the system capacity, and improve the performance of the communication system in terms of data rate and reliability.

The MIMO-OFDM systems described in the reviewed articles were grouped according to the scheme used, and the result is presented in Fig. 1.6. It can be seen that the PAPR techniques providing the greatest amount of reductions are implemented in a generic model (61 articles) or

STBC MIMO system (60 articles). However, PAPR reduction techniques implemented in MU-MIMO, Massive MIMO or V-BLAST are also available. Note that in some cases, the reviewed studies may apply to one or more types of MIMO schemes. Here, when the study is applied to more than one type of MIMO system, we consider the one with the greatest emphasis in the work.

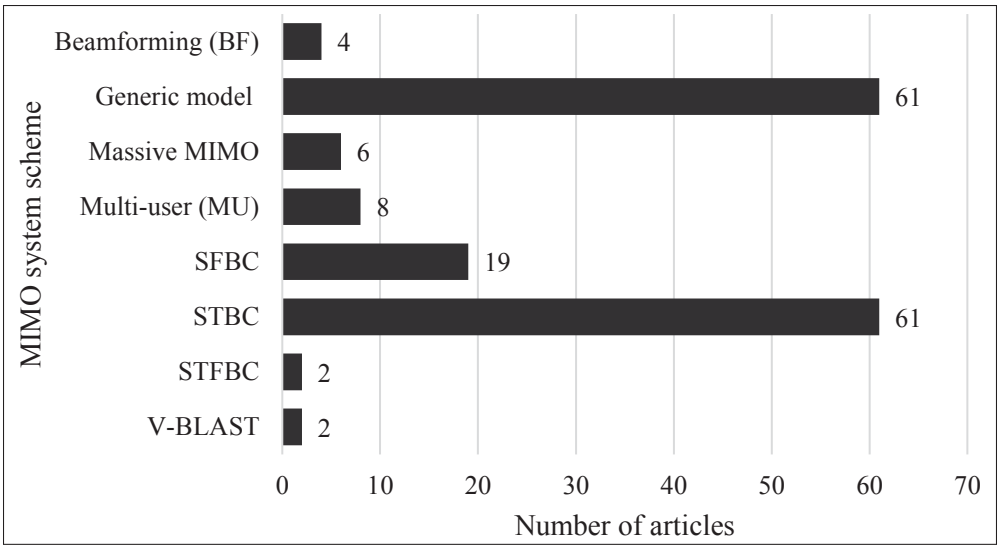

Figure 1.6 Articles per MIMO system type

1.4.4 Proposed classification of PAPR reduction techniques (RQ3)

The techniques proposed in the selected papers were classified based on the taxonomy presented by Sandoval *et al.* (2017), where the PAPR reduction techniques are divided into four categories, namely, Coding (C), Multiple Signaling & Probabilistic (MSP), Signal Distortion (SD), and Hybrid (H).

Fig. 1.7 shows that 83% of the techniques proposed in the selected articles can be considered as Multiple Signaling and Probability methods, 9% as Hybrid, 6% as Signal Distortion, and only 2% were Coding techniques. Meanwhile, Table I-1 presents primary studies grouped by PAPR reduction method and category. For instance, in the Multiple Signal and Probabilistic categories, the most important schemes found are: Active Constellation Extension (ACE),

Cross-Antenna Rotation and Inversion (CARI), Cross-Frequency Permutation and Inversion (CFPI), Precoding, Partial Transmit Sequence (PTS), Selected Mapping (SLM), Tone Reservation (TR), and Wavelet Entropy Algorithm (WEA). On the other hand, Signal Distortion techniques as clipping and peak cancellation methods applied to MIMO-OFDM systems were found in the literature. Additionally, a bar graph including the number of first studies per PAPR reduction technique is shown in Fig. 1.8. For instance, 37% of articles analyzed correspond to the SLM and PTS techniques. Twenty articles are categorized as precoding schemes, and fourteen as hybrid techniques. More details regarding the resulting PAPR reduction techniques are presented in the following section.

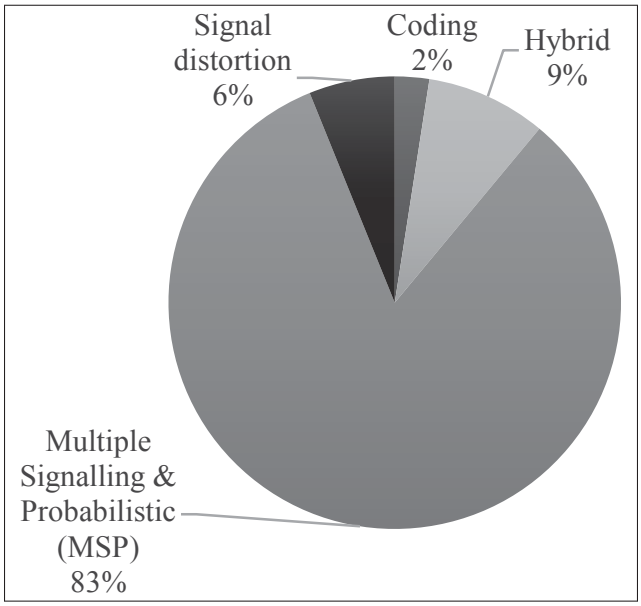

Figure 1.7 Articles per proposed PAPR reduction technique type

1.4.5 Classification of MIMO-OFDM PAPR reduction techniques based on its adaptation to the MIMO structure (RQ4)

Numerous studies have attempted to explain the PAPR problem in a MIMO-OFDM system. They investigate PAPR reduction techniques for a MIMO-OFDM system and propose the extension of OFDM PAPR reduction techniques as PTS, SLM, or TR.

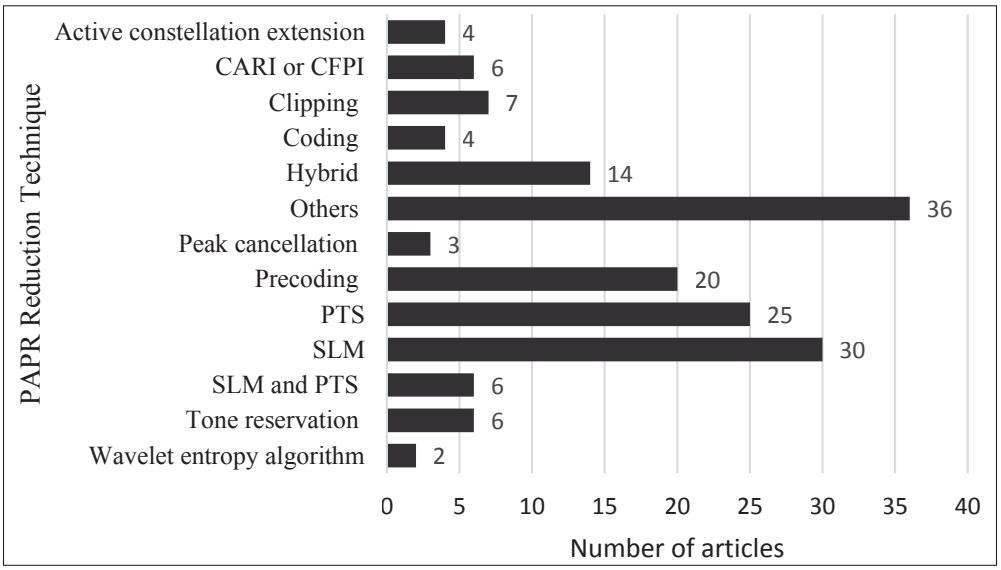

Figure 1.8 Articles per PAPR reduction technique

In recent years, a few authors began to propose alternatives for PAPR reduction that tried to exploit the potential of MIMO systems. Khademi *et al.* (2012) introduced the precoding technique that exploits the Eigen-beamforming mode (EM) in MIMO systems. Using beamforming can significantly improve the received SNR of OFDM systems, and it has been widely adopted in modern MIMO-OFDM. However, the beamforming deteriorates the PAPR because after beamforming the dynamic range of the signals increases (Hung & Tsai, 2014). For this reason, Hung & Tsai (2014) proposed a new algorithm for single-user MIMO-OFDM systems when using beamforming schemes, i.e., maximum ratio transmission (MRT) and equal gain transmission (EGT), which try to adjust the power at some subcarriers after beamforming. The results of Hung & Tsai (2014) show PAPR reduction, and in addition, improve the bit error rate performance. On the other hand, Prabhu *et al.* (2014) analyzed the PAPR problem on massive MIMO-OFDM, and introduced a low-complex PAPR scheme, in which a combination clipping and antenna reservation approach is used to reduce the PAPR. Pandurangan & Perumal (2011) introduced a modified PTS with forward error correcting codes for PAPR reduction in a MIMO-OFDM system and showed that unlike the original PTS technique, the combination of a modified PTS and FEC provides better PAPR reduction and moderate computational complexity in MIMO-OFDM systems.

In the systematic literature review, the articles were classified based on whether the technique proposes an extension of OFDM PAPR reduction techniques or if the scheme exploits the MIMO potential. The result is presented in Fig. 1.9, where is can be seen that the current trend is to take advantage of the MIMO structure in designing the adopted PAPR reduction technique.

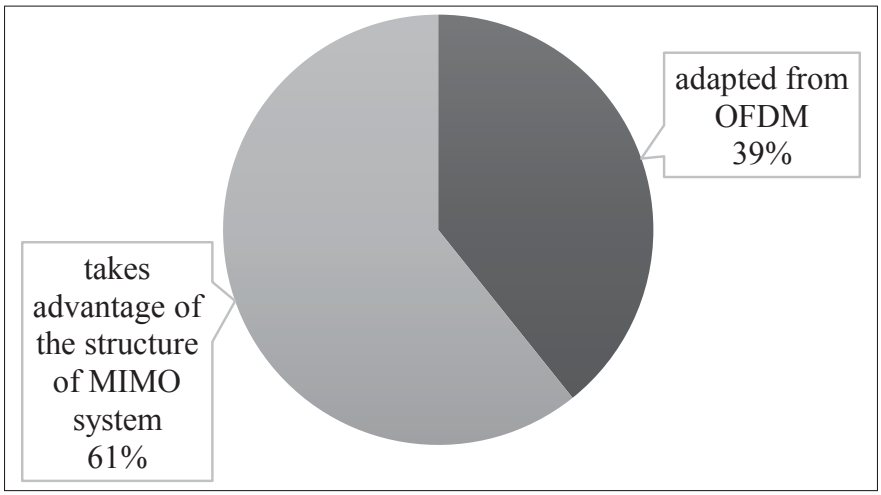

Figure 1.9 Articles per technique approach

1.4.6 Most used PAPR reduction techniques (RQ3) description

1.4.6.1 Coding techniques

The forward error correction (FEC) block can be used to reduce the PAPR if we select the codewords that minimize the PAPR for transmission (Sandoval *et al.*, 2017). These are four articles that describe PAPR reduction schemes based on coding: these include turbo codes (Alakaidi *et al.*, 2006), convolutional codes (Venkataraman *et al.*, 2006), Reed-Solomon codes (Fischer & Siegl, 2009), Reed-Muller (RM) codes and complementary sequence codes (Jinlong & Yuehong, 2009).

1.4.6.2 Precoding techniques

In a precoding scheme, before the OFDM modulator, each information block is multiplied by a precoding matrix. There are several variations of this technique, for example, some variations try to optimize the precoding matrix. This can be seen in Table I-2, where the precoding methods found in the mapping are presented, and their principal characteristics are described.

1.4.6.3 Selected mapping techniques

The conventional SLM technique in an OFDM system is presented in Fig 1.10. The basic idea here is to generate U statistically-independent OFDM frames that represent the same information and to select the $\tilde{u}$th frame with the lowest PAPR for transmission. Nevertheless, to recover data successfully, the receiver needs to know the value of $\tilde{u}$, i.e., the side information (SI) has been used in the transmitter. The number of bits required to represent $\tilde{u}$ is $\log_2(U)$; it is of the highest importance and critical information to the receiver. A strong FEC is required for transmit the side information to avoid errors in the reception, and the strong FEC decreases the transmitting efficiency (Kojima *et al.*, 2010). Other interesting points in SLM design include the method used to generate different phase sequences and the multiple IFFT operations required in the conventional structure, which increase the computational complexity of the system.

There are three main MIMO versions of selected mapping, namely: Ordinary SLM (oSLM) or individual SLM (iSLM), simplified SLM (sSLM) or concurrent SLM (cSLM) and directed SLM (dSLM) (Fischer & Hoch, 2007). The simple extension where an SLM is applied in each of the N_t branches in a MIMO-OFDM system is the oSLM. However, this simple extension rapidly increases the system complexity and the number of SI bits when increasing the number of transmit antennas in the system. A simplified version of SLM proposes to reduce the overheard signalling by applying the same phase factor in all the N_t branches. On the other hand, the directed SLM version is designed to take advantage of the structure of a MIMO system

and proposes to adapt the complexity to optimize the performance of the reduction technique (Fischer & Hoch, 2007).

Table I-3 summarizes the SLM methods found by mapping and describe its significant characteristics.

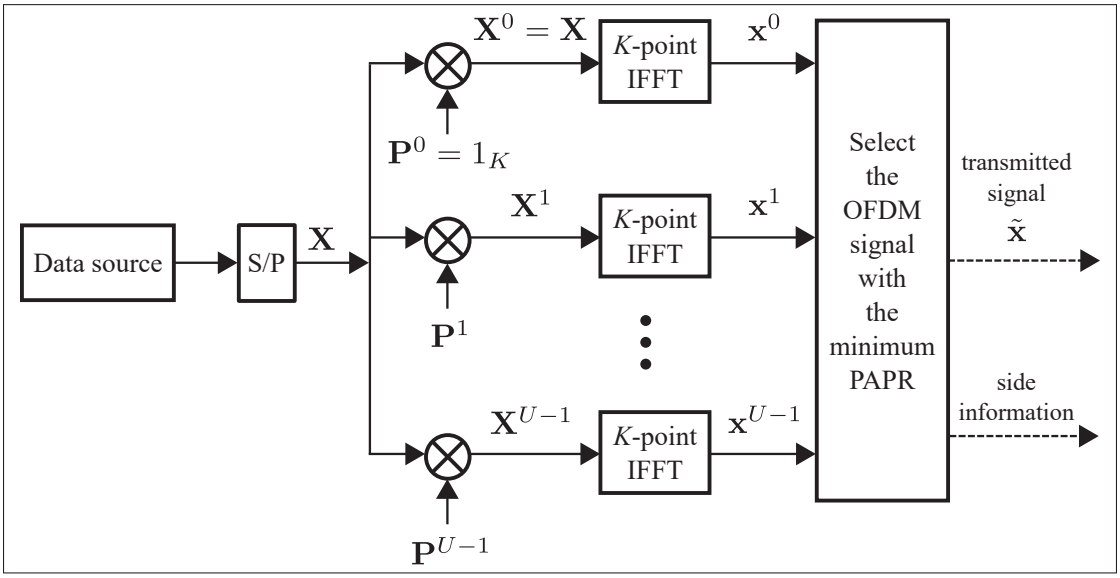

Figure 1.10 SISO-OFDM SLM generic scheme Cho *et al.* (2010a)

1.4.6.4 Partial transmit sequence techniques

In the conventional PTS scheme (see Fig. 1.11), the input symbol sequence is partitioned into non-overlapping subsequences, the IFFT is applied to each subsequent symbol, and then the resulting signals are multiplied by a set of different rotation vectors. All subsequent processing signals are summed, and the PAPR is computed for each resulting subsequence. Finally, the signal sequence with the minimum peak-to-average power ratio is transmitted. Increasing the number of subsequences in PTS allows reducing the PAPR, but however, increases the computational complexity exponentially. As in SLM, the partial transmit sequence needs to transmit side information. There are three subsequence partitioning types, namely, adjacent, interleaved, and pseudo-random partitioning (Muller & Huber, 1997a).

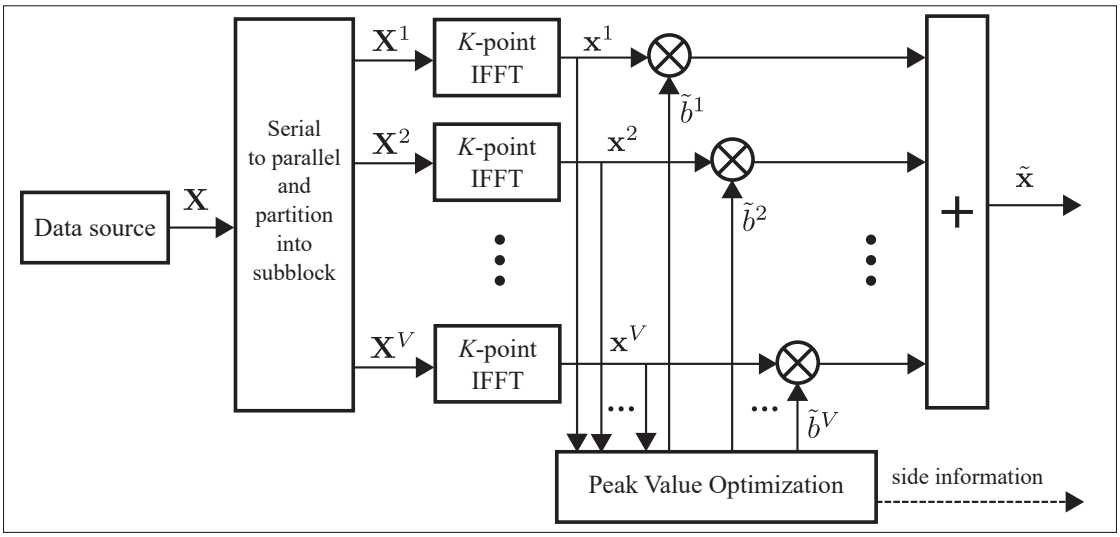

Figure 1.11 SISO-OFDM PTS generic scheme, Cho *et al.* (2010a)

The partial transmit sequence technique for PAPR reduction in MIMO-OFDM systems converts the input data symbols into N_t parallel streams for each transmit antenna, and the conventional PTS method is used in each stream. All transmit antennas in the system use the same set of phase factors as this allows a reduction of the side information. Many variations of this basic system have been devised. Table I-4 presents a summary of the techniques found in this systematic literature review.

1.4.6.5 Tone reservation techniques

In tone reservation (TR), a small number of the N subcarriers (tones) is reserved for peak reduction tones (PRTs). For instance, Fig 1.12 shows the generic model from the TR technique in an OFDM system. The PRTs need to be optimized to minimize the PAPR, and the literature contains different proposals on how to formulate the problem.

The extension of the TR technique can be used to reduce the PAPR of the MIMO-OFDM signal. A simple alternative uses the same position of reserved subcarriers for all transmit antennas and sends side information. In each transmit antenna, PAPR optimization is independent and similar to what is obtained in the OFDM system, and at the receiver, the PRTs are ignored.

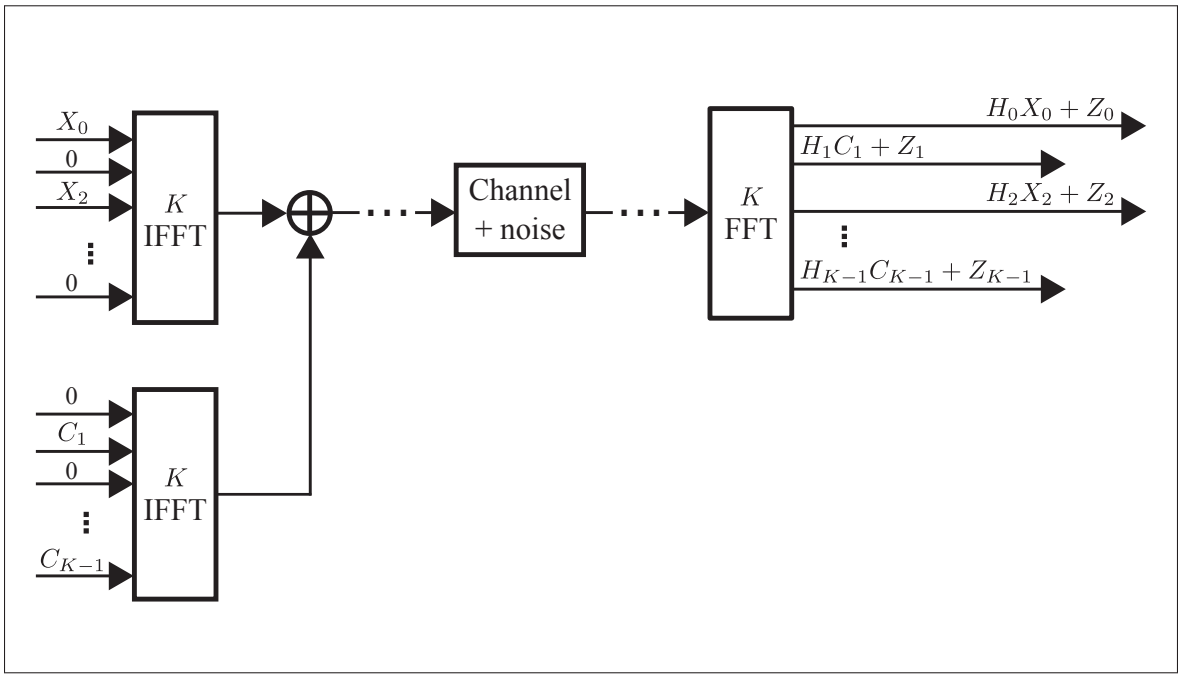

Figure 1.12 SISO-OFDM tone reservation generic scheme, Cho *et al.* (2010a)

Table I-5 summarizes the MIMO-OFDM available tone reservation PAPR reduction techniques and their characteristics.

1.4.6.6 Clipping techniques

Amplitude clipping is a signal distortion scheme in which a specified level limits the time-domain OFDM signal. If we consider a soft threshold, the output signal could be represented by:

$$B(x) = \begin{cases} x, & |x| < A \\ Ae^{j\phi(x)}, & |x| \geq A \end{cases} \tag{1.8}$$

where A is the clipping level and $\phi(x)$ the phase of x.

Clipping is a simple strategy for reducing the peaks in the OFDM signal. Nevertheless, it can produce performance degradation in the form of in-band distortion and out-band radiation. The disadvantages presented by clipping have led to modifications in the conventional technique;

for example, clipping can be combined with filtering (see Fig. 1.12) to avoid out-band radiation. However, it can produce peak regrowth. Another alternative is to use iterative clipping and filtering, which allows controlling the peak regrowth of the signal at the cost of increasing the computational complexity. Table I-6 identifies clipping applications in MIMO and their characteristics.

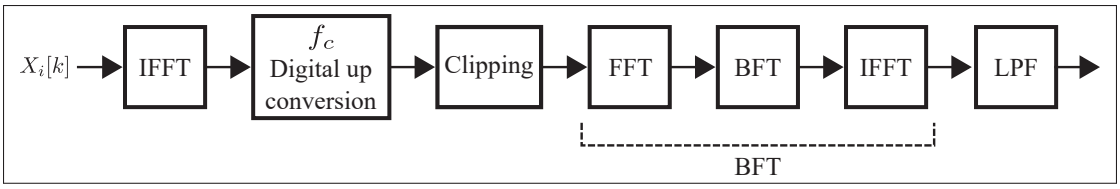

Figure 1.13 SISO-OFDM clipping generic scheme, Cho *et al.* (2010a)

1.4.6.7 Hybrid techniques

Hybrid PAPR reduction techniques exploit the advantage presented by simultaneously using more than one method and combine the methods to achieve better benefits. For example, Distortion techniques are characterized by low complexity but these can produce an increase in BER. On the other hand, MSP techniques do not change the BER of the system, however, they can increase the complexity of the system. Table I-7 shows examples of hybrid methods and describes the techniques that were combined.

1.5 Conclusion

Multiple-input multiple-output orthogonal frequency division multiplexing achieves high spectral efficiency, high capacity, and data throughput. As a result, it has gained favor for use in current and future wireless communications systems, and enjoys a continuous research investments. However, one of the inherited disadvantages of OFDM modulation is the high value of peak-to-average power ratio presents in the OFDM signal due to multiple techniques to reduce the peaks in the OFDM signal have been proposed in the literature.

The present study applies a systematic literature review and groups, classifies and analyzes PAPR reduction techniques for MIMO-OFDM systems available in the literature. Interest in PAPR reduction in MIMO-OFDM systems has gained interest in recent years. Initially, the techniques were aimed at extending the proposed schemes for OFDM. However, currently, there are multiple proposals to take advantage of the structure of MIMO to design new techniques. Besides, the implementation of techniques such as SLM, PTS, and precoding has gained considerable acceptance, and many modifications have been suggested for them. Additionally, in recent years, hybrid techniques, combining more than one PAPR reduction technique, have been attracting increased interest since they allow a combination of the advantages of each individual technique.

CHAPTER 2

HYBRID PEAK-TO-AVERAGE POWER RATIO REDUCTION TECHNIQUES: REVIEW AND PERFORMANCE COMPARISON

Francisco Sandoval[1,3], Gwenael Poitau[2], François Gagnon[3]

[1] Departamento de Ciencias de la Computación y Electrónica, Universidad Técnica Particular de Loja, Loja, 11-01-608, Ecuador
[2] Chief Technology Officer, Ultra Electronics, TCS, Montreal, QC H4T IV7, Canada
[3] Departament of Electrical Engineering, École de Technologie Supérieure, 1100 Notre-Dame West, Montréal, Quebec, Canada H3C 1K3

Paper published in *IEEE Access*, November 2017

Abstract

Orthogonal frequency division multiplexing (OFDM) is an efficient multi-carrier modulation technique for wireless communication. However, one of the main drawbacks encountered in implementing it is its resultant high peak-to-average power ratio (PAPR). Many techniques have been proposed in the literature to substantially decrease the peaks in the OFDM signal. The problem with these, however, is that their effects on other parameters are not always positive. These effects include a decrease in the bit error rate (BER), an increase in complexity, or a reduction in the bit rate. The objective of this paper is to describe the PAPR problem in a bid to reduce the peaks in the OFDM signal. The paper proposes a classification, performance evaluation and optimization of PAPR reduction techniques for commercial, public safety and tactical applications. In the taxonomy proposed herein, we also include a new category, namely, hybrid techniques. Furthermore, we compare the principal characteristics through a complementary cumulative distribution function (CCDF) and BER evaluation, and conclude on the importance of hybrid techniques when the goal is to both improve the BER and reduce the PAPR.

Keywords

Orthogonal frequency division multiplexing, peak-to-average power ratio, high power amplifier, hybrid PAPR reduction technique, commercial communication, tactical communication.

2.1 Introduction

Recent developments in new wireless communication technologies have come about in response to a growing demand for higher data rates due to the popularity of multimedia services, including real-time stream media, gaming, and other social media services. While this demand naturally calls for high bandwidth technologies (Liu *et al.*, 2010), high quality of service (QoS) is nevertheless crucial as well. For example, in Wang *et al.* (2014), it was predicted that 5th generation (5G) mobile networks should achieve 1000 times the system capacity, 10 times the spectral efficiency, higher data rates, 25 times the average cell throughput and other improvements, of the present generation 4G systems.

Orthogonal frequency division multiplexing (OFDM) underlies all 4G wireless communication systems; for instance, it is included in the IEEE 802.16 Worldwide Interoperability for Microwave Access (WiMAX) and Long Term Evolution (LTE) standards. LTE is currently the chosen standard for interoperable Public Safety communications in the US and in other countries. Moreover, multiple tactical waveforms, such as the Universal Networking Waveform (UNW), and Wideband Network Waveform (WNW), leverage the OFDM technology for its inherent mobility robustness. As well, the technology is a popular modulation technique for other wireless digital communication systems, such as IEEE 802.11 a/g/n/ac wireless LANs, Digital Audio Broadcasting (DAB), Digital Video Broadcasting-Terrestrial (DVB-T), and Digital Video Broadcasting by Satellite (DVB-S). Further, combining OFDM with multiple-input multiple-output (MIMO) wireless communication systems results in MIMO-OFDM, one of the most promising techniques for broadband wireless access schemes because in high data rate transmission situations, OFDM decreases the complexity of the MIMO receiver by transform-

ing a frequency-selective MIMO channel into a set of parallel frequency-flat MIMO channels (Yang, 2005).

However, transmit signals in an OFDM system, where the output is the superposition of multiple subcarriers via an inverse fast Fourier transform (IFFT) operation, can have a high peak-to-average power ratio (PAPR), which is effectively one of the main implementation disadvantages of the OFDM system.

If the transmitter has a high PAPR, the average power is significantly reduced, with reference to a constant saturation power. In modern commercial wireless systems, the PAPR problem is more significant in uplink (Anoh *et al.*, 2017) because this is the limiting link in terms of coverage and range (Khan, 2009), and as the mobile terminal is limited in battery power, the efficiency of the power amplifier is critical. A trend in 5G is to enable higher frequency bands to obtain more unused spectrum, and previous research has led to fruitful researches (Rappaport *et al.*, 2013). In the future 5G smartphones where beamforming technique is used, PAPR reduction is more important considering the general low power efficiency of mmWave PAs and poor battery performance investigated in Huo *et al.* (2017). Moreover, in tactical communications, the coverage is a critical point, and vehicle-to-vehicle broadband communication require a strong output power. The problem here is that power amplifiers (PA) equipped with very high power scopes have low cost efficiency and are very expensive (Yi & Linfeng, 2009). As a result, a practical OFDM implementation must consider all measures to reduce the high PAPR. Many authors have considered the PAPR reduction problem and proposed different strategies.

This paper also aims to develop a systematic approach for PAPR reduction under different propagation, topology or traffic conditions. As well, unlike the surveys such as Rahmatallah & Mohan (2013); Vijayarangan & Sukanesh (2009), the work presents a detailed analysis of the motivations to reduce the PAPR in the current communication systems, emphasizing two main motivations such as power savings and coverage gain. The work summarizes the recent literature on hybrid PAPR reduction techniques, compares the important parameters it incorporates, and concludes on its usability in current commercial, public safety and tactical

communications systems. Additionally, the net gain concept is introduced and evaluated as a tool to choose the best PAPR reduction technique under different scenarios.

The rest of this paper is broken down into six sections. Section 2.2 looks at how an OFDM system is affected by the PAPR problem, and presents an OFDM model. Section 2.3 presents the advantages that can be obtained when the PAPR is reduced. The core of this paper is presented in section 2.4, where the PAPR techniques available in the literature are classified and described, and the hybrid category is included and some examples are given. Section 2.5 introduces a simple hybrid PAPR reduction technique, and it compares PAPR reduction rates and BER performance using different techniques. Finally, section 2.6 summarizes and concludes this paper.

2.2 OFDM System Model and PAPR Problem

Orthogonal frequency division multiplexing or OFDM is a multicarrier modulation technique that divides available bandwidth into a number of orthogonal subcarriers which are transmitted with equal intervals, and provides numerous advantages, such as resilience to RF interference, lower multi-path distortion, and ease of integration with MIMO, which increase the spectral efficiency. Fig. 2.1 shows a block diagram of a typical OFDM transmitter and receiver.

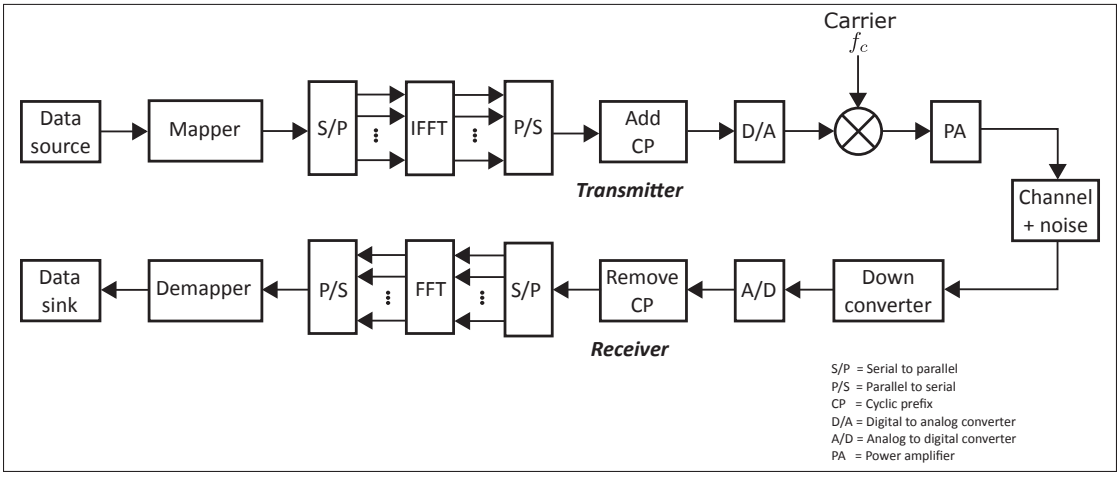

Figure 2.1 Block diagram of transmitter and receiver in an OFDM system

In an OFDM system, a collection of K complex data symbols $X(k)$ are modulated on a set of K orthogonal subcarriers. Hence, an input symbol vector on a frequency domain, called a data block, can be represented by $\mathbf{X} = [X(0),\ X(1),\ldots,X(K-1)]^T$, and the continuous-time baseband OFDM signal $x(t)$, defined as the sum of all K subcarriers with subcarrier spacing $1/Kt_s$, is given by

$$x(t) = \frac{1}{\sqrt{K}} \sum_{k=0}^{K-1} X(k) e^{j2\pi \frac{k}{Kt_s} t},\ 0 \leq t < Kt_s. \tag{2.1}$$

where t_s is the sampling period and $j = \sqrt{-1}$.

Frequently, the instantaneous output of an OFDM signal has large peaks that can be expressed as a PAPR, which is sometimes referred to as PAR. The PAPR of the continuous-time baseband OFDM signal $x(t)$ is defined as the ratio between the maximum instantaneous power and its average power (Jiang & Wu, 2008), that is:

$$\text{PAPR}(x(t)) \triangleq \frac{\max\limits_{0 \leq t \leq Kt_s} |x(t)|^2}{\frac{1}{Kt_s} \int_0^{Kt_s} E\left\{|x(t)|^2\right\} dt}. \tag{2.2}$$

where $E[\cdot]$ denotes the expected value. If the $x(t)$ signal is sampling at the Nyquist rate $t = nt_s$, with integer n, the discrete-time baseband OFDM signal $x(n)$ can be written as:

$$x(n) = \frac{1}{\sqrt{K}} \sum_{k=0}^{K-1} X(k) e^{j2\pi \frac{k}{K} n},\ n = 0, 1, \ldots, K-1, \tag{2.3}$$

and the PAPR in terms of discrete-time baseband OFDM signal can be expressed as:

$$\text{PAPR}(x(n)) \triangleq \frac{\max\limits_{0 \leq n \leq K-1} |x(n)|^2}{\frac{1}{K} \sum\limits_{n=0}^{K-1} |x(n)|^2}. \tag{2.4}$$

In most cases, the PAPR of the discrete OFDM signal is less than the PAPR of the continuous OFDM signals by $0.5 \sim 1$ dB (Lim *et al.*, 2009). Hence, the relationship between PAPRs is

given by

$$\text{PAPR}(x(n)) \leq \text{PAPR}(x(t)). \tag{2.5}$$

2.2.1 The CCDF of the PAPR

The time domain OFDM signal $x(t)$ is a complex number. Assuming that the real and imaginary parts follow a Gaussian distribution, with 0.5 variance and zero mean, in agreement with the central limit theorem when K is sufficiently large, the amplitude of the OFDM signal $|x(t)|$ becomes a Rayleigh distribution and the power distribution is exponential (Han & Lee, 2005). The cumulative distribution function (CDF) of the amplitude of a signal sample is

$$F(z) = 1 - e^{-z}. \tag{2.6}$$

If we assume that the average power of $x(t)$ is equal to one, that is, $E|x(t)|^2 = 1$, the probability distribution function for PAPR less than a certain threshold value is

$$\begin{aligned} \Pr(\text{PAPR} < z) &= (F(z))^K \\ &= (1 - e^{-z})^K. \end{aligned} \tag{2.7}$$

However, when the performance of PAPR reduction techniques is evaluated, the CCDF of the PAPR is more frequently used. The probability that PAPR exceeds a threshold value (i.e., the CCDF) is described by (Han & Lee, 2005)

$$\begin{aligned} \Pr(\text{PAPR} > z) &= 1 - \Pr(\text{PAPR} \leq z) \\ &= 1 - (1 - e^{-z})^K. \end{aligned} \tag{2.8}$$

In the literature, the CCDF of PAPR is usually expressed in terms of the number of subcarriers K. For example, Fig. 2.2 shows the theoretical CCDFs of OFDM signals with different subcarriers (i.e., $K = 64,\ 128,\ 256,\ 512$ and 1024) that are obtained by evaluating (2.8). The graph

shows that the probability of occurrence of a given OFDM symbol decreases with an increase in the number of subcarriers K when compared to a fixed value of PAPR thresholds, PAPR0 (x-axis).

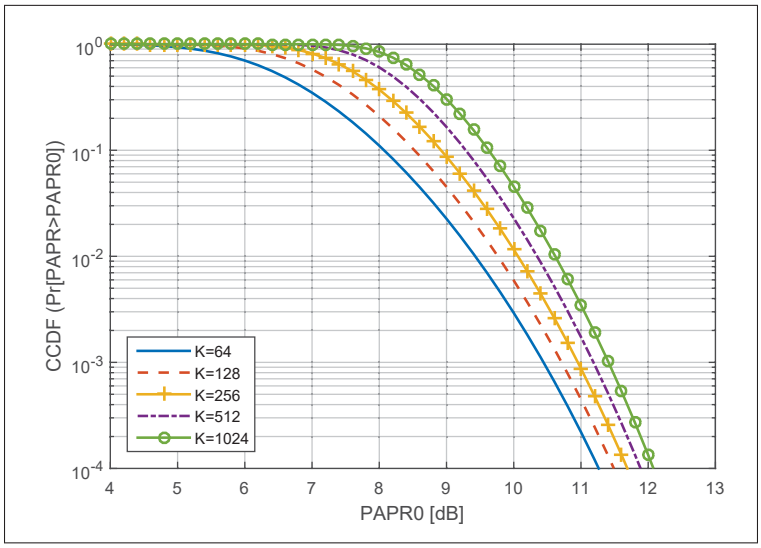

Figure 2.2 Theoretical CCDFs of OFDM signals with different subcarriers

A conventional analysis of the PAPR of OFDM signals (equation (2.8)) provides a good approximation when the number of subcarriers K is relatively small (Ochiai & Imai, 2001; Jiang & Wu, 2008). Ochiai & Imai (2001), and Wei *et al.* (2002) work in an exact distribution of the PAPR in OFDM systems. For instance, Ochiai & Imai (2001) employed the level-crossing rates method, and deduced the following approximation for a large number of subcarriers:

$$\Pr(\text{PAPR} > z) \cong 1 - \exp\left\{-Ke^{-z}\sqrt{\frac{\pi}{3}z}\right\}. \tag{2.9}$$

Meanwhile, Jiang & Wu (2008) developed an approximation of the PAPR of a practical OFDM by employing the extreme value theory; according to that theory, if the number of subcarriers goes to infinity, the complex envelope of a bandlimited uncoded OFDM converges weakly to a Gaussian random process (Jiang & Wu, 2008). The derived expression in Jiang & Wu (2008)

can be written as:

$$\Pr(\text{PAPR} > z) \cong 1 - \exp\left\{-Ke^{-z}\sqrt{\frac{\pi}{3}\log K}\right\}. \tag{2.10}$$

In the case of a coded OFDM signal, the literature provides an approximation of when to use codes that can be modeled as uncorrelated. Many of the standard codes meet this condition; for example, block codes (except repetition codes, and low-rate codes (Wilson, 1995, pg. 527)), some convolutional codes, and turbo codes. Under this condition, Jiang & Wu (2008) demonstrated that the CCDF of the PAPR of coded OFDM can be approximated by the equation (2.10).

2.2.2 Net gain

In order to compare the PAPR reduction techniques for a given requirement, it is important to consider the global gain (net gain) in the system. In this paper, the net gain is composed of the PAPR reduction and the BER performance. Hence, the net gain is defined as a particular case of the fitness function-based approach (Rajbanshi, 2007) where under given channel conditions (AWGN or multi-path), the relative PAPR reduction is

$$Y_1 = -10\log_{10}\left(\frac{\text{PAPR}_{\text{after}}}{\text{PAPR}_{\text{before}}}\right), \tag{2.11}$$

and the relative degradation in BER performance at certain signal to noise ratio (SNR) level can be written as

$$Y_2 = -10\log_{10}\left(\frac{\text{BER}_{\text{after}}}{\text{BER}_{\text{before}}}\right). \tag{2.12}$$

The aggregate fitness value of the PAPR reduction technique is given by Rajbanshi (2007)

$$\Gamma = \sum_{k=1}^{2} \alpha_k \cdot Y_k, \tag{2.13}$$

where

$$\sum_{k=1}^{2} \alpha_k = 1, \tag{2.14}$$

and α_k represents the weights of factors related with the importance level of BER and PAPR reduction in the system.

2.3 Motivation

Transmit signals in an OFDM system can have high peak-to-average power ratio (PAPR), for example, Fig. 2.3 illustrates time domain OFDM subcarriers with $K = 4$ in a QPSK-OFDM system and their sum $|x(t)|$. We see that when the subcarriers have high peaks aligned simultaneously, a high peak appears in the resulting OFDM signal.

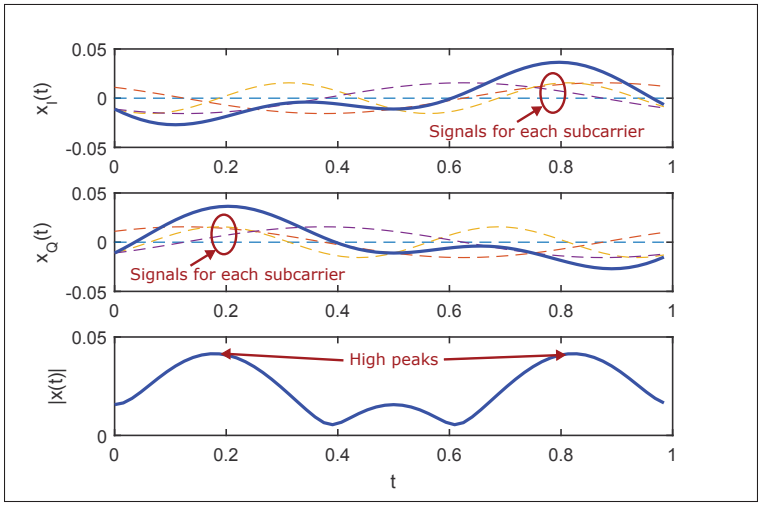

Figure 2.3 Time domain OFDM signals with $K = 4$ for real, imaginary parts and the sum $|x(t)|$, when the modulation is QPSK (Cho *et al.*, 2010a)

An ideal OFDM transmitter requires a linear PA where the output is equal to the input affected by a gain. However, in a real PA, the linear region has a limit, after which the output is equal to the saturation value (or its maximum possible level). The nonlinear PA causes changes in the spectrum and in the constellation signal of the input. As an example, Fig. 2.4 represents the effects of PA on a 16-QAM signal, with the IFFT length being equal to 128. Therefore, the high peaks in the OFDM signal can produce spectral spreading (see Fig. 2.4a) and changes

in the constellation signal how cloud-like shaping (see Fig. 2.4b), attenuation and rotation or warping.

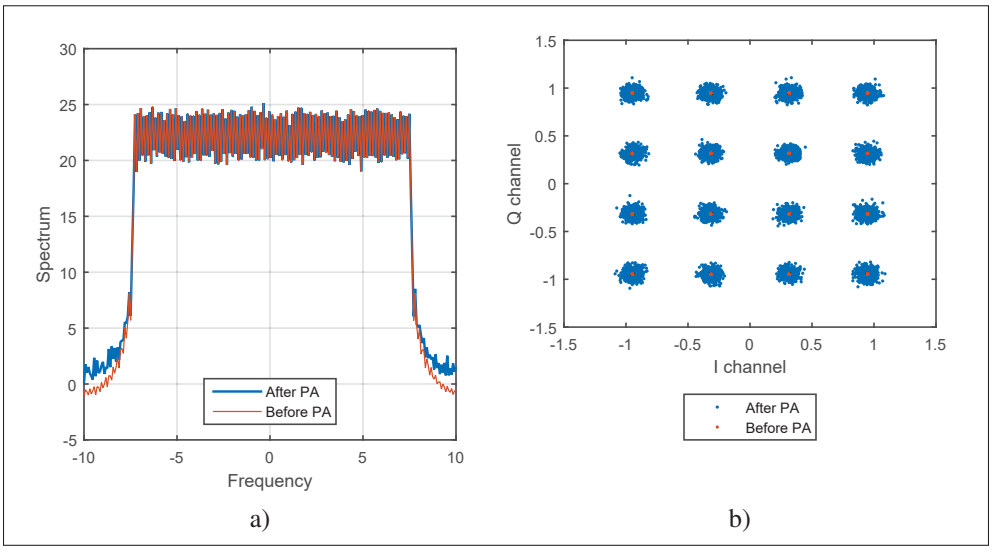

Figure 2.4 Effects of nonlinear PA on (a) signal spectrum and (b) signal constellation (Ramezani, 2007)

The PA is employed in radio systems transmitters to obtain sufficient transmit power, and it usually operates at or near the saturation region to achieve the maximum output power efficiency. This can be seen in Fig. 2.5, which presents a typical input power P_{in} versus output power P_{out} characteristics curve (gain) for a PA. The nonlinear distortion in the PA depends on the back-off of the amplifier, and can be calculated as the input back-off (IBO), which is defined as:

$$\text{IBO} = 10\log_{10}\left(\frac{P_{\text{sat}}}{P_{\text{av}}}\right), \tag{2.15a}$$

or

$$\text{IBO} = [P_{\text{sat}}]_{\text{dB}} - [P_{\text{av}}]_{\text{dB}}, \tag{2.15b}$$

where P_{sat} and P_{av} are the saturation power of the PA and the average power of the input signal, respectively. Moreover, $[P_{\text{sat}}]_{\text{dB}}$ and $[P_{\text{av}}]_{\text{dB}}$ represent the saturation and average powers in dB. The maximum possible output is limited by P_{sat}. To ensure that the peaks in the OFDM signal do not exceed the saturation threshold in the PA, the input back-off should be at least equal to

PAPR (Rahmatallah & Mohan, 2013), i.e., $IBO_1 \leq PAPR$. However, the result of this solution is that the power amplifier works with reduced efficiency (Rahmatallah & Mohan, 2013). For instance, an OFDM signal, such as the one presented in Fig. 2.5 (blue signal, i.e., OFDM signal without PAPR reduction), with an average power P_{av_1}, needs a large input back-off (IBO_1), and consequently, works with very low PA gain (g_1), and low efficiency (η_1). As well, it works with very high nonlinearity. In contrast, an OFDM signal with a good PAPR reduction (Figure 2.5, purple signal) requires very low input back-off (IBO_2), and works with very high PA gain (g_2), high efficiency (η_2), and small nonlinearity.

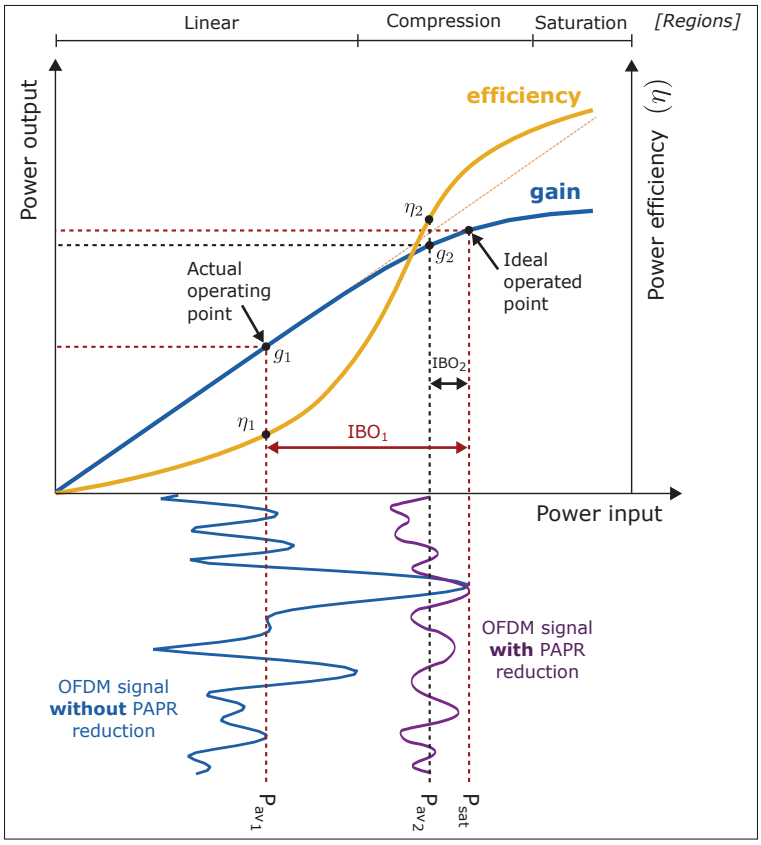

Figure 2.5 Input power versus output power characteristics and efficiency curves for a solid state power amplifier (SSPA)

With a high PAPR, there are very wide variations in the multi-carrier envelope, and as a result, the nonlinear characteristic of PA, excited by a large input, causes in-band distortions and out-

of-band radiation. Therefore, the PA will introduce additional interference into the systems, leading to an increase in BER for high peaks in the OFDM signal. To reduce the signal distortion and improve the BER, we could try to modify the nonlinear components of the system, i.e., the PA or the DAC. With a high PAPR in the system, we require a PA with a wide dynamic range. However, such a PA is not power-efficient, more complex, and is expensive. On the other hand, with a wide variation in the OFDM signal, we need a high precision DAC, which is however, equally expensive. If we were to use a low precision DAC, then we could face the possibility of having significant quantization noise. Since, modifying the nonlinear components to support high PAPR requires drastic sacrifices, the best alternative would be to try to decrease the wide variations in the OFDM signal before tackling the nonlinear devices.

Two additional important motivations for introducing a PAPR reduction technique in commercial and tactical wireless communication systems —power savings and coverage gain— are considered in more detail next.

2.3.1 Power savings

Reducing the PAPR in an OFDM signal can provide significant power savings (Baxley & Zhou, 2004; Rajbanshi, 2007). Power savings becomes more relevant when we have mobile terminals in the system, since these have limited battery life. That is the case with the uplink in a wireless commercial system, and with all nodes in a tactical communications system.

Let us consider Class A power amplifiers, which are the most linear amplifiers, and have a maximum PA efficiency $(\eta_{\max})$ of 50% (Baxley & Zhou, 2004). Assuming an ideal linear model for the power amplifier, where the linear amplification is achieved up to the saturation point (Baxley & Zhou, 2004), the PA efficiency in this amplifier is given by:

$$\eta = \frac{\eta_{\max}}{\text{PAPR}} = \frac{0.5}{\text{PAPR}}, \tag{2.16}$$

where the PAPR is expressed in linear units. To better understand why the PAPR reduction in the OFDM signal may saves power, let us look at an example. Given an OFDM signal

when QPSK is assumed to be the modulation scheme, the oversampling rate is $L = 4$, and the number of subcarriers is $K = 64$ (see Fig. 2.2). Hence, we need to use an input back-off (IBO) equivalent to $\text{PAPR}_{\text{dB}} = 11.4$ dB (≈ 13.80), which is the PAPR at the 10^{-4} probability level, in order to guarantee that no more than 0.01% frames are clipped. Thus, the PA efficiency in this case is $\eta = \frac{0.5}{13.80} \approx 3.6\%$. Now, let us consider the case when a PAPR reduction technique is applied to this system and we achieve a PAPR reduction of 3 dB, i.e., $\text{PAPR}_{\text{dB}} = 8.4$ dB, which is 6.92. So, the PA efficiency is $\eta = \frac{0.5}{6.92} \approx 7.23\%$, which is tantamount to doubling the efficiency.

Table 2.1 analyze the PA efficiency when three type of linear PA are considered, i.e., Class A, B, and C. The maximum PA efficiency is 50%, 78.5%, and 100% for Class A, B, and C, respectively (Johansson & Fritzin, 2014). In Table 2.1, PAPR_1 and η_1 represented the PAPR at the 10^{-4} probability level, and the PA efficiency without PAPR reduction technique, respectively, and PAPR_2 and η_2 are the PAPR at the 10^{-4} probability level, and the PA efficiency, respectively when a PAPR reduction technique is applied to this system and we achieve a PAPR reduction of 3 dB. Similar results are obtained in all cases. Therefore, achieving low power efficiency is thus a strong motivation for using a PAPR reduction technique in the OFDM system.

Table 2.1 A comparison of the PA efficiency with and without PAPR reduction of different PA classes

Class	η_{max} (%) (Johansson & Fritzin, 2014)	PAPR_1 (linear)	η_1	PAPR_2 (linear)	η_2
A	50	13.80	3.62	6.92	7.23
B	78.5	13.80	5.69	6.92	11.35
C	100	13.80	7.24	6.92	14.45

2.3.2 Coverage gain

As with power savings, increasing the coverage and range become more important when we have mobile users on the network. For this reason, coverage and range are key points in tactical

communications, where all users are mobile, and therefore have limited battery power and smaller antennas, as compared to base stations in a commercial system.

In general, a commercial network has user equipment (UE) associated with a Node-B (eNB). A eNB is typically located on a fixed tower and defines a coverage zone, the cell. They are interconnected by an X2 interface (Khan, 2009). The third component is the mobility management entity/gateway (MME/GT), whose main function is idle-mode UE reachability, and is interconnected with the eNBs by an S1 interface (Khan, 2009). In contrast, tactical communications need a highly complex network that is organized in tiers of subnets (Joint Tactical Radio System (JTRS) structure). All the infrastructure's units are mobile, and the nodes are distributed by air, ground or sea. There are two types of subnets: global, which function as gateways in all or part of the network, and local, which use different frequencies. A tier can be comprised of multiple subnets, and only selected nodes can have multichannel capability (Elmasry, 2010). For example, one tier can be the soldier radio waveform (SRW) divided in two categories of subtiers (soldier-to-soldier communications and networking sensors). Another tier is the wideband networking waveform (WNW), which uses an OFDM physical layer and has two subtiers (local subnets for vehicle-to-vehicle communications and global connectivity) (Elmasry, 2010).

The preceding discussion shows that commercial and tactical networks differ in structure, and therefore, increasing coverage poses various challenges. In commercial communications, in order to increase the network coverage, we could, for example, increase the number of cells, and use overlapping cells of different sizes. In addition, as the BS are fixed, the nodes face fewer restrictions in terms of resources, such as transmit power, gain, or height of the antennas. By contrast, in tactical networks, there are no fixed elements, and coverage there is related to the range of each node, and the nodes have limited resources. For instance, an estimation of the range over mountain blockages is modeled by an ITU-R model (Single-Knife Edge) for commercial and tactical applications in Oza *et al.* (2012). The authors conclude that the range of commercial communication is more than four times that of tactical communication with a similar link margin. The research in Oza *et al.* (2012) compares a commercial application BS

versus a Manpack node in tactical communication with the parameters described in Table 2.2. Also, Table 2.2 shows the parameters used for a vehicle-mounted mobile node in a tactical communication network, for comparison.

Table 2.2 Commercial and tactical communications parameters comparison (Oza *et al.*, 2012)

	Commercial Communications	**Tactical Communications**	
	Base Station (BS)	*Manpack*	*Vehicle*
Transmit power [W]	200	5	50
Rx antenna gain [dBi]	0	0	0
Tx/Rx antenna height [m]	15/1	1.7/1.7	2.8/2.8

Common PAPR reduction techniques can reduce the PAPR by about 2 to 4 dBs. This represents a transmit power gain of a few dBs and can have an impact on the range and coverage of the system. Now, an important question is how much a small gain in transmit power can improve the range and coverage of a wireless system. In order to answer this question, we start with a propagation analysis in free space, and then present a model to analyze the range and coverage as a function of transmit power gain. This analysis is based on the work of Khan (2009).

Wireless signal strength decreases as the propagation distance increases. Hence, we need a model which predicts the mean signal strength at the receiver, as a function of the separation between the transmitter and the receiver. A free space model predicts the received signal strength when there is an unobstructed propagation path between the transmitter and the receiver, and it is governed by the Friis free space equation, and can be written as Khan (2009):

$$P_R = P_T G_T G_R \left(\frac{\lambda}{4\pi d} \right)^2, \tag{2.17}$$

where P_R is the received power, P_T represents the radiated power of a source (isotropic radiator), and G_T and G_R are the transmitter and receiver antenna gains, respectively. Also, $(4\pi d)^2$ is the surface area of a sphere of radius d, and the wavelength of the radiation is represented by $\lambda = c/f$, where c and f denote the speed of light and the frequency, respectively. Then, the

total path loss in free space is described by Khan (2009):

$$PL_{\text{FS}} = 32.44 + 20\log_{10}(d) + 20\log_{10}(f) - 10\log_{10} G_T - 10\log_{10} G_R \; [dB]. \tag{2.18}$$

Here, d is given in meters and f in GHz. Therefore, in free space, when the distance is doubled, the path loss increases by $20\log_{10}(2) = 6$ dB. For instance, the additional gain can come from increasing the transmit power by reducing the PAPR in the OFDM system.

Generally, in a practical communication system, path loss increases more than it does in free space, over the same distance. For example, if we consider a two-ray reflection model, which predicts path loss when the signal received consists of two principal components such as the line of sight and a reflected wave, the electric wave power at the receiver is attenuated as $1/d^4$ rather than $1/d^2$ experienced in free space (Khan, 2009). Usually, the power attenuation factor α is denominated path loss exponent, and is a function of the environment. Thus, the received power P_R can be described by Khan (2009)

$$P_R \propto \left(\frac{1}{d}\right)^{\alpha}. \tag{2.19}$$

Assuming a pat loss exponent α and considering that d_0 is the original range and d_1 is the range with a power gain of g_P dBs, the incremental range extension ΔR by a power gain of g_P dBs is given by Khan (2009)

$$\Delta R = \frac{d_1 - d_0}{d_0} = \left(10^{(g_P/10)}\right)^{\frac{1}{\alpha}} - 1. \tag{2.20}$$

Finally, if a circular shape omni-cell is considered, the gain in coverage area ΔA is described by Khan (2009)

$$\begin{aligned}\Delta A &= \frac{A_1 - A_0}{A_0} \\ &= \frac{\pi d_1^2 - \pi d_0^2}{\pi d_0^2} \\ &= \pi \left(\left[\left(10^{(g_P/10)} \right)^{\frac{1}{\alpha}} \right]^2 - 1 \right). \end{aligned} \tag{2.21}$$

The range extension and the coverage area as a function of transmit power gain g_P are plotted in Fig. 2.6. We note that the range extension is small for bigger path loss exponent α, similar to the coverage area. Also, in Fig. 2.6 (left) we can see that a transmit power gain g_P of 3 dB can extend the communication range by ~ 19 to over $\sim 26\%$ for a path loss exponent α in the range of 3 to 4. On the other hand, in Fig. 2.6 (right), with the same value of transmit power gain g_P, i.e., 3 dB, the coverage area gain is between ~ 130 to $\sim 184\%$ for a path loss exponent α in the 3 to 4 range.

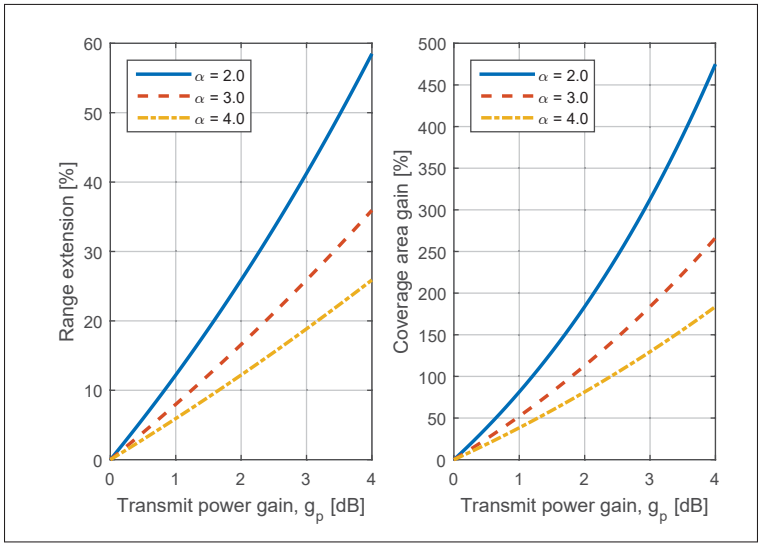

Figure 2.6 Range extension (left) and Coverage area (right) as a function of transmit power gain g_P (Khan, 2009)

In conclusion, it can be seen that reducing the PAPR in the OFDM signal by a few dBs could result in huge improvements in range and coverage area (Khan, 2009).

2.4 PAPR Reduction Techniques

Many authors have considered the PAPR reduction problem and proposed different strategies for reducing the peaks in the multi-carrier signal, and more recently, in the OFDM system. Further, there are different ways to divide the PAPR reduction techniques as detailed next.

Cho *et al.* (2010a) argue that there are five broad categories of PAPR reduction techniques, namely: clipping (includes block-scaling, clipping and filtering, peak windowing and peak cancellation) (O'Neill & Lopes, 1995; Ochiai & Imai, 2000; Ju & Leung, 2003; Ren *et al.*, 2003), coding schemes, adaptive pre-distortion, discrete Fourier transform (DFT) spreading and probabilistic (scrambling) (Bauml *et al.*, 1996; Muller & Huber, 1997b; Cimini & Sollenberger, 2000), which includes selected mapping, partial transmit sequence, tone reservation, and tone injection techniques.

Alternatively, the work in Vijayarangan & Sukanesh (2009) classified the PAPR techniques into two broad types: signal distortion and signal scrambling. Signal distortion techniques such as signal clipping, peak windowing or nonlinear companding transform (NCT), reduce high peaks in the OFDM signal by distorting the signal before the amplification, and the signal scrambling techniques are all variations of how to scramble codes to decrease the PAPR (Vijayarangan & Sukanesh, 2009). The scrambling techniques may be divided into two main sub-groups: without explicit side information, for instance, the Hadamard transform method or Dummy sequence insertion, and with explicit side information including coding-based schemes, such as block coding schemes, sub-block coding schemes or block coding with error correction. We also have probabilistic schemes, including, for example, selected mapping (SLM), partial transmit sequence (PTS), tone reservation (TR), tone injection (TI) and active constellation extension.

Another categorization is described by Rajbanshi (2007), who divided the PAPR reduction techniques into deterministic and probabilistic approaches. The deterministic schemes try to ensure that the PAPR of the signal does not exceed a predefined limit, in contrast to probabilistic schemes which minimize the probability that the PAPR of a signal exceeds a predefined limit.

Finally, Rahmatallah & Mohan (2013) defined three main categories in their taxonomy: signal distortion, multiple signaling techniques and probabilistic techniques, and coding techniques.

The taxonomy presented by Rahmatallah & Mohan (2013) is selected here for describe the PAPR reduction techniques. However, in this work, we add a new category, namely, hybrid techniques, which groups together the methods that combine two or more than two techniques for PAPR reduction. Hybrid methods have gained interest in recent years as they can combine the advantages present in two or more techniques. They can achieve better overall results such as an improved PAPR reduction, an increase in performances of the system, at the cost of only a slight increase in complexity.

Fig. 2.7 shows the four categories of PAPR reduction techniques and examples of each category. Next, we will briefly describe some schemes in each category of the PAPR reduction classification, and discuss the advantages and disadvantages of these techniques.

2.4.1 Coding Based Techniques

The coding PAPR reduction technique consists in choosing the codewords that minimize the PAPR. By way of illustration, Fig. 2.8 shows the PAPR of a four subcarrier signal as a function of time, for all possible data words d, increasing sequentially from $0_{\text{dec}}(\prime 0000\prime_{\text{bin}})$ to $15_{\text{dec}}(\prime 1111\prime_{\text{bin}})$. As can be seen from Fig. 2.8, four words result in the maximum PAPR: the two code sequence with all bits equal, i.e., the words $0_{\text{dec}}(\prime 0000\prime_{\text{bin}})$ and $15_{\text{dec}}(\prime 1111\prime_{\text{bin}})$, and the two data words with all bits alternating, i.e., $5_{\text{dec}}(\prime 0101\prime_{\text{bin}})$ and $10_{\text{dec}}(\prime 1010\prime_{\text{bin}})$. It is understandable that we could reduce the PAPR of this OFDM signal by avoiding the use of these words.

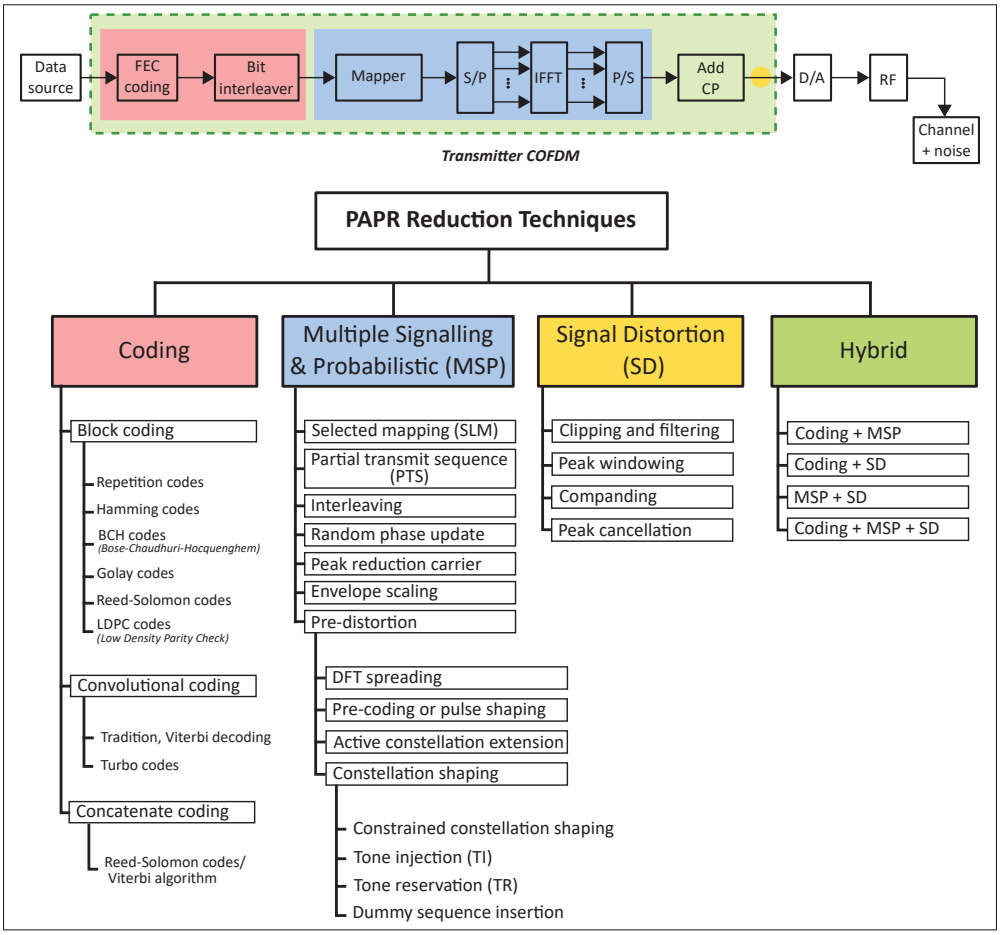

Figure 2.7 PAPR reduction techniques

The PAPR reduction techniques classification proposed here suggest three types of coding-based PAPR reduction schemes, namely, block coding schemes, convolutional codes schemes, and concatenate coding schemes in concordance with the forward error correction (FEC) categorization. Examples of coding schemes are presented below.

2.4.1.1 Simple Odd Parity Code

Wilkinson & Jones (1995) proposed PAPR reduction using a simple odd parity code (SOPC). Based on the idea presented as an example in Fig. 2.8, Wilkinson & Jones (1995) showed that the PAPR of a four-carrier signal can be reduced from 6.02 dB to 2.48 dB with a 3/4 rate block code by avoiding the transmission of words with high PAPR; in the case of 4 bits,

Wilkinson & Jones (1995) used 3 bits for data transmission and one bit for the odd parity check (see Fig. 2.9a).

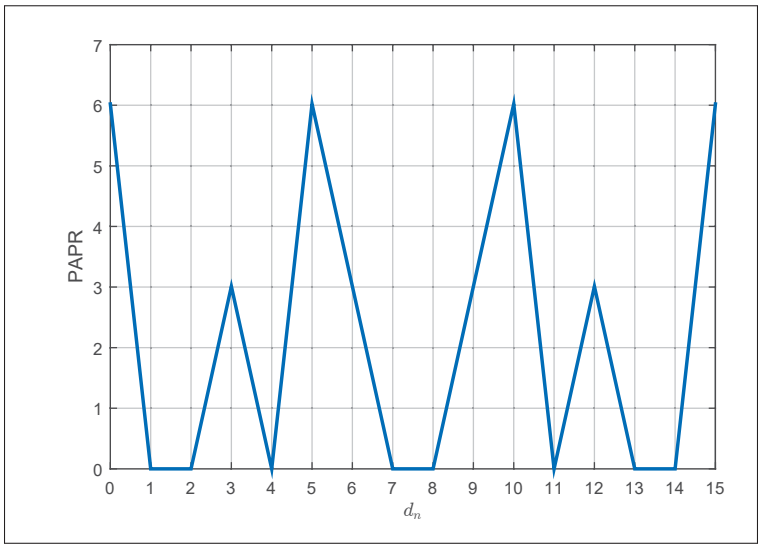

Figure 2.8 PAPR of a four subcarrier signal for all possible data words d_n

2.4.1.2 Modified Code Repetition

A reduction of the peaks in a multi-carrier signal by a modified code repetition (MCR) is presented in Ngajikin *et al.* (2003) for a BPSK OFDM signal. Code repetition is a basic forward error correction code, where the idea is to repeat the message several times. For example, for $k = 4$ number of repetitions, the input bit 0 produces the output $'0000'$, and with the input 1, the output will be $'1111'$. Ngajikin *et al.* (2003) used a repetition code and modified the last bit of the word (less significant bit (LSB)), by toggling up, i.e., with $k = 4$ the output will be $'1110'$ if the input is 1 and $'0001'$ if the input is 0. It is clear from Fig. 2.8 that these words dot not have the maximum PAPR.

The decoding process for a repetition code word can be run by maximum likelihood, or simply by choosing the output bit based on the majority bits in the code word (Ngajikin *et al.*, 2003).

MCR is restricted by modulation, and to a small number of subcarriers. However, MCR provides error correction, and using it with an interleaver could increase the PAPR reduction capabilities.

2.4.1.3 Complement Block Coding

In the complement block coding (CBC) PAPR reduction technique (Jiang & Zhu, 2005), a complementary sequence is added to the information sequence. If the code length K is the number of subcarriers, and we use k complement bits (CBs), where one CB is the inverse of the selected information bit (IB), the number of information bits in a block code is therefore $K-k$ (see Fig. 2.9b).

The CBC technique can provide detection and correction capabilities. Additionally, as CBC does not generate alternate or all-equal bit sequences, it reduces the PAPR of the OFDM signal.

2.4.1.4 Sub-block complementary coding

Sub-block complementary coding (SBCC) (Jiang & Zhu, 2004b) is an effective technique involving large frame sizes, since it breaks the long information sequence into several equal-sized sub-blocks, with each sub-block encoded with a complementary error correction code (see Fig. 2.9c). (Jiang & Zhu, 2004b) demonstrated that over a BPSK-OFDM system with $K = 16$ subcarriers and a code rate $R = 3/4$, the PAPR reduction is 6.03 dB when the SBCC is used.

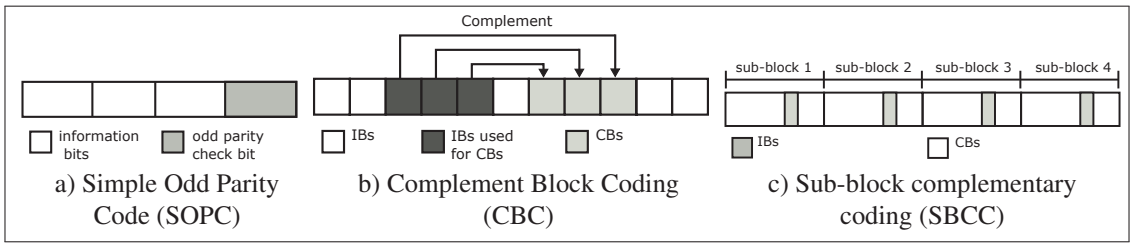

Figure 2.9 Examples of Coding-based techniques

2.4.1.5 Golay complementary sequences

Wilkinson & Jones (1995); Jiang *et al.* (2004b) used Golay complementary sequences to achieve PAPR reduction, and showed that applying these sequences can reduce the PAPR by about 3 dB. Budisin (1992) reported that the power spectrum of the Golay complementary sequences present the complementary property, and the spectrum is approximately flat. Also, Davis & Jedwab (1999) proposed error correcting codes to achieve lower PAPR by determining the connection between Golay complementary sequences and second-order Reed-Muller codes.

In addition, Nee (1996) showed the possibility of using Golay complementary codes both for error correction and PAPR reduction.

2.4.2 Multiple Signaling and Probabilistic Techniques

Multiple signaling techniques, generate a permutation of the multi-carrier signal and choose the signal with the minimum PAPR for transmission, while probabilistic techniques, modify different parameters in the OFDM signal, and optimize them to minimize the PAPR.

These techniques have the advantages of introducing no distortion in the transmitted signal and achieving significant PAPR reduction. However, they also involve certain drawbacks, such as a loss in data rate due to the transmission of several side information bits or increased complexity and transmission delay (Mahajan & Mukhare, 2012). Next, we present examples of such techniques.

2.4.2.1 Selected Mapping

Selected mapping (SLM) is an important PAPR reduction technique, which has been used extensively as it provides considerable gains. SLM was proposed for the first time by Bäuml *et al.* (1996) in 1996, and then by Muller & Huber (1997b) in 1997.

The structure of the conventional SLM technique for PAPR reduction is presented in Fig. 2.10. The input data block $\mathbf{X} = [X_0, X_1, \cdots, X_{K-1}]^T$ after a serial-to-parallel conversion is multiplied by U different phase sequences $P^u = \left[P_0^u, P_1^u, \cdots, P_{K-1}^u\right]^T$, where $P_v^u = e^{j\varphi_v^u}$ and $\varphi_v^u \in [0, 2\pi)$ for $v = 0, 1, \cdots, K-1$ and $u = 1, 2, \cdots, U$. As a result, U statistically independent sequences $\mathbf{X}^u = \left[X_1^u, X_2^u, \cdots, X_{K-1}^u\right]$, which represent the same input data block, are generated and forwarded to the IFFT operation simultaneously to produce the U independent sequences $\mathbf{x}^u = \left[x_0^u, x_1^u, \cdots, x_{K-1}^u\right]^T$. Finally, the PAPR of the $\mathbf{x}^u$ vectors are evaluated separately and the sequence $\tilde{x} = x^{\tilde{u}}$ with the lowest PAPR is selected for final serial transmission (Cho *et al.*, 2010a), as

$$\tilde{u} = \underset{u=1,2,\cdots,U}{\operatorname{argmin}} \left(\max_{k=0,1,\cdots,K-1} |x_k^u| \right). \tag{2.22}$$

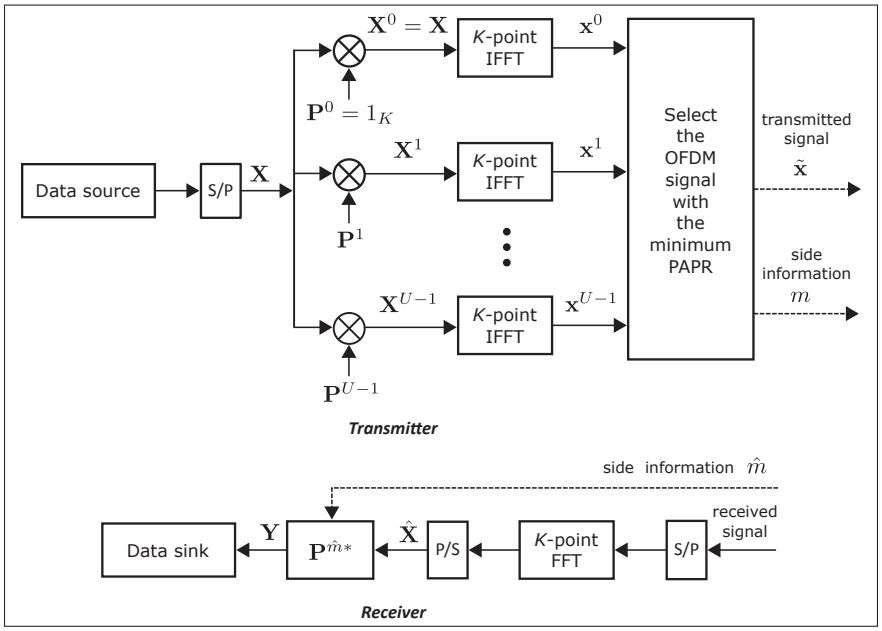

Figure 2.10 Block diagram of selected mapping technique for PAPR reduction

The conventional selected mapping technique needs to send the index u that identifies the selected phase sequence P^u as side information to allow the receiver to recover the original data block. Also, we note that U IFFT operations are needed in implementing the SLM method: for

each data block, the technique requires $\lfloor \log_2 U \rfloor$ bits of side information, where $\lfloor x \rfloor$ denotes the greatest integer less than x. In the SLM technique, the side information is very important at the receiver, and as a result, channel coding is usually used to guarantee a reliable transmission.

In recent years, most research efforts have paid particular attention to reducing the disadvantages of the conventional SLM technique. To that end, two basic approaches are currently adopted: SLM algorithms without side information (Breiling *et al.*, 2000; Jayalath & Tellambura, 2002, 2005; Vallavaraj *et al.*, 2008; Goff *et al.*, 2009; Kojima *et al.*, 2010), and SLM algorithms with low-complexity (Lim *et al.*, 2005; Heo *et al.*, 2007; Ghassemi & Gulliver, 2008; Jeon *et al.*, 2011; Ma *et al.*, 2011).

2.4.2.2 Partial Transmit Sequence (PTS)

A flexible PAPR reduction technique for the OFDM system, which combines partial transmit sequences was presented in Muller & Huber (1997b). In the PTS scheme (Fig. 2.11), the input symbol sequence $\mathbf{X}$ of K symbols is partitioned into V non-overlapping subsequences $\mathbf{X}^1, \cdots, \mathbf{X}^V$, the IFFT is applied to each symbol subsequence, and then the resulting signals are multiplied by a set of different rotation vectors $\tilde{\mathbf{b}}^1, \cdots, \tilde{\mathbf{b}}^V$. When all the signals are processed, subsequences are summed, and the PAPR is computed for each resulting subsequence. Finally, the signal sequence with the minimum peak-to-average power ratio is transmitted.

When the PTS scheme is used, the search complexity is an important parameter in the transmitter because it increases exponentially with the number of subsequences. Therefore, the selection of the rotation vectors must be limited to a set with a finite number of elements. Also, we should note that, like the SLM scheme, the classical PTS technique requires side information.

The PAPR reduction performance with PTS scheme depends on the number of subsequences, the number of rotation vectors, and finally, the method used to divide the sequences into multiple non-overlapping subsequences. Three subsequence partitioning types are available, namely, adjacent, interleaved, and pseudo-random partitioning (Muller & Huber, 1997a).

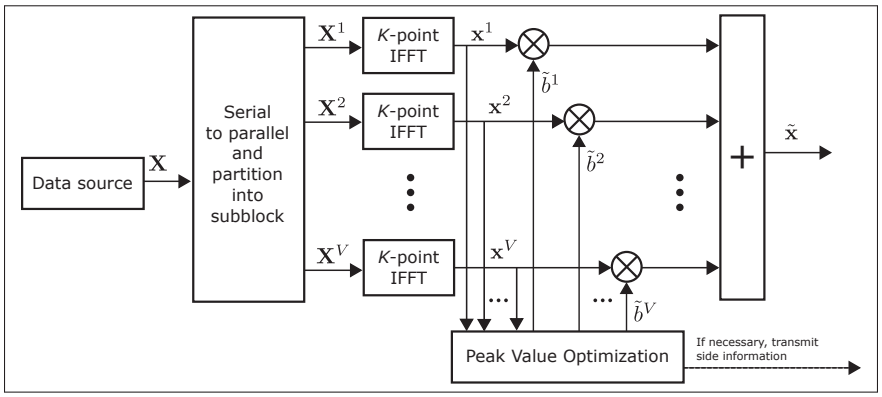

Figure 2.11 Block diagram of PTS technique for PAPR reduction (Cho *et al.*, 2010a)

2.4.2.3 Interleaving

In the interleaving technique, introduced by Jayalath & Tellambura (2000), a $K-1$ permuted sequence from the same information is generated by $K-1$ random interleaved signals. Then, the PAPR of the original information and the permuted sequences are computed using K over-sampled FFTs, and similarly to the selected mapping technique, the sequence with the lowest PAPR is chosen for transmission. The transmitter needs only transmit the information about which interleaver is used to recover the original data block at the receiver. Two interleaver types are proposed in Jayalath & Tellambura (2000), namely, random interleavers (RI) and periodic interleavers.

Although this technique is less complex than the PTS method, it however achieves comparable results, and the PAPR reduction performance depends on the number and the design of interleavers. Additionally, an interleaving block is considered on systems which use forward error correcting technique to spread the burst of errors. In tactical communication it reduces the effects of pulsed jamming (Puspitaningayu & Hendrantoro, 2014).

2.4.2.4 DFT-Spreading Technique

This is a useful technique that can achieve a similar PAPR as a single-carrier transmission. Here, the input signal is spread by a DFT, which can be following by the IFFT. Nowadays, the DFT-spreading technique is used for uplink transmissions in mobile communications. The technique, also known as the Single Carrier-FDMA (SC-FDMA) (see Fig. 2.12), has been adopted for uplink transmissions in the 3GPP LTE standard (Bruninghaus & Rohling, 1998; Galda & Rohling, 2002; Myung *et al.*, 2006b,a).

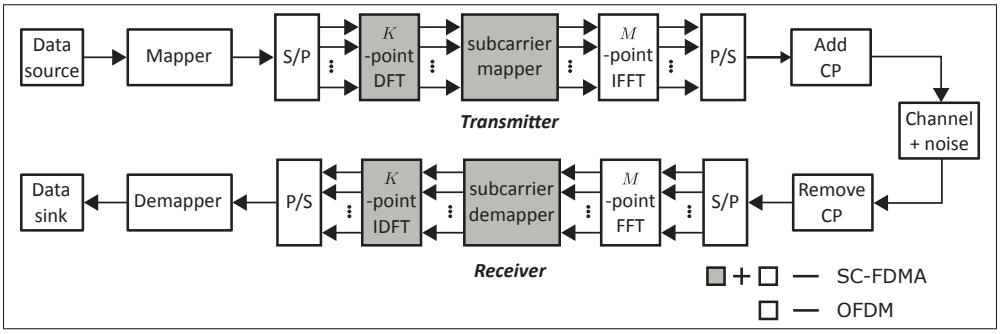

Figure 2.12 Block diagram for single carrier-FDMA (SC-FDMA) technique for PAPR reduction

While in a downlink transmission in mobile communications with an orthogonal frequency division multiple access (OFDMA) system, the subcarriers are partitioned and assigned to multiple mobile terminals (users), in uplink, each terminal uses a subset of subcarriers M to transmit its data, and the rest of the subcarriers are filled with zeros (Cho *et al.*, 2010a). Hence, an M-point DFT is used for spreading in the DFT-spreading technique, and the output of DFT is assigned to the subcarriers of the IFFT. The PAPR reduction performance of this technique depends on how the subcarriers are assigned to each terminal (Myung *et al.*, 2006b). Two options are described in the literature for apportioning subcarriers: the localized SC-FDMA (LFDMA), in which each terminal uses a set of adjacent subcarriers to transmit its symbols, and the distributed SC-FDMA (DFDMA), in which the subcarriers used by a terminal are spread over the entire signal band. When DFDMA distributes occupied subcarriers at an equidistance, it is referred to as an interleaved FDMA (IFDMA) (Myung *et al.*, 2006b).

SC-FDMA has similar overall complexity and throughput performance as OFDMA, but while the PAPR performance of IFDMA is better than that of LFDMA, LFDMA with channel-dependent scheduling does result in higher throughput.

2.4.2.5 Tone Reservation

This method partitions the K subcarriers (tones) into peak reduction tones (PRTs) and data tones (Tellado-Mourelo, 1999), i.e., it reserves a small set of subcarriers and peak reduction tones that are optimized for PAPR reduction (see Fig. 2.13). The receiver and the transmitter need to know the positions of the PRTs.

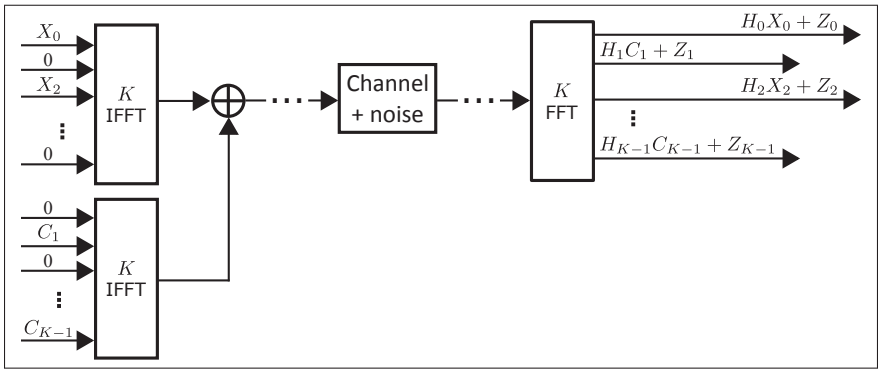

Figure 2.13 Block diagram of tone reservation technique for PAPR reduction (Cho *et al.*, 2010a)

An interesting problem to solve here is the strategy for calculating the PRTs that reduce the PAPR; to that end, Tellado-Mourelo (1999) demonstrated that this problem can be solved if it is considered as a convex problem. Tellado-Mourelo (1999) further showed that reserving a small part of subcarriers leads to a large PAPR reduction; moreover, this scheme does not require a complex algorithm in the transmitter, and there is no added complexity at the receiver. On the other hand, with the TR technique, the subcarriers reserved for the PRTs cause data rate decreases, and additional processing power is required in the transmitter. Thus, the amount of PAPR reduction seen when the tone reservation scheme is used depends on various factors,

such as the complexity that can be used, and the number of peak reduction tones and their location.

2.4.2.6 Tone Injection

A tone injection (Tellado-Mourelo, 1999) is another transformed input constellation method that can be used to reduce the PAPR without decreasing the data rate.

The TI technique expands the original constellation size into equivalent points in the larger constellation that is like to injecting a tone into the OFDM signal, with a specific frequency and phase to minimize the PAPR (see Fig. 2.14), hence the name of the technique. Although the TI technique does not decrease the data rate, as it does not use an additional subcarrier for PRTs, its method requires extra signal power to transmit the symbols due to the increased constellation size. Furthermore, the technique can add problems in the transmitter because the injected and information signals occupy the same frequency band.

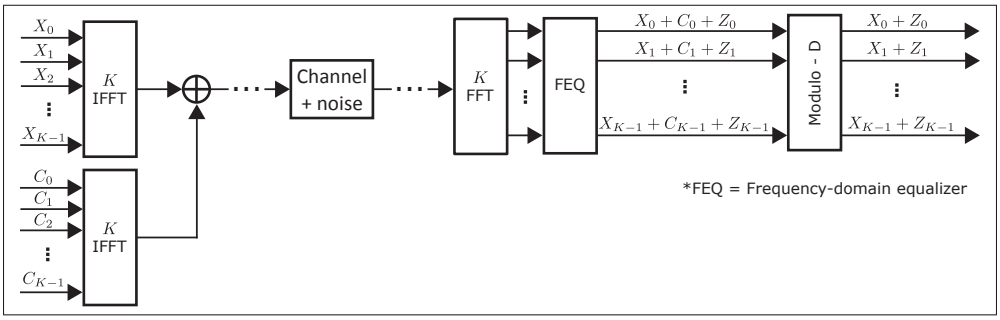

Figure 2.14 Block diagram of tone injection technique for PAPR reduction (Cho *et al.*, 2010a)

2.4.2.7 Dummy Sequence Insertion

In the dummy sequence insertion (DSI) method, suggested in Ryu *et al.* (2004), a dummy sequence is added to the input data before the IFFT stage to reduce the peaks in the OFDM signal. Originally, Ryu *et al.* (2004) proposed four methods for using a dummy sequence in this DSI method. Method 1 inserts the complementary sequence, method 2 uses a correlation

sequence as the dummy sequence. In method 3, the all-zero sequence is the dummy sequence, and the all-one sequence is the dummy sequence in method 4. In all cases, a dummy sequence is inserted before IFFT, and after the parallel-to-serial conversion, the PAPR is checked. If the PAPR is lower than a given limit, it is transmitted. Otherwise, a feedback is used to provide notification that the DSI process must be repeated using another sequence.

One advantage of the dummy sequence method is that it does not require side information as the dummy sequence is only used for peaks reduction and at the receiver, and can be discarded after the FFT operation. Hence, unlike the conventional partial transmit sequence (PTS) and selected level mapping (SLM) techniques, the DSI method does not increase the receiver system complexity, and is independent of the dummy sequence error.

The dummy sequence insertion method got better results than the PTS technique in terms of BER performance, and is more efficient in transmitting than the conventional block coding technique. However, the DSI method performs worse than the block coding and conventional PTS techniques in terms of PAPR reduction. Additionally, Ryu *et al.* (2004) proved that the DSI method 1 is better than the other methods.

2.4.3 Signal Distortion Techniques

Signal distortion techniques, such as signal clipping, peak windowing and nonlinear companding transform (NCT), reduce high peaks in the OFDM signal by distorting the signal before amplification. A major advantage of these techniques is their simplicity. Signal distortion methods do not require extra side information, but these techniques introduce both in-band and out-of-band interference and complexity.

2.4.3.1 Amplitude Clipping

Amplitude clipping (O'Neill & Lopes, 1995) is the simplest scheme for PAPR reduction, and limits the peak envelope of the input signal to a pre-specified level. The output signal of a soft

threshold can be given as:

$$B(x) = \begin{cases} x, & |x| < A \\ Ae^{j\phi(x)}, & |x| \geq A \end{cases} \tag{2.23}$$

where A represents the clipping level and $\phi(x)$ is the phase of x. While the signal distortion technique guarantees peak reduction, it does however have some drawbacks.

First, clipping causes in-band signal distortion, which produces a degradation in the bit error rate. Also, clipping the OFDM signal envelope causes out-of-band radiation, resulting in interference for the adjacent channels. Several strategies have been developed to reduce these disadvantages. For example, the out-of-band signals generated by clipping can be reduced or removed by filtering, but this can also produce peak regrowth. For this reason, to obtain an appropriate PAPR reduction, iterative clipping and filtering must be used (Anoh *et al.*, 2017). However, this adds computational complexity to the system (Armstrong, 2002; Chen & Haimovich, 2003; Li & Cimini, 1997).

2.4.3.2 Peak Windowing

In the peak windowing method, the original OFDM signal is multiplied by a correcting function (Nee & de Wild, 1998) such as Gaussian-shaped, Kaiser, Hamming or cosine window. Ideally, the correcting function frequency spectrum must be close to rectangular in the in-band frequency. Unlike amplitude clipping, peak windowing suppresses out-of-band radiation while reducing the peak signal. When the windowing technique is used, PAPR can be reduced down to about 4 dB, independent of the number of subcarriers, with a loss of SNR, caused by signal distortion, and an increase in out-of-band interference (Vijayarangan & Sukanesh, 2009).

2.4.3.3 Companding

A companding (compressing and expanding) technique was proposed by Wang *et al.* (1999a) to reduce the PAPR of the OFDM signal, based on the speech processing algorithm $\mu-$law. To implement the companding technique in the OFDM signal, the signal is companded and

quantized before being converted into an analog waveform. At the receiver, the received signal is first converted into digital form, and expanded. The result in Wang *et al.* (1999a) shows that companding is an effective method for reducing the PAPR in OFDM systems, which does not require side information, and hence does not reduce the bit rate. Also, the number of subcarriers does not affect the companding complexity. However, the quantization error for large signals is significant due to companding, which means that this technique can degrade the system BER performance.

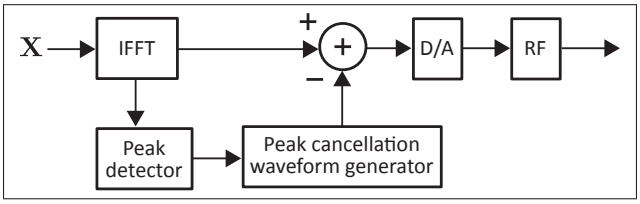

Figure 2.15 Block diagram of peak windowing technique for PAPR reduction (Rahmatallah & Mohan, 2013)

There are four classes of companding transforms, namely, linear symmetrical transform (LST), linear asymmetrical transform (LAST), nonlinear symmetrical transform (NLST) and nonlinear asymmetrical transform (NLAST) (Rahmatallah & Mohan, 2013). An example of nonlinear companding transform is presented in (Jiang & Zhu, 2004a; Jiang *et al.*, 2005), which show two different types: based on error function (Jiang & Zhu, 2004a) and based on exponential function (Jiang *et al.*, 2005). These techniques provide good system performance, including BER and PAPR reduction, no bandwidth expansion, and low implementation complexity.

2.4.4 Hybrid Techniques

In recent years, some hybrid methods have also been proposed in the literature. These schemes combine two or more methods for PAPR reduction, and can be categorized into: Coding plus Multiple Signaling and Probabilistic techniques (C+MSP), Coding plus Signal Distortion techniques (C+SD), Multiple Signaling and Probabilistic plus Signal Distortion techniques (MSP+SD), and a combination of three methods, i.e., Coding plus Multiple Signaling and

Probabilistic plus Signal Distortion techniques (C+MSP+SD). Some examples for each category are summarized in Table 2.3.

Table 2.3 PAPR Reduction Hybrid Techniques

	Coding (C)	Multiple Signaling & Probabilistic (MSP)	Signal Distortion (SD)	Ref.
C + MSP	Error-Correcting Code (ECC)	PTS		(Ghassemi & Gulliver, 2010)
	Concatenated low density parity check (LDPC) codes	PTS (low complexity)		(Joshi & Saini, 2015)
	Error control (EC) (Convolutional, Turbo or LDPC)	SLM		(Xin & Fair, 2004; Abouda, 2004) (Breiling *et al.*, 2001)
	Correction sub-code + Scrambling subcode	SLM		(Chen & Liang, 2007b)
	Binary cyclic codes	SLM (without SI)		(Chen & Liang, 2007a)
	Turbo code	SLM (without SI)		(c. Tsai *et al.*, 2008)
C + SD	FEC coding		Clipping	(Choubey & HOD, 2014)
	FEC coding		Companding	(Choubey & Jain, 2014)
MSP + SD		Interleaving	Companding	(Sakran *et al.*, 2009)
		PTS	Clipping	(Cuteanu & Isar, 2012)
		Interleaver	Peak windowing	(Sakran *et al.*, 2008)
C + MSP + SD	FEC (Modified repeat accumulate (RA))	SLM (without SI)	Clipping	(Carson & Gulliver, 2002)
	LDPC or RA encoder	SLM (without SI)	Clipping	(Yue & Wang, 2006)
	Convolutional Code	SLM	Companding	(Sharma & Verma, 2011)

Nowadays, hybrid techniques are considered a good option for PAPR reduction as they have the advantages of allowing both or more techniques to be used in hybridization, albeit with slight increases in complexity. Examples of hybrid techniques are the methods that combine a coding-based PAPR reduction scheme with MSP or SD techniques. To date, several studies have examined the combination of the coding peak-to-average power ratio reduction with other PAPR techniques, such as clipping, selected mapping and partial transmit sequence. Probabilistic methods, such as PTS and SLM, achieve significant PAPR reduction with a small data rate loss. On the other hand, coding techniques present good error control properties.

2.4.4.1 Partial Transmit Sequence Using Error-Correcting Code (PTS-ECC)

One of the main disadvantages with practically implementing a PTS scheme is the high computational complexity it involves due to the required computation of multiple IFFTs, which is proportional to the number of sub-blocks. Thus, Ghassemi & Gulliver (2010) proposed a new PTS sub-block partitioning based on error-correcting codes (ECCs). The PTS-ECC

technique presents better PAPR reduction than ordinary PTS (O-PTS), using, for example, pseudo-random sub-blocking partitions, while implementing the PTS with low complexity.

2.4.4.2 Error Control Selected Mapping (EC-SLM)

This hybrid technique, which combines coding with a multiple signaling scheme is presented in Xin & Fair (2004) for a BPSK-OFDM system. This scheme is based on Breiling *et al.* (2001), who proposed an extension of SLM (concatenated SLM) that employs a label insertion and scrambling for avoiding the transmission side information. Also, Breiling *et al.* (2001) proposed the use of error control and interleaving blocks (π) to improve the BER. The EC-SLM scheme integrates PAPR reduction with error control in OFDM systems, as can be seen in Fig. 2.16, which shows the structure of an EC-SLM transmitter and receiver. The EC-SLM does not require the transmission of side information, and uses linear block codes and convolutional or turbo codes for error correction. In contrast with the concatenated SLM scheme, EC-SLM coding eliminates error propagation, and results in superior BER performance; however, the PAPR performance of EC-SLM PAPR is slightly worse than that of the concatenated SLM scheme.

Subsequently, in Abouda (2004) the authors proposed a PAPR reduction technique using turbo coding and selected mapping. Again, they demonstrated that the (Turbo) encoder can be used for error correction and PAPR reduction, and that the turbo code improves the PAPR and BER performance as compared to an OFDM system with uncoded data, which uses SLM for PAPR reduction. Next, Chen & Liang (2007b) extended the EC-SLM technique with the use of cyclic codes with SLM for BPSK, and combining block-coded modulation (BCM) with SLM for 16-QAM OFDM.

2.4.4.3 Error Control Selected Mapping with Clipping (EC-SLM-CP)

A complete hybrid scheme with one technique of each category is given in Carson & Gulliver (2002), where a modified repeat accumulate (RA) code, selected mapping, and clipping are

combined. The RA code is a repetition code with an accumulator, followed by an interleaver (π) that generates good sequences in relation to PAPR reduction and allows an improvement of BER performance. On the other hand, the EC-SLM-CP uses the modified SLM with label insertion to avoid transmitting side information, followed by a four-stage linear-feedback shift register (LFSR), and the signal is transformed into orthogonal channels by the IFFT. Finally, in the transmitter the signal is clipped in order to reduce the PAPR. The complete block diagram of the EC-SLM-CP technique is shown in Fig. 2.17.

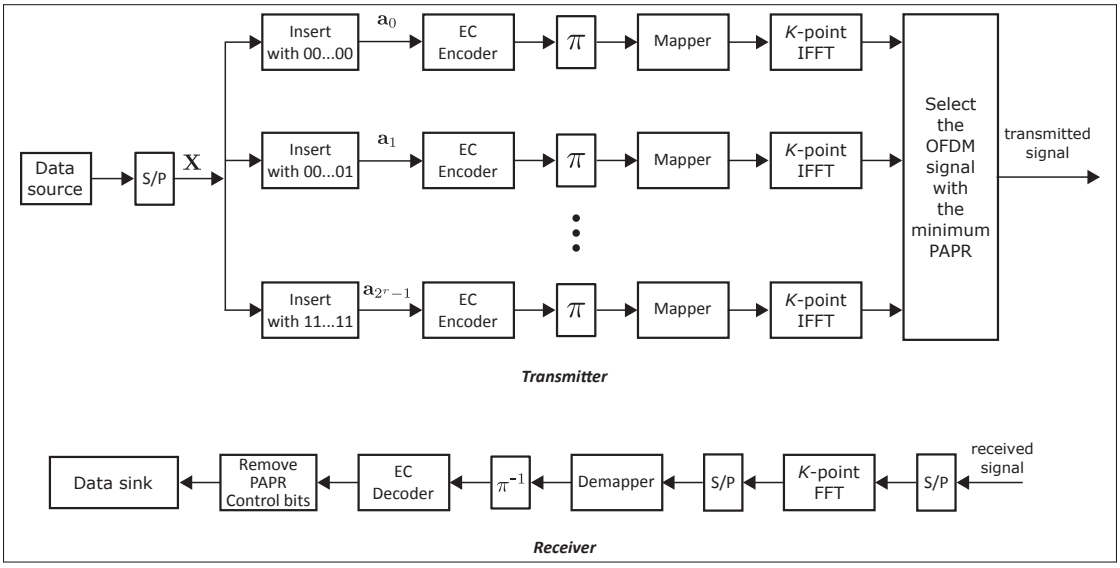

Figure 2.16 Block diagram of an EC-SLM transmitter and receiver (Xin & Fair, 2004)

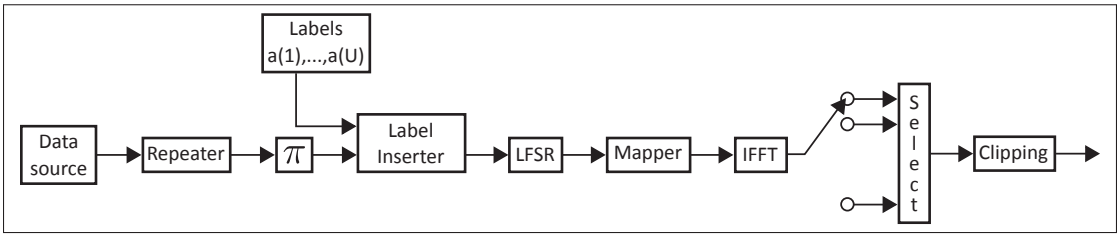

Figure 2.17 Block diagram of EC-SLM-CP technique (Carson & Gulliver, 2002)

A similar technique is applied by Yue & Wang (2006), who suggests the use of random-like codes, such as turbo codes, low-density parity-check (LDPC) codes, and modified repeat ac-

cumulate (RA) codes, combined with a modified SLM. In addition, to avoid transmitting side information, a label insertion scrambler is used, along with a soft amplitude limiter (SAL) for clipping the signal. This technique provides good PAPR reduction and, BER improvement, avoids transmitting side information, and unlike the Carson & Gulliver (2002) scheme, Yue & Wang (2006) does not need an LFSR to implement scrambling.

As has been widely discussed, when different PAPR reduction techniques are considered, all methods show advantages and disadvantages, i.e., each technique must pay a price for peak reduction. A number of authors Han & Lee (2005); Jiang & Wu (2008); Vijayarangan & Sukanesh (2009) suggest that the following important factors must be considered when choosing a specific PAPR reduction: PAPR reduction capability, power increase in transmit signal, BER increase at the receiver, loss in data rate, computational complexity, and bandwidth expansion. For instance, for the technique based on channel coding, although it reduces the PAPR and improves the BER, it produces data rate loss, and sometimes requires extra memory. SLM reduces the PAPR, but results in more computational complexity, and in a loss in data rate from the side information. Finally, the clipping technique is a simple scheme that causes in-band signal distortion and out-of-band radiation.

2.5 Modified Code Repetition, Selected Mapping and Clipping (MCR-SLM-CP)

We now propose a simple hybrid PAPR reduction scheme that combines one technique per category, such as modified code repetition (MCR), selected mapping (SLM), and clipping. This will allow us to compare the different techniques, which we will do in the following section. The structure for the individual schemes were introduced into sections 2.4.1.2, 2.4.2.1, and 2.4.3.1 for MCR, SLM, and in the clipping section, respectively. For the coding category, we use an interleaving in addition to the MCR block. Different types of interleavers are available, depending on how the bits are rearranged, and it is clear that the kind of interleaver used has an impact on the PAPR reduction achieved. In this work, a block interleaver, which writes across rows in the input and reads down columns in the output, is used. Also, the SLM tech-

nique requires side information. Fig. 2.18 shows the complete diagram for the MCR-SLM-CP transmitter.

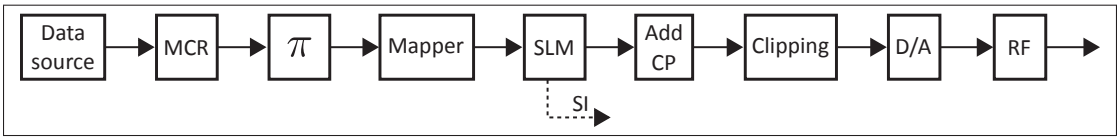

Figure 2.18 Block diagram of MCR-SLM-CP hybrid technique

2.5.1 Comparison of PAPR Reduction Techniques

We will now carry out a comparison of different PAPR reduction techniques in each category. The PAPR reduction techniques chosen to evaluate the performance are modified code repetition (MCR), selected mapping (SLM), and clipping (CP).

In the simulation, we consider an OFDM base-band signal with $K = 512$ subcarriers, a cyclic prefix length of 128 (guard interval percentage equal to 25%), a binary phase shift keying (BPSK), and an oversampling rate $L = 1$. An additive white Gaussian noise (AWGN) channel is assumed, the forward error correction block includes an MCR plus block interleaving, and the MCR decoding is implemented using majority logic detection. For the SLM technique, the rotation factor is defined as $P_v^u \in [\pm 1, \pm j]$, it can be implemented without any multiplications (Bäuml *et al.*, 1996).

As illustrated in Fig. 2.19, different curves of the complementary cumulative distribution function (CCDF) of the PAPR are given, and evaluated, for example: the conventional OFDM system without PAPR reduction (reference); the PAPR reduction schemes, namely, clipping with a clipping level equal to 70% and 50% (curves 3 and 4, respectively); the SLM scheme with 4 phase sequences (curve 2); and the MCR scheme with a code rate $R = 1/4$ (curve 5). Also, a hybrid technique is presented, i.e., the MCR-SLM-CP scheme with two variations of parameters: code rate $R = 1/4$, $U = 4$ and clipping level equal to 70% (curve 6) and code rate $R = 1/4$, $U = 8$ and clipping level equal to 50% (curve 7). The algorithm is executed $N_s = 300000$ times for conventional OFDM, CP 70%, CP 50%, and MCR ($R = 1/4$), and

$N_s = 100000$ for SLM ($U = 4$), MCR+SLM ($U = 4$)+CP 70%, and MCR+SLM ($U = 8$)+CP 50%.

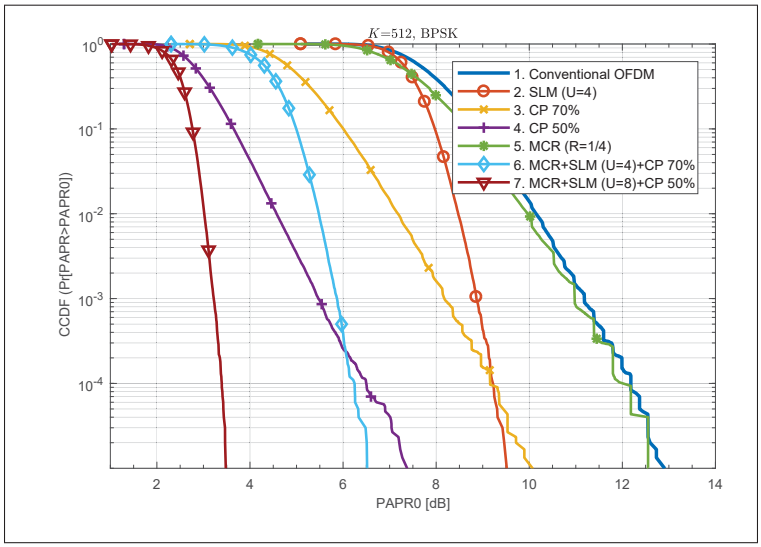

Figure 2.19 Comparisons of CCDF in OFDM-BPSK system for PAPR reduction techniques with $N_s = 3e+5$ for conventional OFDM, CP 70%, CP 50%, and MCR ($R = 1/4$), and $N_s = 1e+5$ for SLM ($U = 4$), MCR+SLM ($U = 4$)+CP 70%, and MCR+SLM ($U = 8$)+CP 50%

After analyzing these curves, it is clear that all the techniques improve the PAPR performance of a conventional OFDM system. To compare the results, we take a reference value of CCDF 10^{-4} for all cases. For instance, the SLM technique ($U = 4$) improves the PAPR performance by 2.96 dB over the conventional OFDM signal. The PAPR performance, for the clipping with clipping level equal to 70% and 50% improves the PAPR performance by 3.02 dB, and 5.68 dB, respectively. In contrast, the PAPR reduction with a coding based technique MCR (code rate $R = 1/4$) is only 0.25 dB better than the reference OFDM signal. On the other hand, the hybrid PAPR reduction technique curves 6 and 7 improve the PAPR performances by 5.93 dB, and 8.78 dB, respectively, over the conventional OFDM signal. That is, the MCR + SLM ($U = 8$) + CP (50%) technique provides the greatest reduction in the CCDF of the PAPR, while the CCDF provides the greatest reduction with clipping at 50% as compared to the three individual

schemes. However, a high percentage of clipping causes in-band signal distortion, and out-of-band radiation, resulting in bit error rate degradation and adjacent channel interference (see Fig. 2.20), respectively.

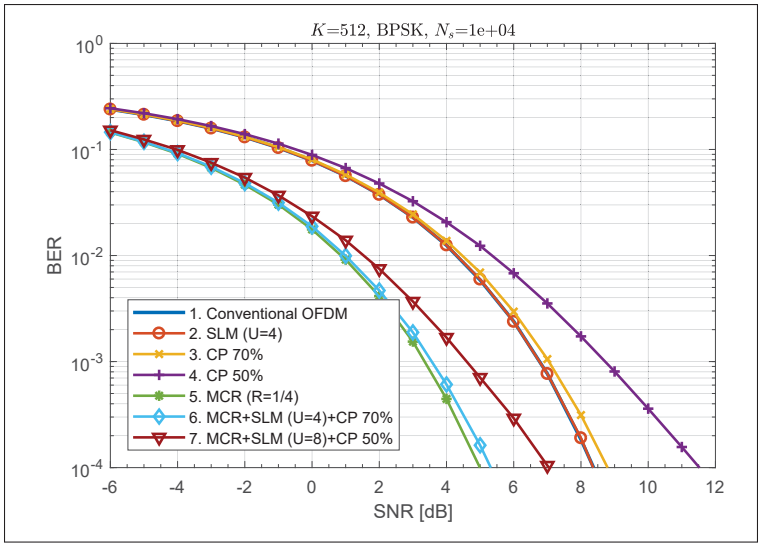

Figure 2.20 Comparisons of BER in OFDM-BPSK system for PAPR reduction techniques

Figure 2.20 shows the performance of BER versus SNR for different PAPR reduction techniques and for the conventional OFDM signal (approximately similar BER than SLM ($U = 4$), and close to CP 70 %) when the AWGN channel is considered. It is seen that using a clipping PAPR reduction technique produces a BER degradation compared to the performance bound. For example, when the performance bound is considered, the minimum SNR needed to achieve a BER of 10^{-3} is 6.8 dB. However, in the clipping PAPR reduction technique, with a 50% clipping level, an SNR of 8.6 dB is required. On the other hand, one advantage presented by MCR is the reduction of the BER given a fixed value of SNR when compare with the conventional OFDM signal. For instance, the minimum SNR required for a BER of 10^{-3} is achieved with MCR, and is equal to 3.4 dB.

The net gain defined in the equation (2.13) is calculated for all case studied.

The results for a net gain are presented in the Table 2.4. A large value for the Y_1 implies better PAPR reduction. In the same way, a large value for the Y_2 implies better performance (less BER). Additionally, three net gain have been analyzed: first, when $\alpha_1 = \alpha_2 = 0.5$, i.e., equal importance for BER improvement and PAPR reduction; second, when $\alpha_1 = 0.25$ and $\alpha_2 = 0.75$, i.e., it is more important to achieve BER improvement; and third, when $\alpha_1 = 0.75$ and $\alpha_2 = 0.25$, i.e., it is more important to achieve PAPR reduction. In the Table 2.4, the best net gain for each case (Γ_1, Γ_2 and Γ_3) is highlighted by the gray box.

When we analyzed the net gain for the different techniques in Table 2.4, we could appreciate the importance of hybrid techniques, which can combine a technique with good PAPR reduction performance and one with BER reduction to provide an improvement in both factors.

Table 2.4 Net gain of PAPR reduction techniques

PAPR Reduction Technique	Y_1	Y_2	Net Gain		
			Γ_1	Γ_2	Γ_3
	PAPR Reduction $(\text{CCDF} = 10^{-3})$	E_bN_0 Reduction $(\text{BER} = 10^{-4})$	$\alpha_1 = 0.5$ $\alpha_2 = 0.5$	$\alpha_1 = 0.25$ $\alpha_2 = 0.75$	$\alpha_1 = 0.75$ $\alpha_2 = 0.25$
2. SLM ($U = 4$)	2.60	0.00	1.30	0.65	1.95
3. Clipping 70%	3.20	-0.40	1.40	0.50	2.30
4. Clipping 50%	6.20	-3.00	1.60	-0.70	3.90
5. MCR ($R = 1/4$)	0.40	3.40	1.90	2.65	1.15
6. MCR+SLM ($U = 4$)+CP 70%	5.60	3.10	4.35	3.73	4.98
7. MCR+SLM ($U = 8$)+CP 50%	8.20	1.20	4.70	2.95	6.45

Therefore, net gain concept could be considered as a tool to define the technique to be used in a given situation, for this, we must define the priority given to each parameter, i.e. the weights of factors α_k, such as, the PAPR reduction or the degradation in BER, and is possible to add others as the computational complexity of the technique, the increase in transmit power or reduction in goodput (Rajbanshi, 2007).

2.6 Conclusion

Orthogonal frequency division multiplexing is a multi-carrier modulation technique used for both wired and wireless communications, and has a lot of applications in current communi-

cations systems. However, a major drawback of the OFDM signal is in the form of its high peaks in the envelope, which cause saturations in the power amplifier at the transmitter. PAPR reductions in OFDM systems could lead to power savings and in great improvements in range and coverage area. Meanwhile, in modern wireless communication many parameters can be changed in an OFDM system and be digitally adapted based on channel status, and traffic type to achieve improvements in PAPR reduction.

In this work, we started by studying theoretical concepts, such as the OFDM system, the PAPR problem, and the motivations for reducing the high peaks in a multi-carrier signal envelope. An extensive literature review for PAPR reduction methods was presented.

Finally, we concluded that a good strategy for reducing the PAPR an OFDM signal involves the use of a hybrid technique because such techniques can take advantage of different individual techniques, while reducing the high peaks in the signal, and can improve the BER performance.

CHAPTER 3

OPTIMIZING FORWARD ERROR CORRECTION CODES FOR COFDM WITH REDUCED PAPR

Francisco Sandoval[1,3], Gwenael Poitau[2], François Gagnon[3]

[1] Departamento de Ciencias de la Computación y Electrónica, Universidad Técnica Particular de Loja, Loja, 11-01-608, Ecuador
[2] Chief Technology Officer, Ultra Electronics, TCS, Montreal, QC H4T IV7, Canada
[3] Departament of Electrical Engineering, École de Technologie Supérieure, 1100 Notre-Dame West, Montréal, Quebec, Canada H3C 1K3

Paper published in *IEEE Transactions on Communications*, April 2019

Abstract

Coded orthogonal frequency division multiplexing (COFDM) is a popular modulation technique for wireless communication that guarantees reliable transmission of data over noisy wireless channels. However, a major disadvantage in implementing it is its resulting high peak to average power ratio (PAPR). Including forward error correction (FEC) in the orthogonal frequency division multiplexing (OFDM) system enables the avoidance of transmission errors. Nevertheless, the selected code may impact the value of PAPR. The objective of this paper is to analyze the impact of FEC on the PAPR for the COFDM system based on the autocorrelation of the signal, before the inverse fast Fourier transform (IFFT) block in the COFDM system, the evaluation of the complementary cumulative distribution function (CCDF) of PAPR, and the bit error rate (BER). The autocorrelation of the COFDM system is calculated based on a Markov Chain Model. From the results, we can reach a conclusion on the characteristics we need to consider in order to choose the codes relating to the PAPR performance in the COFDM system.

Keywords

Autocorrelation, coded OFDM, complementary cumulative distribution function, peak to average power ratio.

3.1 Introduction

Orthogonal frequency division multiplexing (OFDM) offers high spectrum efficiency and capacity, is flexible (Hwang *et al.*, 2009), and is a popular modulation technique for wireless digital communication systems such as 4G wireless communication systems, public safety systems, tactical communication systems, etc. Examples of such systems include IEEE 802.11 a/g/n/ac wireless LANs, Digital Audio Broadcasting (DAB), and Digital Video Broadcasting-Terrestrial (DVB-T).

The main implementation drawback of OFDM, however, is the high peak to average power ratio (PAPR) it produces (Han & Lee, 2005). When a significant PAPR appears in the transmitter, we require a power amplifier with wide dynamic range that is not power-efficient, and is expensive (Rahmatallah & Mohan, 2013). Therefore, many techniques have been proposed in the literature to reduce the PAPR (Sandoval *et al.*, 2017), including selected mapping (SLM), partial transmit sequence (PTS), signal clipping and filtering.

Interestingly, in the literature, coding techniques such as block codes, Golay complementary sequences, and second-order Reed-Muller codes (Rahmatallah & Mohan, 2013) are also used to reduce the PAPR. This suggests a possibility of using coding techniques to obtain both benefits, error control and PAPR reduction.

For example, Wilkinson & Jones (1995) proposed PAPR reduction using a simple odd parity code (SOPC) which is based on a four-carrier signal with a 3/4 rate block code demonstrated that the PAPR could be reduced from 6.02 dB to 2.48 dB in the case of 4 bits, 3 bits could be used for data transmission and one for the odd parity check. Wilkinson & Jones (1995) and Jiang *et al.* (2004b) proposed the use of Golay complementary sequences to achieve the

reduction of PAPR because the power spectrum of the Golay complementary sequences is approximately flat (Budisin, 1992). Another technique suggested for PAPR reduction is the complement block coding (CBC) (Jiang & Zhu, 2005). The CBC is a code with detection and correction capabilities. The CBC can contribute in the reduction of the PAPR in the OFDM signal because it does not generate all-equal bit sequences. In the case of large frame size, the sub-block complementary coding (SBCC) (Jiang & Zhu, 2004b) can be used. In SBCC, the information sequence is broken into several equal-sized sub-blocks, and each sub-block is encoded with a complementary error correction code.

This paper analyzes the impact of FEC on the PAPR for the COFDM system. As will be shown later, several of the FEC, frequently used in the current communication systems, caused degradation of the PAPR compared to the OFDM system. To that end, we conducted an analysis comparing the CCDF of PAPR to the autocorrelation of the COFDM signal before the inverse fast Fourier transform (IFFT) block. This allowed us to deduce the principal coding characteristics that generate the peak factor after the IFFT block, following which we could then choose the parameters of the coded structure in order to reduce the peak power. The analysis for convolutional codes of this study is emphasized; as well as a simple example of the linear block codes which is studied, based on the repetition codes.

Convolutional codes are widely used in current communication systems, for example, these are present in the audiovisual systems that require error correction in real time such as Digital Video Broadcasting by Satellite (DVB-S), and Digital Video Broadcasting-Terrestrial (DVB-T). Moreover, the convolutional codes are the FEC codes for tactical communication such as Wideband Network Waveform (WNW) (Oguntade, 2010). However, according to the knowledge of the authors, there is no extensive analysis of the choice of the convolutional codes parameters in relation to PAPR optimization.

PAPR reduction techniques based on codes such as SOPC, CBC, SBCC, and Golay Codes, are outside of the analysis made in this work and their comparisons with the formulation presented in this document is open for future work.

This paper is divided into five sections, including this introduction. Section 3.2 presents the Forward Error Correction (FEC) theory, the COFDM system model, the PAPR problem in a multicarrier system, and describes the distribution of PAPR for the COFDM system. Section 3.3 analyzes the autocorrelation characteristics of the COFDM based on a Markov Chain Model, and its relation to the peak factor of the COFDM signal. Additionally, this section introduces an upper bound on the peak factor of the COFDM signal, and its discussion for linear block codes and convolutional codes. The analysis of PAPR degradation in COFDM systems is reviewed in Section 3.4. Two cases are studied: the repetition code in Section 3.4.1 and the convolutional codes based on the study of four important parameters: the code rate, the code structure, the maximum free distance, and the constraint length, in Section 3.4.2. The net gain concept is used in Section 3.5 to define the optimal convolutional code as a means to avoid an increase in the PAPR. In addition, the decoder complexity is discussed in Section 3.5.1. The final section concludes the work.

3.2 Background

3.2.1 Forward Error Correction

Mobile channels are very hostile environments characterized by the presence of several noise sources such as white noise, impulse noise, echo, attenuation, intermodulation noise, and phase jitter. However, the real systems can be resolved successfully thanks to the inclusion in the systems of techniques such as the error control that permits robust transmission of data.

Forward error correction (FEC) is an error control method for data transmission where the transmitter adds redundant data to its messages with the objective of detecting and correcting errors without the need to re-transmit additional data. There are two main categories of FEC codes, depending on how redundancy is added, namely block codes and convolutional codes (Jiang, 2010).

3.2.1.1 Block Codes

To construct a block code, we started by splitting the information sequence (for binary digits we have a binary block code) into 2^k message blocks of fixed length, with k information digits. The encoder mapped each input message into a coded word sequence of length η, where $\eta > k$. Hence, there were 2^k code words, and the rate of the code was k/η.

A linear block code $\mathscr{C}$ consists of a set of M code words (vectors) of length η denoted by $\mathbf{c}_m = (c_{m1}, c_{m2}, \cdots, c_{m\eta})$, $1 \leq m \leq M$, where for any two code words $\mathbf{c}_1$, $\mathbf{c}_2 \in \mathscr{C}$, we have $\mathbf{c}_1 + \mathbf{c}_2 \in \mathscr{C}$ (Proakis & Salehi, 2008).

In a linear block code, the transformation from information sequences, represented by a binary vector $\mathbf{u}_m$ of length k, to code words $\mathbf{c}_m$, can be given in matrix form by:

$$\mathbf{c}_m = \mathbf{u}_m \mathbf{G},\ 1 \leq m \leq 2^k, \tag{3.1}$$

where the matrix $\mathbf{G}$ of dimension $k \times \eta$ is the generation matrix. If a generation matrix of a linear block code is in the form of:

$$\mathbf{G} = [\mathbf{I}_k | \mathbf{P}], \tag{3.2}$$

we have systematic coding. In equation (3.2), $\mathbf{I}_k$ represents a $k \times k$ identity matrix and $\mathbf{P}$ is the parity matrix of dimension $k \times (\eta - k)$ (Proakis & Salehi, 2008).

Examples of block error correction codes are Repetition Codes, Hamming Codes, Reed-Solomon (RS) Codes, Bose-Chaudhuri-Hocquenghem (BCH) Codes, Golay Codes, and Low-Density Parity Check (LDPC) Codes.

3.2.1.2 Convolutional Codes

Unlike the block code, the convolutional code (CC) contains memory, i.e., the encoder output depends on the current and the previous input bits, Hence, a convolutional code can be easily implemented using a linear finite state shift register, and it can be characterized by three param-

eters (η, k, V), where η represents the code word length, k the input length, and the constraint length V is given by the number of bits stored in each shift register, plus the current input bits. So, similar to linear block codes, the code rate is given by k/η.

Although coding a convolutional code is a simple task, its decoding is much more complex. There are several proposed algorithms for decoding and one of the most known is the Viterbi algorithm (VA) which is an optimal algorithm (maximum-likelihood).

The VA calculates the distance (measure of similarity) between the received signal and all the trellis paths entering each state at a specific time. The Viterbi algorithm removes the trellis paths that can not be used by candidates for the maximum likelihood choice (Sklar, 2001). To remove, the VA, it chooses the path with the minimum metric between two paths that enter the same state, the path chosen is called surviving path (Sklar, 2001). The selection of surviving paths is made for all states.

There are two approaches to perform decoding namely hard decision decoding that receives a simple bitstream on its input, and the soft decision decoding (Proakis & Salehi, 2008).

The implementation of the VA consists of three main parts: the branch metric (BM) calculation, the path metric (PM) calculation, and the trace back (TB) operation. The branch metric is a measurement of the distance between the information transmitted and received. In the case of a hard decision decoding, the BM is the Hamming distance between the expected parity bits and the received ones. For a soft decision decoder, a BM is measured using the Euclidean distance. The PM is the sum of metrics of all branches in the path. For every encoder state, the path metric calculation calculates a metric for the survivor path ending in this state. Meanwhile, trace back is an operation used for hardware implementations that allows for the reduction of the information that must be stored in respect of the survivor's paths.

3.2.2 COFDM System Model

OFDM is a digital multiplexing and modulation technique that can be easily implemented due to the IFFT. If we consider N IFFT points, $\{X[l]\}_{l=0}^{N-1}$ represents the frequency-domain signal, where l is the frequency index. The discrete-time baseband OFDM signal $x[n]$ after applying IFFT is given by

$$x[n] = \frac{1}{\sqrt{N}} \sum_{l=0}^{N-1} X[l] e^{\mathrm{j}2\pi \frac{ln}{\mathscr{L}N}},\ n = 0, 1, \ldots, \mathscr{L}N - 1, \tag{3.3}$$

where n denotes the discrete-time index, j is the imaginary unit, and $\mathscr{L}$ is the oversampling rate.

The typical COFDM transmitter and receiver are presented in Fig. 3.1. First, the input information source is transformed into a sequence of channel symbols (code symbols) by the FEC coding block where one block code or convolutional code method can be used. Generally, on fading channels, the channel coding is combined with an interleaving block to mitigate the effect of error bursts (Goldsmith, 2004, pg. 267). The bit interleaver block reorders the code symbols aiming at spreading out the burst errors. There are two main forms of interleaver: a block structure or a convolutional structure (Proakis & Salehi, 2008). Next, the interleaver symbols or code symbols (when bit interleaver is not used) are mapped using a phase shift keying (PSK) or quadrature amplitude modulation (QAM). To generate the OFDM symbol, the input signal is serial-to-parallel (S/P) converter followed by an inverse fast Fourier transformer (IFFT). The OFDM symbol is parallel-to-serial (P/S) converter, a cyclic prefix (CP) of length N_{cp} is added, and the output is processed by the digital-to-analog (D/A) converter. Finally, the signal is prepared by the RF components to be transmitted through for the channel. At the receiver's end, the reverse process is performed.

3.2.3 PAPR Problem

A high peak to average power ratio (PAPR) can appear in the discrete-time OFDM signal when the N independent data symbols modulated on the N orthogonal subcarriers are added to the

same phase. The PAPR in terms of discrete-time baseband OFDM signal can be written as:

$$\mathrm{PAPR}(x[n]) \triangleq \frac{\max\limits_{0\le n\le N-1} |x[n]|^2}{\frac{1}{N}\sum\limits_{n=0}^{N-1} |x[n]|^2}. \tag{3.4}$$

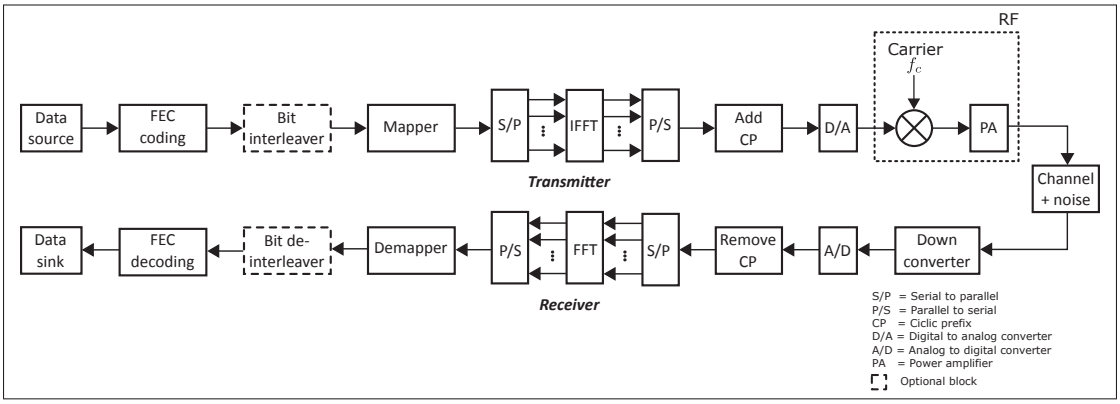

Figure 3.1 Block diagram of transmitter and receiver in a coded OFDM system

3.2.4 Net gain

In order to determine an appropriate FEC code to avoid increasing the PAPR, it is important to consider a global gain (net gain) in the system. In this work, the net gain is defined as a particular case of the fitness function-based approach (Rajbanshi, 2007), where two factors of interest are considered: the PAPR reduction and the BER performance. Hence, under given channel conditions (AWGN or multi-path), the relative PAPR reduction can be written as:

$$Y_1 = -10\log_{10}\left(\frac{\mathrm{PAPR}_{\mathrm{after}}}{\mathrm{PAPR}_{\mathrm{before}}}\right), \tag{3.5}$$

and if we consider a certain signal to noise ratio (SNR) level, the relative degradation in BER performance is given by

$$Y_2 = -10\log_{10}\left(\frac{\mathrm{BER}_{\mathrm{after}}}{\mathrm{BER}_{\mathrm{before}}}\right). \tag{3.6}$$

So, if α_u represents the weights of factors related to the significance level of PAPR reduction ($u = 1$), and BER ($u = 2$) in the system, the aggregate fitness value is (Sandoval *et al.*, 2017)

$$\Gamma = \sum_{u=1}^{2} \alpha_u \cdot Y_u, \tag{3.7}$$

where

$$\sum_{u=1}^{2} \alpha_u = 1, \tag{3.8}$$

3.2.5 Distribution of the PARP for COFDM Signal

The complementary cumulative distribution function (CCDF) of PAPR represents the probability that the peak to average power ratio of the OFDM signal exceeds a given threshold γ (also represented by PAPR0), i.e. $\Pr(\text{PAPR} > \gamma)$. The CCDF is an important performance measure for evaluating PAPR reduction techniques, and we can use it to determine an appropriate value for the output back-off of a high power amplifier (HPA) (Jiang & Wu, 2008).

A widely used simple approximation of the CCDF, is obtained based on the central limit theorem. Considering this principle, the real and imaginary parts of the time domain signal follow a Gaussian distribution with zero as the mean and a variance equal to 0.5 (Han & Lee, 2005). Therefore, in this case, the amplitude and power of the OFDM signal can be represented by a Rayleigh and chi-square distribution, respectively (Han & Lee, 2005).

On the other hand, in Jiang & Wu (2008), the extremal value theory of Gaussian random processes is used to achieve an accurate approximation for the CCDF of a bandlimited uncoded OFDM signal equal to:

$$\Pr(\text{PAPR} > \gamma) \cong 1 - \exp\left\{-Ne^{-\gamma}\sqrt{\frac{\pi}{3}\log N}\right\}. \tag{3.9}$$

In a practical implementation of the OFDM system there are three types of subcarriers namely data, pilot and null subcarriers. These subcarriers are allocated with unequal transmission

power in order to make efficient use of limited power (Jiang *et al.*, 2008). Based on that, more sophisticated CCDF expression derived by the aid of the Extreme Value Theory for Chi-squared-2 process for adaptive OFDM systems with unequal power allocation to subcarriers is given by Jiang & Wu (2008) as

$$\Pr(\text{PAPR} > \gamma) \approx 1 - \exp\left\{ -2e^{-\gamma} \sqrt{\frac{\pi\gamma \sum_{l=-L}^{L} l^2 \sigma_l^2}{\sum_{l=-L}^{L} \sigma_l^2}} \right\} \tag{3.10}$$

where σ_l^2 denotes the transmission power allocated to the l-th subcarrier, $L = N_{\text{active}}/2$ if the subcarrier at DC is inactive; otherwise $L = (N_{\text{active}} - 1)/2$ if the DC subcarrier is active, N_{active} represents the active subcarriers (data subcarriers and pilot subcarriers), N_{inactive} corresponds to the inactive subcarriers (null subcarriers). Hence, the total number of subcarriers is $N = N_{\text{active}} + N_{\text{inactive}}$.

As highlighted by Jiang *et al.* (2008) the PAPR distribution in OFDM systems is strongly impacted by the transmission power allocation. The expression in (3.10) is a general PAPR distribution and is valid for both cases where it is assumed that equal power is allocated to active subcarriers, and for the case with unequal power allocation to each subcarriers. In the first case with equal power allocated to the active subcarriers, $\sigma_l^2 = \rho P_{\text{av}}$, where $0 \leq \rho \leq N/N_{\text{active}}$, and P_{av} is the average power of the OFDM signal. Throughout this work, we assume equal power allocation to each active subcarrier to be $\rho = 1$.

Additionally, Jiang & Wu (2008) considered the COFDM signal restricted to the case of codes that can be represented as uncorrected, and we demonstrated that the distribution of PAPR can be modeled by (3.9). The uncorrelated condition for forward error correction codes is met for many of the currently used codes, including, for instance, block codes (except repetition codes, and low rate codes (Wilson, 1995, pg. 527)), some convolutional codes, and turbo codes.

The question, therefore, is whether it possible to establish the behavior of PAPR distribution in the case where uncorrelated codes are used. We discuss this important question below, based on the relation between the autocorrelation and the maximum PAPR of the COFDM.

3.3 Autocorrelation Characteristics of COFDM Signal

In this section, we present a study about the autocorrelation before the IFFT block in an uncoded and in a coded OFDM system, and its relation to the CCDF of PAPR. In the case of COFDM, we propose that the Markov Chain Model is used, as given in Mannerkoski & Koivunen (2000), to calculate the autocorrelation function of the coded sequence, and we analyze some characteristics of the forward error correction codes that affect the PAPR.

3.3.1 Autocorrelation characteristics of uncoded OFDM signal

In an uncoded OFDM signal, the autocorrelation function for the frequency-domain signal, $X[l]$, is defined by:

$$\rho[l] = \sum_{n=1}^{N-l} X[n+l] \cdot X^*[n] \quad \text{for } l = 0, \cdots, N-1. \tag{3.11}$$

An interesting relationship that depends only on the data sequence is highlighted in Tellambura (1997), between the autocorrelation of the IFFT input and the maximum PAPR of the uncoded OFDM signal, and can be given by:

$$\text{PAPR} \leq \Lambda = 1 + \frac{2}{N} \sum_{l=1}^{N-1} |\rho[l]|, \tag{3.12}$$

which describes an upper bound on the peak factor of the uncoded OFDM signal and provides a good approximation. Note that, based on (3.12), for the PAPR of the OFDM signal to be small, the values of the autocorrelation coefficients of the input sequences be small as well (Ermolova & Vainikainen, 2003). Therefore, this is not a necessary condition (Er-

molova & Vainikainen, 2003). To compare the CCDF of PAPR of different OFDM signals, the autocorrelation can thus not be the only metric.

3.3.2 Markov Chain model for autocorrelation of coded OFDM

The analytical expression for the autocorrelation function of typical code words with length η can be calculated based on a Markov Chain Model (Mannerkoski & Koivunen, 2000; Bilardi *et al.*, 1983). Let s_i be the state at time t, and s_j, the state at the next time $t+1$ with $i = 0, \cdots, K-1$, and $j = 0, \cdots, K-1$. Each state s_i has an associated output code word vector $\mathbf{c}_i = [c_i(0), \cdots, c_i(\eta-1)]$. We assume a *Mealy machine*; also known as a *finite-state synchronous sequential machine*, i.e., the output code word is a function of the current state only (Mannerkoski & Koivunen, 2000). This represents a general assumption, and as will be shown in the following sections, multiple forward error correction codes can be represented by this model, both linear block codes such as repetition codes, systematic Hamming codes, and Reed-Solomon (RS) codes; as well as convolutional codes. Then, the complete statistics of the stationary processes are given by the transition probability matrix, $\mathbf{\Pi} \triangleq [p_{ij}]_{K\times K}$, where p_{ij} are the probabilities of the transition from state s_i to state s_j. Additionally, we can define the state correlation matrix by the expression:

$$\mathbf{R}(k) = \begin{cases} \mathbf{D}\mathbf{\Pi}^k, & k \geq 0 \\ (\mathbf{\Pi}^H)^{-k}\mathbf{D}, & k < 0 \end{cases}, \tag{3.13}$$

where the powers of $\mathbf{\Pi}^k$ are the $k-$step transition probability matrix. In equation (3.13), $\mathbf{D} = \text{diag}(p_0, \cdots, p_{K-1})$ is a diagonal matrix, where p_i for $i = 0, \cdots, K-1$ represents the steady-state probabilities of states s_i, and we can summarize these probabilities in the vector $\mathbf{p} = [p_0, \cdots, p_{K-1}]$. Another important matrix for which we need to define the autocorrelation is:

$$\mathbf{C} = \begin{bmatrix} c_0(0) & \cdots & c_0(\eta-1) \\ \vdots & \ddots & \vdots \\ c_{K-1}(0) & \cdots & c_{K-1}(\eta-1) \end{bmatrix}, \tag{3.14}$$

that has the K code words $\mathbf{c}_i$ corresponding to the K states s_i.

The discrete autocorrelation function of the coded sequence can be defined when we know the state transition matrix and all the possible code words and is given by Mannerkoski & Koivunen (2000):

$$\rho[j] = \sum_k \sum_i \mathbf{c}^H(i)\mathbf{R}(k)\mathbf{c}(i+j-\eta k) \tag{3.15}$$

where $0 \leq i \leq \eta - 1 \cap 0 \leq i+j-\eta k \leq \eta - 1$ describes the ranges of i and k. In equation (3.15), $\mathbf{c}(i) = [c_0(i), \cdots, c_{K-1}(i)]^T$ is a column vector of the matrix $\mathbf{C}$, and $\mathbf{R}(k)$ represents the state correlation matrix defined in (3.13).

3.3.3 Upper bound on peak factor of coded OFDM signal analysis

In Section 3.3.1, we present an upper bound on the peak factor of the OFDM signal. Next, in Section 3.3.2, we describe a method for computing the autocorrelation function of a coded OFDM sequence. If we substitute (3.15) into (3.12), we can define an upper bound on the peak factor of a coded OFDM signal, and some characteristics that may limit the increase of PAPR in a coded OFDM system can be established.

We then study a particular case in relation to the FEC code used in the OFDM system, first, with a linear block code, and next with a convolutional code.

3.3.3.1 Linear block code

In the case of linear block codes, the Markov model is simple because, if we consider an $L-$ary code, all the transition probability from state s_i to state s_j are equal to $1/K$, where $K = L^M$ represents the number of states; i.e., the transition probability matrix can be given by (Mannerkoski & Koivunen, 2000):

$$\mathbf{\Pi} = \begin{bmatrix} 1/K & \cdots & 1/K \\ \vdots & \ddots & \vdots \\ 1/K & \cdots & 1/K \end{bmatrix}, \tag{3.16}$$

Moreover, the steady-state probabilities $p_i = 1/K$ for all $i = 0, \cdots, K-1$. Hence, the diagonal matrix $\mathbf{D}$ is computed as (Mannerkoski & Koivunen, 2000):

$$\mathbf{D} = \text{diag}(1/K, \cdots, 1/K). \tag{3.17}$$

So, the state correlation matrix is reduced to (Mannerkoski & Koivunen, 2000):

$$\mathbf{R}(k) = \begin{cases} \mathbf{D}, & k = 0 \\ \mathbf{D\Pi}, & \text{otherwise} \end{cases}. \tag{3.18}$$

Finally, we can find the autocorrelation function of an encoded OFDM signal from (3.15). By replacing the values and simplifying (3.15), we get the following result:

$$\rho[j] = \begin{cases} \dfrac{1}{K} \cdot \displaystyle\sum_i \mathbf{c}^H(i) \cdot \mathbf{c}(i+j), & k = 0 \\ \dfrac{1}{K^2} \cdot \displaystyle\sum_k \sum_i \mathbf{c}^H(i) \cdot \mathbf{c}(i+j-\eta k), & \text{otherwise} \end{cases}, \tag{3.19}$$

Hence, when the number of states or code words K increases, the autocorrelation $\rho[j]$ decreases, and this can have an impact on the PAPR bound expressed in (3.12).

The autocorrelation functions for some examples of linear block codes are presented by Mannerkoski and Koivunen in Mannerkoski & Koivunen (2000), for instance, a systematic Hamming code with generation matrix $\mathbf{G} = [\mathbf{I}_4|\mathbf{P}]$, where the parity matrix is defined by

$$\mathbf{P} = \begin{bmatrix} 1 & 0 & 1 \\ 1 & 1 & 1 \\ 1 & 1 & 0 \\ 0 & 1 & 1 \end{bmatrix}, \tag{3.20}$$

is considered. In this case, the number of states and code words is equal to $K = 2^4$, and Mannerkoski & Koivunen (2000) demonstrated that the absolute value of the analytical $\rho[j]$ (equation (3.15)) of the encoded sequence is equal to the Dirac delta function $\delta(j)$, i.e., we

have whiteness autocorrelation. However, there are other linear block codes where $\rho[j]$ is not perfectly white (Mannerkoski & Koivunen, 2000), and codes with colored autocorrelation, such as repetition codes (Mannerkoski & Koivunen, 2000), are present.

Repetition is a simple solution introduced in coding theory, where the idea is to repeat the message η times for transmission. For example, in the case of $\eta = 4$, the generation matrix is given by $\mathbf{G} = [1\ 1\ 1\ 1]$, and there are two states s_0 and s_1 associated to the symbols 0 and 1, i.e, $K = 2$ and $\mathbf{\Pi}$ is a (2×2) matrix with all elements equal to $1/2$. Therefore, the column vector of the matrix $\mathbf{C}$ is $\mathbf{c}(i) = [-1\ 1]^T$ for all i, where $i = 0, ..., 3$, i.e., $\mathbf{C}$ is a matrix of dimension (2×4). The autocorrelation $\rho[j]$ can be computed by (3.15) and is presented in Fig. 3.2a, where it is possible to see that the repetition encoded sequence has colored autocorrelation. Additionally, the case is considered when $\eta = 8$. In this case, $\mathbf{C}$ is a matrix of (8×2) with the same columns given by $\mathbf{c}(i) = [-1\ 1]^T$ for $i = 0, ..., 7$, and the state correlation matrix $\mathbf{\Pi}$ is equal to that in the case of $\eta = 4$. The autocorrelation is given in Fig. 3.2b, and in this is intuitively clear that there is an increase in the autocorrelation when η increases.

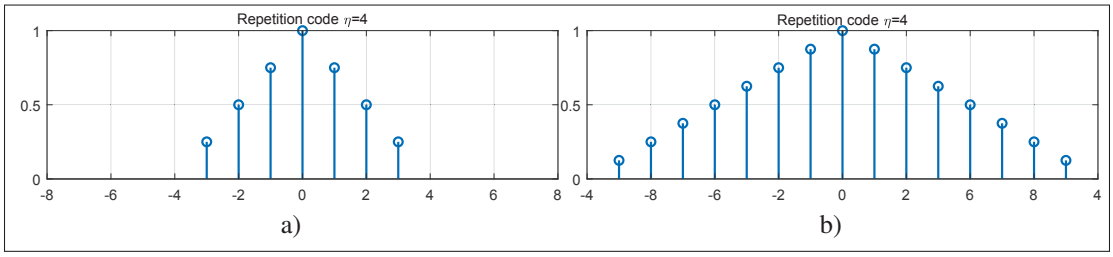

Figure 3.2 (a) Autocorrelation of repetition code with $\eta = 4$, (b) Autocorrelation of repetition code with $\eta = 8$

Note that BPSK modulation has been used in the example of repetition code to find the matrix $\mathbf{C}$. BPSK is considered here to simplify the calculations, but under a similar procedure high modulations can be included in the demonstration. Besides, when mapper operation is considered in the $\mathbf{C}$ matrix, the autocorrelation of the coded sequence calculated by (3.15) corresponds to the autocorrelation before the IFFT block in the COFDM system in Fig. 3.1;

therefore, the calculated autocorrelation value allows finding the upper bound on the peak factor of the coded OFDM when (3.12) is used.

Another interesting example presented in Mannerkoski & Koivunen (2000) analyzes the Reed-Solomon (RS) Codes case, where it is important to highlight the large value for the number of code words and K states. For instance, with a $\eta = 7$, $M = 3$, and 8-QAM RS-code there are a total of $K = 8^3$, and for a $\eta = 15$, $M = 5$, and 16-QAM RS-code, there are $K = 16^5$ code words and states (Mannerkoski & Koivunen, 2000). Therefore, when this large value of K is considered in the inverse relation presented in (3.19) between the autocorrelation and the number of code words and states, it is clear that the value of autocorrelation tends to white.

3.3.3.2 Convolutional Code

Consider the convolutional encoder $(2,1,3)$ with generators given in octal form equal to $[7,5]$ (see Fig. 3.3a); thus, the code rate is $R = k/\eta = 1/2$, and the state diagram has $2^{k(V-1)}$ possible states (see Fig. 3.3b). On the other hand, the states of the Markov chair are defined by the register contents (Mannerkoski & Koivunen, 2000). So, there are $K = 2^3$ possible states of the Markov chair, and 2^3 possible code words. Hence, the transition probability matrix is given by:

$$\mathbf{\Pi} = \begin{bmatrix} 1/2 & 0 & 0 & 0 & 1/2 & 0 & 0 & 0 \\ 1/2 & 0 & 0 & 0 & 1/2 & 0 & 0 & 0 \\ 0 & 1/2 & 0 & 0 & 0 & 1/2 & 0 & 0 \\ 0 & 1/2 & 0 & 0 & 0 & 1/2 & 0 & 0 \\ 0 & 0 & 1/2 & 0 & 0 & 0 & 1/2 & 0 \\ 0 & 0 & 1/2 & 0 & 0 & 0 & 1/2 & 0 \\ 0 & 0 & 0 & 1/2 & 0 & 0 & 0 & 1/2 \\ 0 & 0 & 0 & 1/2 & 0 & 0 & 0 & 1/2 \end{bmatrix}, \tag{3.21}$$

All states and the register content possibilities are presented in Table 3.1. Unlike the linear block code in Section 3.3.3.1, when convolutional codes are used, the state transition matrix is not identical and the result is not general (Mannerkoski & Koivunen, 2000). Moreover, we need the code word matrix $\mathbf{C}$ for the $(2,1,3)$ convolutional code, which can be created based on the output of the convolutional encoder presented in the third column of Table 3.1 for each state. The elements of the code word matrix are presented in the fourth column of the Table 3.1

and results of changing the output code words (third column) to obtain a zero-mean sequence in the output of the convolutional encoder (Mannerkoski & Koivunen, 2000), i.e., we change 0 by -1 and 1 by $+1$ (BPSK modulation, for simplicity).

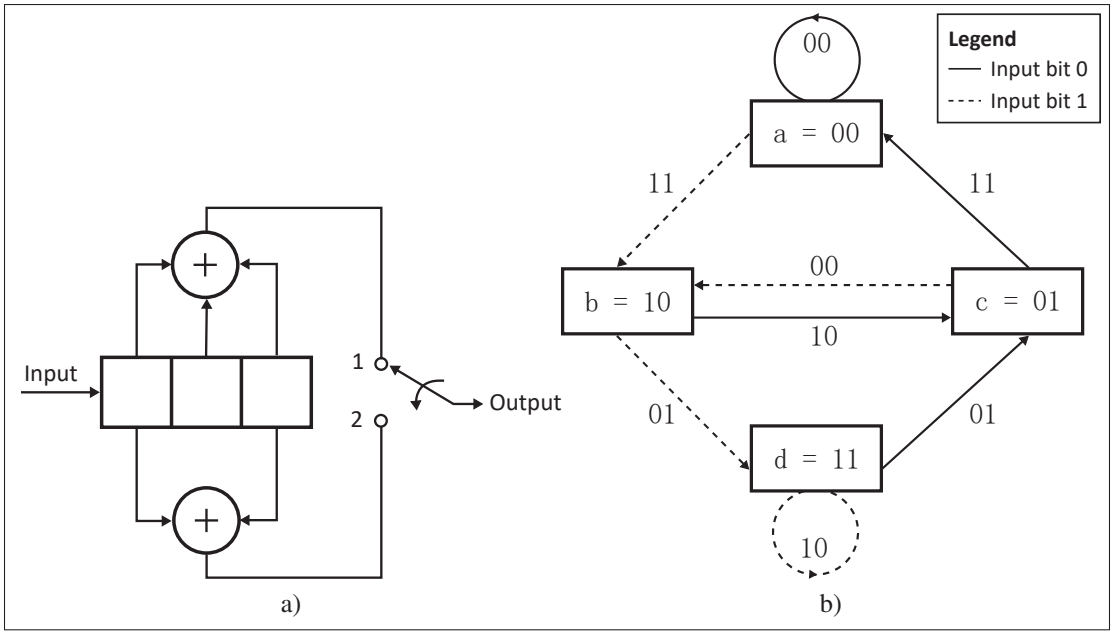

Figure 3.3 (a) $(2,1,3)$ convolutional encoder, (b) state diagram for $(2,1,3)$ convolutional encoder (Sklar, 2001)

The autocorrelation for the convolutional code can be found by the expression in (3.15), and similar to the example presented for repetition code, the upper bound on the peak factor is given by the substitution of the autocorrelation value in (3.12).

In some cases, e.g., a $\eta = 7, M = 3$, and 8-QAM Reed-Solomon code, computing the matrix $\mathbf{\Pi}$ is too expensive (Mannerkoski & Koivunen, 2000). Therefore, we can estimate the autocorrelation by the expression (Mannerkoski & Koivunen, 2000):

$$\hat{\rho}[j] = \frac{1}{N_s} \sum_{n=1}^{N_s} [w(n)w^*(n-j)], \tag{3.22}$$

where N_s is the number of samples and $w(n)$ the output of the convolutional encoder. This expression is used in this paper to find the simulation result in Section 3.4.

Table 3.1 Register Contents, Output Code Words and Elements of the Code Word Matrix for Convolutional Code $(2,1,3)$

State s_i	Register contents	Output	**C** elements
s_0	000	00	-1,-1
s_1	001	11	1,1
s_2	010	10	1,-1
s_3	011	01	-1,1
s_4	100	11	1,1
s_5	101	00	-1,-1
s_6	110	01	-1,1
s_7	111	10	1,-1

3.4 Analysis of PAPR Degradation in COFDM

In this section, we present a validation of the concepts presented in Section 3.3.2, based on the calculation of the CCDF of PAPR, the BER, and the autocorrelation of the signal before the IFFT block. First, in the case of linear block codes, for simplicity, we consider as an example, repetition codes with and without interleaving, and a simple variation called a modified code repetition (MCR). Then, the influence of the convolutional codes is analyzed.

3.4.1 Linear block code: Repetition code

The behavior of the autocorrelation in relation to the value of the CCDF of PAPR in a COFDM signal when using linear block codes is studied based on the use of repetition codes in the system.

In the case of repetition code, according to the analysis presented in Section 3.3.3.1, we know that the variable parameter that affect the autocorrelation of the code word is the code rate R. Thus, it is also known that for the calculation of the autocorrelation through (3.15) both the matrix $\mathbf{\Pi}$ and $\mathbf{D}$ remain constant and the column vector $\mathbf{c}(i)$ is identical for all i, but the number of columns of the matrix $\mathbf{C}$ changes according to η which, as shown in Fig 3.2, can modify the

autocorrelation. The impact of code rate over the autocorrelation and the CCDF in COFDM signal is analyzed in Fig. 3.4 where the CCDF of PAPR of COFDM signals with repetition codes (RC) for different code rate value is plotted (see Fig. 3.4a). The reference is the OFDM signal and a BPSK modulation is used for all cases. Also, Fig. 3.4b shows the autocorrelation for repetition code with code rates $1/2, 1/4$ and $1/8$, and based on these, the value of the upper bound peak factor Λ for repetition code with $R = 1/2, 1/4$, and $1/8$ is 15.4629 dB, 16.8448 dB, and 17.4570 dB, respectively. Therefore, it is possible to see that the reduction of the code rate for a repetition code, can increase the autocorrelation, and also the PAPR of COFDM system.

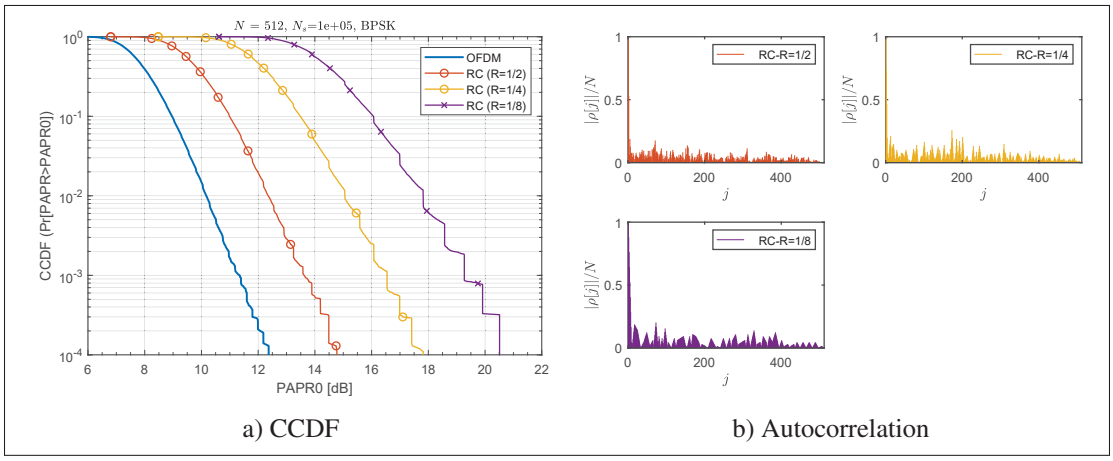

Figure 3.4 COFDM system with repetition code with code rate $1/2, 1/4$, and $1/8$, $N = 512$ subcarriers, and $N_s = 10^5$ OFDM symbols simulated.

As we have seen, the use of repetition codes generates colored autocorrelation. To achieve an autocorrelation closer to white, we also tested the use of a repetition code plus a block interleaver. The block interleaver used in this work writes across rows in the input and reads down columns in the output. Additionally, we evaluated the use of the modified code repetition (MCR) technique presented in Ngajikin *et al.* (2003), which allows a reduction of the peaks for a BPSK OFDM signal. Ngajikin *et al.* (2003) suggested using a repetition code and modified the last bit of the word, by toggling up. For example, for $k = 4$ number of repetitions, the input bit 0 produces the output $'0000'$ when code repetition is used, and in the case of MCR, the output will be $'0001'$. Two code rates are analyzed: $R = 1/4$, and $R = 1/8$.

The CCDF of PAPR of the COFDM signals with repetition codes (RC), repetition codes plus interleaver (RC+Int), and MCR plus interleaver (MCR+Int), for BPSK and QPSK modulation are show in Fig. 3.5a for code rate $1/4$, and in Fig. 3.6a for code rate $1/8$. Also, the conventional OFDM with BPSK and QPSK modulation is added for comparison. With code rate $1/4$, the use of a repetition code with QPSK presents a large value of PAPR, and compared to conventional OFDM BPSK signal, MRC plus interleaver with BPSK slight decrease can be achieved. On the other hand, the BER performance for the OFDM signal plus RC, RC+Int, and MRC+Int with code rates $1/4$ and $1/8$ are presented in Fig. 3.5b, and Fig. 3.6b, respectively. For same BER value, the better SNR are given for the MRC+Int and RC+Int than RC alone. Meanwhile, Fig. 3.5c and Fig. 3.6c show the autocorrelation for all cases with code rates $1/4$ and $1/8$, respectively. In the cases analyzed, the OFDM signal with repetition code presents a large value of autocorrelation and a large value of PAPR. Finally, the value of the upper bound peak factor Λ for repetition code, repetition code plus interleaver, and MCR plus interleaver for BPSK and QPSK modulation with code rates $1/4$ and $1/8$ is presented in Table 3.2.

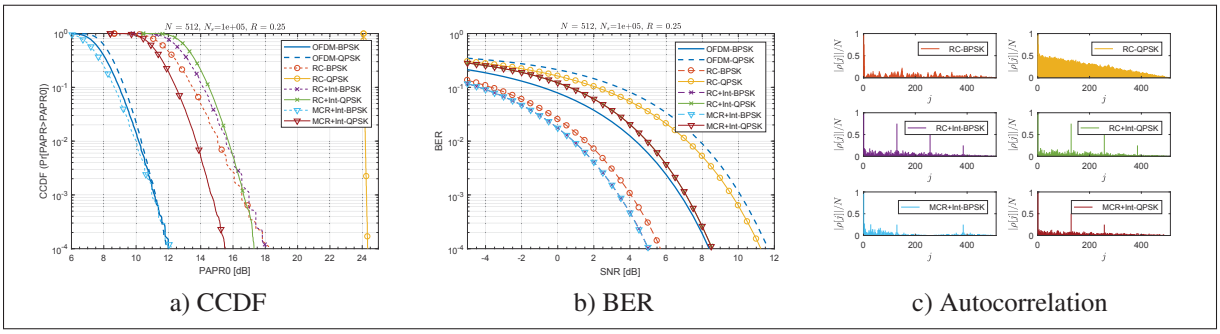

a) CCDF b) BER c) Autocorrelation

Figure 3.5 COFDM system with repetition code, repetition code plus interleaving and MCR plus interleaving with code rate $1/4$, $N = 512$ subcarriers, and $N_s = 10^5$ OFDM symbols simulated.

3.4.2 Convolutional codes

If a convolutional code is used in the COFDM system, the autocorrelation, and consequently, the PAPR of the OFDM signal, depends on the code word, i.e., the code rate, the code structure, and the state correlation matrix that is related to the constraint length V. On the one hand, it

is known that lower code rate leads to better performance. However, a more powerful code leads to extra redundancy and less bandwidth efficiency. On the other hand, more coding gain and more powerful convolutional code are obtained when a longer constraint length is used. However, the larger constraint length leads to more complex decoder and more decoding delays (Proakis & Salehi, 2008).

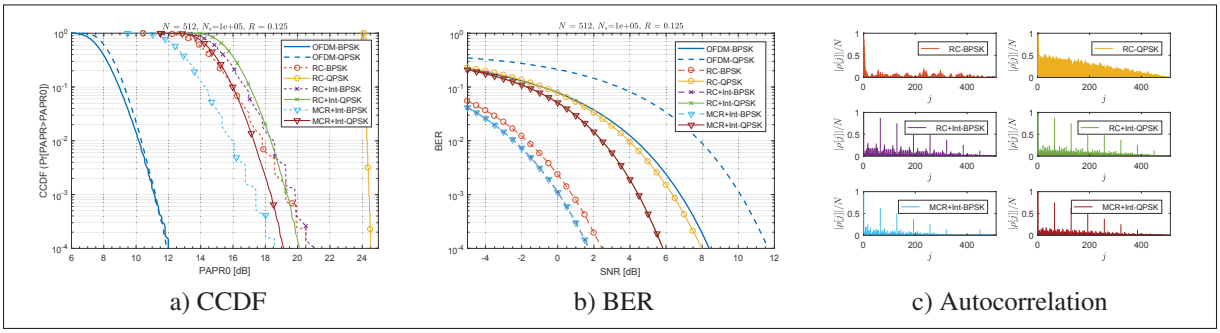

a) CCDF b) BER c) Autocorrelation

Figure 3.6 COFDM system with repetition code, repetition code plus interleaving and MCR plus interleaving with code rate $R = 1/8$, $N = 512$ subcarriers, and $N_s = 10^5$ OFDM symbols simulated.

Table 3.2 Λ for COFDM used in the linear block code examples

Code Rate (R)	Code	Modulation	Λ (dB)
1/4	RC	BPSK	16.5170
1/4	RC	QPSK	24.0986
1/4	RC+Int	BPSK	15.8130
1/4	RC+Int	QPSK	16.4278
1/4	MCR+Int	BPSK	13.9808
1/4	MCR+Int	QPSK	15.7127
1/8	RC	BPSK	17.0850
1/8	RC	QPSK	24.0916
1/8	RC+Int	BPSK	17.4964
1/8	RC+Int	QPSK	18.1708
1/8	MCR+Int	BPSK	14.8961
1/8	MCR+Int	QPSK	16.8202

Below, we study in more detail these important parameters, i.e., the code rate R, the code structure, and the constraint length V, and we analyze how they affect the PAPR of an OFDM signal. This can be an important point to take into account when designing an encoder. Also, we include in the discussion the maximum free distance Convolutional codes in case of code rates $1/2, 1/4$ and $1/8$ and compare its CCDF of PAPR, its BER, and its autocorrelation. In all simulations for the case of convolutional codes in this section, we consider an OFDM signal with $K = 256$ subcarriers, a guard interval percentage equal to 25%, a quadrature phase-shift keying (QPSK), and an oversampling rate $\mathscr{L} = 1$. An additive white Gaussian noise (AWGN) channel is assumed, and the receiver uses a hard Viterbi decoder with memory truncation and traceback depth defined by $2.5 \cdot [(V-1)/(1-R)]$ (Moision, 2008). The algorithm is executed $N_s = 10^5$ times in each case.

3.4.2.1 Code rate

Considering a forward error correction (FEC) code, the code rate is the proportion between the length of information digits and the length of the code word sequence. For instance, if the code rate is equal to $2/3$, then for each three bits, two correspond to data, and one is a redundancy. Typical convolutional code rate values are $1/2, 1/4, 1/8, 2/3, 3/4, 5/6$ and $7/8$.

A study examining the influence of the code rates of nonrecursive nonsystematic convolutional codes on the peak degradation of the COFDM signal is presented in Frontana & Fair (2007), where it is concluded that the PAPR can be increased in the case of a code rate $R < 1/2$ and relatively low constraint lengths $V = 3$ through $V = 6$ (Frontana & Fair, 2007). This conclusion is based on simulation results only.

Consider three convolutional codes with code rate $1/2, 1/4$ and $1/8$, similar constraint length $V = 3$, and without a significant structure defined by the polynomials in octal form: $[5,7]$, $[1,3,7,3]$, and $[1,5,7,3,1,5,3,7]$, respectively. For all three cases, there are $K = 2^3$ possible states of the Markov chain, and the same possible code words. The transition probability matrix is given by (3.21) and all states, register contents, and output possibilities are presented in

Table 3.3. The code word matrix **C** is obtained from Table 3.3 for each code word by the application of a BPSK mapped to the output when each code word is used. Therefore, the resulting code word matrices **C** has dimensions of (8×2), (8×4), and (8×8) for $R = 1/2, 1/4$, and $1/8$, respectively. Thus, in the case of constant constraint length, the autocorrelation changes according to the code word matrix. In this case, when analyzing the first two states for the three examples cases, we can observe an output similar to that in the example presented with repetition code. So the autocorrelation increases, in these cases, when the code word decrease, as analyzed in Fig. 3.2. Although this conclusion is based on a particular example, it is intuitively clear, that there are more options to have states that generate long chains of repetition at the output when the code rate decreases.

Table 3.3
States, Register Contents, and Output Code Words for Convolutional code: $(V = 3; [5,7])$, $(V = 3; [1,3,7,3])$, and $(V = 3; [1,5,7,3,1,5,3,7])$

State s_i	Register contents	Output		
		$[5,7]$	$[1,3,7,3]$	$[1,5,7,3,1,5,3,7]$
s_0	000	00	0000	00000000
s_1	001	11	1111	11111111
s_2	010	01	0111	00110011
s_3	011	10	1000	11001100
s_4	100	11	0010	01100101
s_5	101	00	1101	10011010
s_6	110	10	0101	01010110
s_7	111	01	1010	10101001

The CCDF of PAPR (see Fig. 3.7a), and the BER (see Fig. 3.7b) of the COFDM signals with convolutional codes $[5,7]$, $[1,3,7,3]$, and $[1,5,7,3,1,5,3,7]$ are calculated. We can see that the code rate decrease may increase the PAPR in the COFDM signal. In this example, only the polynomial $[5,7]$ corresponds to a maximum free distance code. For instance, in the example proposed here, the convolutional code OFDM signal with code rate 1/2 (see curve CC-OFDM, $R = 1/2$ in Fig. 3.7a) has a similar CCDF of PAPR as the OFDM signal. However, the curves

with code rates 1/4 and 1/8 (see curves CC-OFDM, $R = 1/4$, and CC-OFDM, $R = 1/8$ in Fig. 3.7a, respectively), when the CCDF is equal to 10^{-4} lose 3.2, and 5.1 dB, respectively, in the PAPR as compared to the OFDM signal. Meanwhile, the BER curves; (Fig. 3.7b) report the expected behavior when using different code rates. Next, the normalized value of absolute autocorrelation of the COFDM signals with convolutional codes represented by the polynomials $[5,7]$, $[1,3,7,3]$, and $[1,5,7,3,1,5,3,7]$ is presented in Fig. 3.7c. Additionally, the value of the upper bound on the peak factor Λ described in (3.12), based on the autocorrelation calculated in Fig. 3.7c is calculated. For the case of code rate $R = 1/2, 1/4$, and $1/8$ the upper bound on the peak factor (Λ) is 12.7012 dB, 13.8997 dB, and 15.5053 dB, respectively.

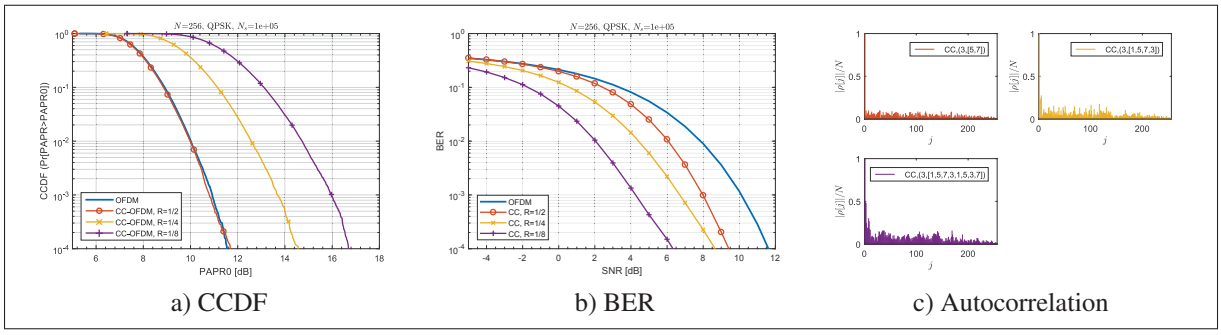

a) CCDF b) BER c) Autocorrelation

Figure 3.7 COFDM-QPSK system for different convolutional code rate with $N = 256$ subcarriers, and $N_s = 10^5$ OFDM symbols simulated.

3.4.2.2 Code structure

There are many code structures that can be used to generate the convolutional code; however, each code structure differs in its results in terms of error detection and error correction capabilities, and can also generate different values of PAPR for the system. For example, Frontana & Fair (2007), through simulation results, suggest that a significant structure in the convolutional encoder can lead to a degradation in the PAPR because it may cause a constructive summation on many of the subcarriers (Frontana & Fair, 2007).

We consider that a convolutional code has a significant structure if at least two consecutive bits of the resulting code word is obtained by the same generator (this means that we get same bits

in these positions). For example, in the convolutional code ($V = 3$; [5,7,7,7]) with code rate $R = 1/4$ the last three bits of each 4-bit code word are identical.

To quantify the effect of the significant structure of the convolutional code in the autocorrelation of the code word, we define the structure number (ς) as the number of consecutive generators existing in the generation of the code. For instance, the structure number for the convolutional code $V = 3$; [5,7,7,7] is $\varsigma = 3$.

The effect of the convolutional code structure on the value of autocorrelation is analyzed below. We consider four different polynomials, with a similar code rate $R = 1/4$, and constraint length $V = 3$, described in octal form by: $[1,3,5,7]$, $[5,5,7,7]$, $[5,7,7,7]$, and $[7,7,7,7]$ with structure number equal to $\varsigma = 1$, $\varsigma = 4$, $\varsigma = 3$, and $\varsigma = 4$, respectively. Again, $K = 3$, and the transition probability matrix is given by (3.21). All states, register contents, and output possibilities are presented in Table 3.4. The code word matrix has a dimension of (8×4) and it is constructed, with each output, by mapping $0 \rightarrow -1$ and $1 \rightarrow +1$. When analyzing the outputs in Table 3.4, it is possible to see that the repetition increases when the significant structure in the convolutional code also increases.

Table 3.4
States, Register Contents, and Output Code Words for Convolutional codes: $(V = 3; [1,3,5,7])$, $(V = 3; [5,5,7,7])$, $(V = 3; [5,7,7,7])$, and $(V = 3; [7,7,7,7])$

State s_i	Register contents	Output			
		$[1,3,5,7]$	$[5,5,7,7]$	$[5,7,7,7]$	$[7,7,7,7]$
s_0	000	0000	0000	0000	0000
s_1	001	1111	1111	1111	1111
s_2	010	0101	0011	0111	1111
s_3	011	1010	1100	1000	0000
s_4	100	0011	1111	1111	1111
s_5	101	1100	0000	0000	0000
s_6	110	0110	1100	1000	0000
s_7	111	1001	0011	0111	1111

The effect is calculated by simulating the PAPR (Fig. 3.8a), the BER (Fig. 3.8b) and the absolute value of its autocorrelation (Fig. 3.8c); in a COFDM system with QPSK modulation. It can be concluded from the results that when a significant structure is presented in the convolutional code, the absolute value of the autocorrelation increases, and consequently, may produce a PAPR increase. For this example, it was observed that when the value of the structure number (ς) increased, the autocorrelation and the PAPR also increased. For instance, if we consider the CCDF of PAPR equal to 10^{-4}, for $\varsigma = 1$ ($[1,3,5,7]$) the PAPR is 14 dB, for $\varsigma = 3$ ($[5,7,7,7]$) is 17.8 dB, and for $\varsigma = 4$ ($[5,5,7,7]$, and $[7,7,7,7]$) are 21.3 dB and 21.5 dB, respectively. Regarding the BER results, it is important to highlight that only the polynomial $[5,7,7,7]$ is a maximum free distance code. The value of the upper bound peak factor Λ is equal to 14.3922 dB, 21.1666 dB, 16.31143 dB, and 21.1875 dB when the convolutional codes $(V = 3; [1,3,5,7])$, $(V = 3; [5,5,7,7])$, $(V = 3; [5,7,7,7])$, and $(V = 3; [7,7,7,7])$ are used in the COFDM system.

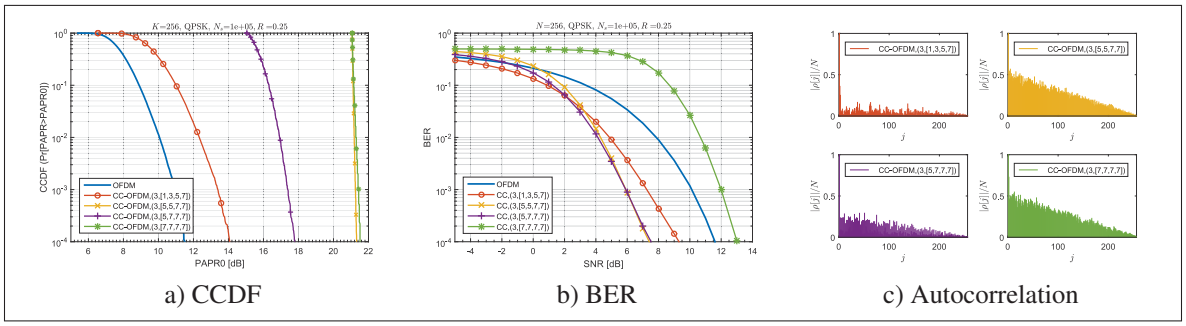

a) CCDF b) BER c) Autocorrelation

Figure 3.8 COFDM-QPSK system for different convolutional code structures with code rate $R = 1/4$, $N = 256$ subcarriers, and $N_s = 10^5$ OFDM symbols simulated.

3.4.2.3 Maximum free distance Convolutional codes

The free distance (d_{free}) is a minimal Hamming distance between different encoded sequences (Proakis & Salehi, 2008), and is related to the correcting capability of the code. In Table 3.5 the maximum free distance codes for code rates $1/2, 1/4$, and $1/8$ are presented.

The free distance is analyzed as a parameter here since the convolutional codes, with maximum free distance, represent the most used codes. In addition, the free distance impacts on the performance of the system. This effect will be included later in the calculation of the net gain and the convolutional code optimization.

In Fig. 3.9a, we present the CCDF of the PAPR for a selected group of maximum free distance codes in Table 3.5. We can see in Fig. 3.9a that in the case of free distance convolutional codes with $R = 1/2$, all curves have the same response with respect to the CCDF of PAPR. However, when we consider the case with $R = 1/4$, the convolutional code $(V = 5; [25, 27, 33, 37])$ loses approximately 1 dB, and the codes $(V = 3; [5, 7, 7, 7])$ and $(V = 7; [135, 135, 147, 163])$ lose approximately 6 dB as compared to the OFDM signal. On the other hand, when the code rate is $R = 1/8$, all curves experience degradation. For instance, if we consider the CCDF of PAPR equal to 10^{-4}, the curve "CC, $V = 3$" loses 8.63 dB as compared with the OFDM curve. Similarly, the curve "CC, $V = 4$" loses 6.83 dB, "CC, $V = 5$" loses 4.85 dB, "CC, $V = 6$" loses 1.07 dB, "CC, $V = 7$" loses 4.35 dB, and "CC, $V = 8$" loses 3.81 dB.

Table 3.5 presents the value of structure number ς for each generator. When the code rate is $R = 1/2$, all the generators show a structure number equal to 1 and all the codes experience same PAPR results. In the case of code rate $R = 1/4$ all the generators present $\varsigma = 1$ except for the codes with $V = 3, V = 4,$ and $V = 7$. The code with constraint length $V = 3$ has the highest value of ς and the highest value of PAPR. The code with $V = 7$ that has $\varsigma = 2$ experience high value of PAPR, too. However, there is an exception in the case of $V = 4$, since it experiences a similar PAPR value as the reference OFDM signal although it has a value of $\varsigma = 2$. In contrast, the code with $V = 5$ with a value of $\varsigma = 1$, also has a value of PAPR greater than the reference signal OFDM. For codes with code rate $R = 1/8$ there is a direct relation between the increase of the structure number ς and that of the PAPR for all cases is observed.

Additionally, the BER for the maximum free distance codes with a constraint length between 3 and 8 are presented in Fig. 3.9b. Finally, we present the estimation of the normalized

autocorrelation for four examples of each code rate in Fig. 3.10a, Fig. 3.10b, and Fig. 3.10c, respectively. The upper bound peak factor Λ for all possible cases is presented in Table 3.6.

Table 3.5 Maximum Free Distance Codes (Proakis & Salehi, 2008) with code rate $1/2$, $1/4$, and $1/8$, and the structure number (ς) for each code

Constraint Length (V)	Rate 1/2				Rate 1/4						Rate 1/8									
	Generators in Octal		d_{free}	ς	Generators in Octal				d_{free}	ς	Generators in Octal								d_{free}	ς
3	5	7	5	1	5	7	7	7	10	3	7	7	5	5	5	7	7	7	21	8
4	15	17	6	1	13	15	15	17	13	2	17	17	13	13	13	15	15	17	26	7
5	23	35	7	1	25	27	33	37	16	1	27	33	25	25	35	33	25	25	32	4
6	53	75	8	1	53	67	71	75	18	1	57	73	51	65	75	47	67	57	36	1
7	133	171	10	1	135	135	147	163	20	2	153	111	165	173	135	135	147	137	40	2
8	247	371	10	1	235	275	313	357	22	1	275	275	253	371	331	235	213	357	45	2

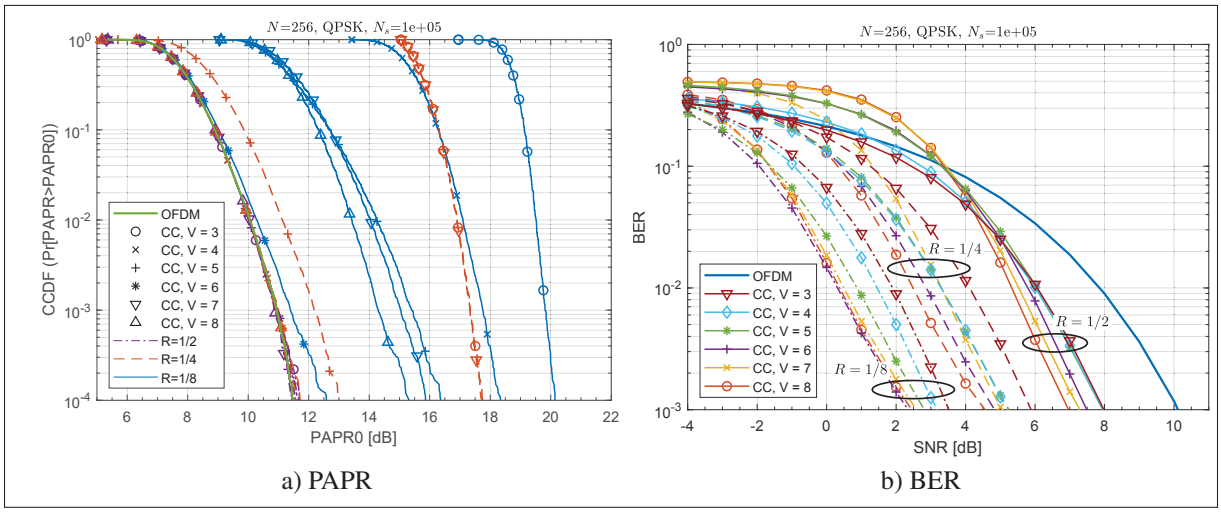

a) PAPR b) BER

Figure 3.9 COFDM-QPSK system for different maximum free distance convolutional codes with $N = 256$ subcarriers, constraint length V between 3 and 8, $N_s = 10^5$ OFDM symbols simulated, and code rates $R = 1/2$, $R = 1/4$, and $R = 1/8$.

3.4.2.4 Constraint length

The constraint length parameter is linked to the possibility of having memory in the convolutional codes, i.e., if we consider one information bit in the input of the convolutional encoder, the constraint length represents the maximum number of encoder outputs that can be affected (Lin & Costello, 2004). Frontana & Fair (2007) demonstrated by simulation that in an OFDM

system, the PAPR performance experiences degradation when the constraint length is low. To analyze the effect of the constraint length on the COFDM system, we consider the examples proposed in Section 3.4.2.3.

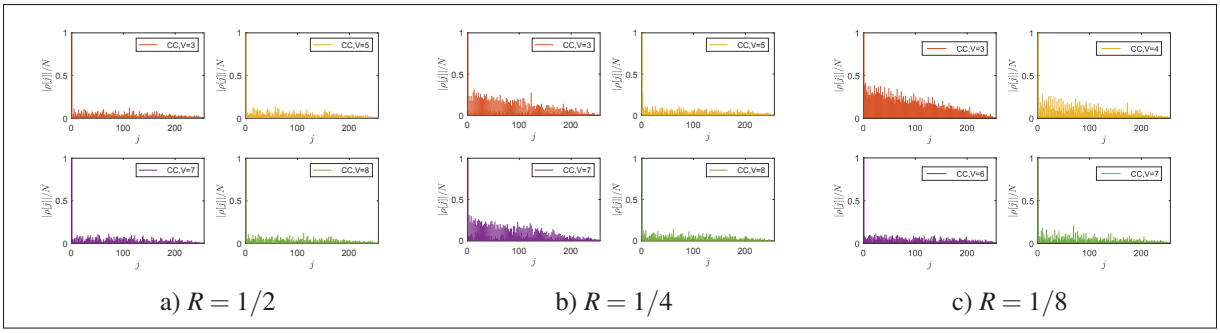

a) $R = 1/2$ b) $R = 1/4$ c) $R = 1/8$

Figure 3.10 Autocorrelation for COFDM-QPSK system with $N = 256$ subcarriers, $N_s = 10^5$ OFDM symbols simulated, different maximum free distance convolutional codes, and code rates $R = 1/2$, $R = 1/4$, and $R = 1/8$.

Table 3.6 Λ for COFDM used for free distance code example

Constraint length (V)	Λ (dB)		
	R=1/2	R=1/4	R=1/8
3	12.8131	16.0999	19.1310
4	12.9730	12.4933	15.7781
5	12.9761	13.2805	13.4960
6	12.9150	13.1190	13.2172
7	13.0507	16.3264	13.3310
8	13.1398	13.0456	13.5317

For the proposed examples, the code rate can assume the values of $1/2, 1/4$, and $1/8$, while the constraint length varies between 3 to 8, and the structure number is a variable for the cases $R = 1/4$ and $R = 1/8$. Since, the constraint length is a variable, the matrices $\mathbf{\Pi}, \mathbf{D}$, and $\mathbf{C}$ are also variables as well as the number of states and possible code words that change in relation to $K = 2^V$.

In the case of code rate $R = 1/2$ (Fig. 3.9a), we can see that changes in constraint length do not affect the CCDF of PAPR performance. In the second example, with code rate $1/4$ (Fig. 3.9a), the situation differs. The performance of the CCDF of PAPR in the COFDM system with convolutional codes, with $V = 3$, $V = 5$, and $V = 7$, is worse than for the OFDM system. However, it is important to highlight that the polynomial of convolutional codes with $V = 3$ and $V = 7$ present a significant structure as well. In example three, in the COFDM system with $R = 1/8$ (Fig. 3.9a), the behavior is different. All the polynomials experience losses, and we can see that when the polynomial with the least constraint length has worst CCDF of PAPR, except in the case of a polynomial with $V = 7$. In this case, the polynomial with $V = 6, 7$ and 8 do not have a significant structure. Therefore, in this case, the law that stipulates that the PAPR increases when the value of the constraint length decreases predominates.

3.5 Optimal Convolutional Code to Avoid an Increase in the PAPR Based on Net Gain

To define the optimal convolutional code of a given rate with a given constraint length, we use the net gain concept defined in Section 3.2.4 to compare all the maximum free distance codes for code rates $1/2, 1/4$ and $1/8$ presented in Table 3.5. The procedure followed to obtain the optimal codes is presented in Fig. 3.11, where N_c is the number of codes to compare, Γ_{opt} is the optimal net gain for all codes, and N_{opt} is the optimal code chosen.

In addition, we need to provide a specific value for the CCDF of PAPR and the BER to make the net gain comparison. These values may vary for different services offered by a system. For example, in a multimedia connection, we can consider three components with different quality of service (QoS), such as voice, video, and packet data. For voice service, the error probably in the region of 10^{-3} is typical (Richardson, 2005). The video service has a greater sensibility to errors, and it regularly requires a BER in the region of 10^{-6} (Richardson, 2005). On the other hand, For the packet data communications, in the case of high-speed Internet access, acceptable BER is 10^{-9} (Richardson, 2005). In this work, a BER equal to 10^{-3} is used for net gain evaluation as in the case of digitized voice service (Goldsmith, 2004, pg. 181). On the other hand, as shown in this case, a simulation is carried out using the Monte

Carlo method, to generate a comparison with a reasonable uncertainty data when the observer value is $10^{-\rho}$, leastwise $N_s = 10^{\rho+1}$ bits are processed through the system which produces a confidence interval of about $(2\hat{p}, 0.5\hat{p})$, where $\hat{p}$ is the estimator of the BER (Jeruchim, 1984).

In the case of the CCDF of PAPR, the typical values used in the literature for the comparison of PAPR reduction techniques are between 10^{-3} (Han & Lee, 2005; Jiang & Wu, 2008) to 10^{-5} (Muller & Huber, 1997c), so here 10^{-4} is used as a reference for net gain calculation.

If we change the reference value for the BER or the CCDF of PAPR, significant changes may occur in the result of the net gain, so it is advisable to perform the net gain calculation according to the application system.

Three cases of net gain were calculated: 1), when $\alpha_1 = \alpha_2 = 0.5$, i.e., equal importance for PAPR and BER improvement; 2), when $\alpha_1 = 0.75$ and $\alpha_2 = 0.25$, it is more important to achieve a reduced value of PAPR; and 3), when $\alpha_1 = 0.25$ and $\alpha_2 = 0.75$, it is more important to achieve BER improvement. The net results gain for different maximum free distance convolutional codes with code rates $1/2, 1/4$ and $1/8$ are shown in Table 3.7. We consider the basic OFDM system as a reference. A large value for the Y_1 implies a lower value of PAPR, and a large value for the variable Y_2 implies a better performance (less BER) as compared to conventional OFDM. ΔPAPR represents the variation between the PAPR value for OFDM signal and the COFDM signal at a specific value of CCDF. Similarly, ΔSNR is the variation between the SNR value for the reference signal and the COFDM signal at a specific value of BER.

Table 3.7 Net gain for different maximum free distance convolutional code with code rate equal to $1/2, 1/4$, and $1/8$

				Y_1						Y_2			Net Gain								
													Γ_1			Γ_2			Γ_3		
	PAPR Value (CCDF = 10^{-4})			ΔPAPR (CCDF = 10^{-4})			SNR Value (BER = 10^{-3})			SNR Variation (BER = 10^{-3})			$\alpha_1 = 0.5$ $\alpha_2 = 0.5$			$\alpha_1 = 0.75$ $\alpha_2 = 0.25$			$\alpha_1 = 0.25$ $\alpha_2 = 0.75$		
V \ R	1/2	1/4	1/8	1/2	1/4	1/8	1/2	1/4	1/8	1/2	1/4	1/8	1/2	1/4	1/8	1/2	1/4	1/8	1/2	1/4	1/8
OFDM	11.52			-	-	-	10.1			-	-	-	-	-	-	-	-	-	-	-	-
3	11.58	17.70	20.14	-0.06	-6.18	-8.62	7.98	5.88	3.52	2.12	4.22	6.58	1.03	-0.98	-1.02	0.48	-3.58	-4.32	1.58	1.62	2.78
4	11.62	11.53	18.34	-0.1	-0.01	-6.82	7.95	5.21	3.18	2.15	4.89	6.92	1.03	2.44	0.05	0.46	1.22	-3.89	1.59	3.67	3.49
5	11.60	12.86	16.36	-0.08	-1.34	-4.84	7.95	5.25	2.81	2.15	4.85	7.29	1.04	1.76	1.23	0.48	0.21	-1.81	1.59	3.30	4.26
6	11.77	11.55	12.58	-0.25	-0.03	-1.06	7.49	4.83	2.35	2.61	5.27	7.75	1.18	2.62	3.35	0.47	1.30	1.14	1.90	3.95	5.55
7	11.58	17.65	15.86	-0.06	-6.13	-4.34	7.29	5.05	2.58	2.81	5.05	7.52	1.38	-0.54	1.59	0.66	-3.34	-1.38	2.09	2.26	4.56
8	11.63	11.65	15.32	-0.11	-0.13	-3.80	6.96	4.56	2.45	3.14	5.54	7.65	1.52	2.71	1.93	0.70	1.29	-0.94	2.33	4.12	4.79

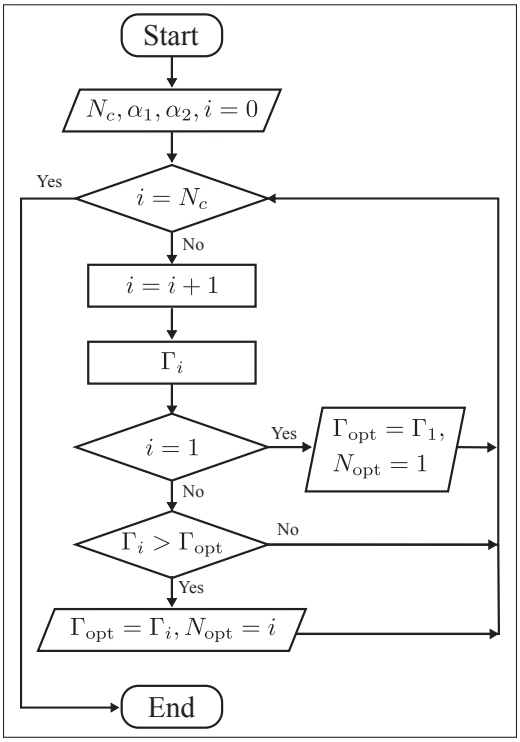

Figure 3.11 Algorithm to calculate the optimal code to avoid an increase in the PAPR based on the net gain

The net gain calculated in the first case, $\alpha_1 = \alpha_2 = 0.5$, for code rates $1/2, 1/4$ and $1/8$ is presented in Fig. 3.12a, where it can be seen that in the case of code rate $1/2$, the best options for the convolutional code are the code with constraint length $V = 8$. When the code rate is equal to $1/4$, the worst results seen are for codes with constraint lengths 3, and 7, and the convolutional codes with constraint lengths 4, 6, and 8 have good performance. In the case of code rate $1/8$, the best option is the convolutional code with constraint length 6. Based on these results, it can be affirmed that the best codes with maximum free distance codes for code rates $1/2, 1/4$ and $1/8$, with $\alpha_1 = \alpha_2 = 0.5$, are the codes with constraint lengths equal to 8, 8, and 6, respectively. The best net gain for each case is highlighted in gray in Table 3.7, 3.7.

Additionally, in Fig. 3.12b the variation of PAPR Y_1 (left axis), and the variation of BER performance Y_2 (right axis) in the case $\alpha_1 = \alpha_2 = 0.5$ is plotted for code rates $1/2, 1/4$ and $1/8$, and different values of constrain length (V).

Considering the left axis (Y_1), we can see that in the case of code rate 1/2, for different value of constraint length, slight differences are present. However, with the code rate equaling 1/4 or 1/8, differences in the PAPR of approximatively 6 dB for the case of R = 1/4, or 8 dB in the case of code rate 1/8 are shown, between codes with different constraint length. The smallest PAPR is presented for cases with constraint length equal to 3 and 7 (R = 1/2), 8 (R = 1/4), and 6 (R = 1/8). Besides, it can be seen that for all tested cases there are PAPR degradation; however, the system can be optimized through an accurate selection of the code which can lead to minimum increments for all cases.

Also, in Fig 3.12b, it can also seen that the variation of the SNR is in conformity with the literature results for convolutional codes, and we see that the reduction of the BER is impacted by choice of the code rate (lower code rate, greater reduction), and the constraint length. It should be remembered at this point that all the codes analyzed are the maximum free distance codes and that the distance free increases when there is an increment in the constraint length.

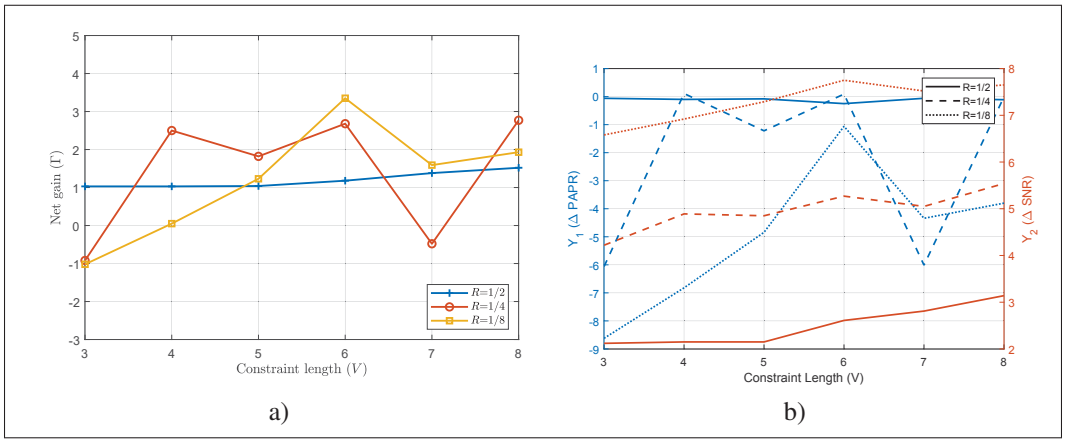

Figure 3.12 (a) Net gain with $\alpha_1 = \alpha_2 = 0.5$ for different maximum free distance convolutional codes with code rate 1/2, 1/4, and 1/8, (b) Y_1 versus Y_2 for different constraint length (V) with code rate $1/2, 1/4$, and $1/8$

3.5.1 Decoder complexity

A parameter that is an important measure to evaluate coding scheme in practice is the decoding complexity. Next we analyze the computational complexity taking as an example the convolutional codes.

If we consider a Viterbi decoder for a binary convolutional code with k input bits and constraint length V, there are $2^{k(V-1)}$ states. Therefore, there are $2^{k(V-1)}$ surviving paths at each state and $2^{k(V-1)}$ metrics (Proakis & Salehi, 2008). The calculation of a metric is required for each path that converges at a common node, so 2^k metrics for each node is calculated. In the VA, of the 2^k paths that merge at each node, only one survives. So, in conclusion the number of calculations at each stage increases exponentially with k and V (Proakis & Salehi, 2008). Due to this exponential growth of complexity, the VA is used mainly with short constraint lengths ($V \leq 10$).

On the other hand, the computational complexity measurement of convolutional codes for software implementations on the Viterbi algorithm operating with hard decision decoder can be defined in terms of arithmetic operation namely summations, bit comparisons and integer comparisons. McEliece & Lin (1996) defined decoding complexity measure of a trellis module (repeated copies of the trellis (McEliece & Lin, 1996)) as the total number of edge symbols in the module normalized by the number of information bits (Benchimol *et al.*, 2014) called complexity of the module M that represents the additive complexity of the trellis module M. On the other hand, Benchimol *et al.* (2014) raised the need to consider the computational complexity in the number of comparisons made by defining the total number of comparisons in M as the merge complexity that is equal to the total number of edges reaching it minus one (Benchimol *et al.*, 2014), at a specific state of M.

We see that complexity has a considerable impact when choosing an optimal convolutional code, so, an algorithm to calculate the optimal code can be included in the calculation as described above, by considering one more parameter in the aggregate fitness value in (3.7), the

relative increase in system complexity (Rajbanshi, 2007), i.e.,

$$Y_3 = -10\log_{10}\left(\frac{\text{Complexity}_{\text{after}}}{\text{Complexity}_{\text{before}}}\right). \tag{3.23}$$

so the expression in (3.7) can be rewritten as:

$$\Gamma = \sum_{u=1}^{3} \alpha_u \cdot Y_u, \tag{3.24}$$

where

$$\sum_{u=1}^{3} \alpha_u = 1, \tag{3.25}$$

As with the computational complexity, other parameters can be added and taken into account for the selection of an optimal code in relation to the particular needs of a system and the same procedure is feasible to establish the optimal code.

3.6 Conclusion

Orthogonal frequency division multiplexing (OFDM) is an attractive modulation technique for transmitting signals over wireless channels. This modulation has a lot of applications in current communications systems, and its performance can be improved by using forward error correction (FEC) codes. However, one of the main disadvantages with the OFDM system is the high peaks present in the envelope of its signal, which affects the performance of the system mainly at the level of nonlinear components.

In this work, we studied the effect of using FEC on the value of the CCDF of PAPR when a COFDM system is implemented. First, we introduced the OFDM model and discussed the exact evaluation of the CCDF of PAPR in the OFDM system. Next, we introduced the formulation of autocorrelation for uncoded and coded OFDM systems, and presented an upper bound on the peak factor of uncoded OFDM signals. Additionally, we explained a strategy for evaluating the autocorrelation for coded OFDM signals based on the Markov Chain Model,

and we related the autocorrelation with the value of the CCDF of PAPR in the case of linear block codes and convolutional codes. The optimal maximum free distance convolutional codes with given constraint lengths were selected based on the value of the net gain for code rates $1/2, 1/4$ and $1/8$, and we concluded that the codes with $R = 1/2, V = 8$; $R = 1/4, V = 8$; and $R = 1/8, V = 6$ are the best option (for $\alpha_1 = \alpha_2 = 0.5$).

Finally, we concluded that based on the autocorrelation we could show some characteristics that may affect the value of the CCDF of PAPR. First, in the linear block code, the number of possible code words and the structure of the code word are important parameters. On the other hand, with convolutional codes, the important parameters are the code rate, the constraint length, and the structure of the code.

In convolutional codes, the PAPR can be increased when low code rate and relative low constraint length is used. Due to low code rate there are more options to have states that generate long chains of repetition at the output. In addition, significant structure in the convolutional encoder can increase the peak in the COFDM signal because the repetition in the output increases when there is an increment in the significant structure.

The results in the work, will contribute to correctly choosing the codes to be used in conjunction with an OFDM system in order to not increase the PAPR.

CHAPTER 4

ON OPTIMIZING THE PAPR OF OFDM SIGNALS WITH CODING, COMPANDING, AND MIMO

Francisco Sandoval[1,3], Gwenael Poitau[2], François Gagnon[3]

[1] Departamento de Ciencias de la Computación y Electrónica, Universidad Técnica Particular de Loja, Loja, 11-01-608, Ecuador
[2] Chief Technology Officer, Ultra Electronics, TCS, Montreal, QC H4T IV7, Canada
[3] Departament of Electrical Engineering, École de Technologie Supérieure, 1100 Notre-Dame West, Montréal, Quebec, Canada H3C 1K3

Paper published in *IEEE Access*, February 2019

Abstract

One main disadvantage of the multiple-input multiple-output orthogonal frequency division multiplexing (MIMO-OFDM) system is that the signals transmitted on each antenna may experience high peak-to-average power ratio (PAPR). We will present a new hybrid PAPR reduction technique that combines and optimizes three methods, namely, convolutional code, successive suboptimal cross-antenna rotation and inversion (SS-CARI), and an iterative modified companding and filtering. Results for the hybrid PAPR reduction technique show that this scheme significantly reduces the PAPR, as compared to SS-CARI alone; it can improve the bit error rate (BER) to levels better than what obtains with the space-time block coding (STBC) MIMO-OFDM system, and the spectral splatter due to companding is also controlled by the use of frequency domain filtering. In addition, it is a flexible technique in which the net gain can be optimized based on the requirements of scheme parameters, such as the code rate, the constraint length of the convolutional code, the number of subblocks for SS-CARI , and the companding parameters.

Keywords

Companding, convolutional codes, multiple-input multiple-output (MIMO), orthogonal frequency division multiplexing (OFDM), peak-to-average power ratio (PAPR), signal scrambling, space-time block coding (STBC).

4.1 Introduction

The use of multiple antennas both at the transmitter and at the receiver represents a standard method for improving the performance and increasing the capacity of wireless communications systems; furthermore, it can provide spatial diversity when an orthogonal space-time block coding (STBC) is used (Cho *et al.*, 2010b). Multiple-input multiple-output (MIMO) can also improve the system capacity, as compared to single-input single-output (SISO) systems with flat Rayleigh fading or narrowband channels (Foschini, 1996). However, when MIMO is used in wideband channels, intersymbol interference (ISI) becomes a problem, and consequently orthogonal frequency division multiplexing (OFDM) is combined with MIMO to improve capacity and achieve ISI mitigation.

One of the main implementation drawbacks of OFDM is its inherent high peak-to-average power ratio (PAPR). This problem has been extensively studied, and multiple schemes have been proposed to reduce the PAPR in the OFDM signal. For example, Sandoval *et al.* (2017) classifies PAPR reduction methods under four technique categories: coding, multiple signaling and probabilistic (MSP), signal distortion (SD), and hybrid. Coding schemes choose the codewords that produce the minimum PAPR for transmission; multiple signaling techniques generate a given number of multi-carrier signal permutations and select the one that minimizes the peaks in the envelope; probabilistic methods likewise try to minimize the PAPR by modifying and optimizing one or more parameters in the OFDM signal; signal distortion schemes are the simplest to implement, and distort the signal before the high power amplifier in order to reduce the PAPR. Finally, hybrid techniques take advantage of different individual methods and combine two or more schemes to realize optimal PAPR reduction.

High PAPR is also an issue in MIMO-OFDM systems, and usually, works that propose to reduce the peaks in such systems proceed by either the OFDM techniques or by taking advantage of MIMO architecture to propose new techniques.

The companding scheme is an example of a signal distortion technique that can be extended to MIMO-OFDM; it compand the OFDM signal at the transmitter and decompand it at the receiver, based on different companding transforms (Wang *et al.*, 1999a; Huang *et al.*, 2004), such as $\mu-$law, $A-$law, exponential, etc. Unlike other distortion techniques, such as clipping, where the idea is to reduce the peaks of the OFDM signal, companding increases the average power of the signal, which can in turn substantially reduce the PAPR, in addition to operating the power amplifier more effectively (Vallavaraj *et al.*, 2010), because when the mean power of the system increases, most subcarriers can operate at the maximum power available (Vallavaraj, 2008); less input back-off (IBO) is then required than in the case of general OFDM or of the clipping OFDM signal (Vallavaraj, 2008). However, in the classic $\mu-$law compander transform (uCT), the trade-off between PAPR reduction and bit error rate (BER) performance is critical, and the use of compander PAPR reduction technique can increase the out-of-band radiation. In that context, Vallavaraj *et al.* (2004) proposed a modified $\mu-$law compander transform (MuCT) scheme that added a new companding profile parameter, called the peak ratio (PR), which can help achieve better BER performance (Vallavaraj *et al.*, 2010).

However, distortion techniques, such as companding, have the disadvantage of possibly negatively affecting the performance of the system. In addition, they can increase the out-of-band radiation.

On the other hand, an MSP PAPR reduction scheme that uses the additional degree of freedom provided by the MIMO system is the successive suboptimal cross-antenna rotation and inversion (SS-CARI) proposed by Tan *et al.* (2005). However, the PAPR reduction obtained with the SS-CARI scheme is limited (Su *et al.*, 2011), and does not grow linearly with an increase in complexity or the number of permutations. Although SS-CARI does not change the BER performance of the system, the SS-CARI method requires additional side information (SI) that

leads to a reduced data rate. In addition, the SI is a critical data that can significantly impact the BER if the SI is not recovered at the receiver. Consequently, the literature provides several proposals without side information as the blind cross-antenna successive shifting rotation and inversion (Blind-CASSRI) (Chang *et al.*, 2014).

A coding PAPR reduction technique is interesting for the MIMO-OFDM system as a method for reducing the peaks in the OFDM signal while improving the BER performance. For instance, the impact of convolutional codes (CC) is analyzed in the OFDM system by Frontana & Fair (2007), and shows that the selection of the generator polynomial for the CC can substantially affect the PAPR performance.

The aim of this paper is to propose a new hybrid PAPR reduction technique for an STBC MIMO-OFDM system, in which the convolutional code is optimized to avoid PAPR degradation; the technique combines the SS-CARI with iterative modified companding and filtering methods. This is a new technique aimed at considerably improving the system through significant PAPR reduction, BER gain as compared to the basic MIMO-OFDM system, low complexity, and reduced spectral splatter.

The paper is organized as follows. In Section 4.2, we introduce the system model and the theoretical concepts. The third section covers the description of the new hybrid PAPR reduction technique, while its performance evaluation is presented in Section 4.4. The final section gives a brief summary and brings together the key findings.

4.2 Background

4.2.1 System Model

Generally, OFDM modulation and MIMO systems allow easy integration and an increase in spectral efficiency. If we consider a MIMO-OFDM system with N_t transmit antennas, N_r receive antennas, and N subcarriers, the frequency-domain signal is therefore represented by $\{X_i[k]\}_{k=0}^{N-1}$ where k is the frequency index, and an assumption of N IFFT points from the ith

transmit antenna. After applying the IFFT, the discrete-time baseband OFDM signal $x_i[n]$ is given by

$$x_i[n] = \frac{1}{\sqrt{N}} \sum_{k=0}^{N-1} X_i[k] e^{\mathrm{j}2\pi \frac{kn}{LN}},\ n = 0, 1, \ldots, LN-1, \tag{4.1}$$

where n denotes the discrete-time index, j is the imaginary unit, and L is the oversampling factor. The discrete-time baseband signal (L-times oversampled) can have about the same peaks as the continuous-time baseband signal when $L \geq 4$ (Cho *et al.*, 2010a).

The PAPR of the discrete-time OFDM baseband signal is defined as the ratio between the maximum instantaneous power and its average power (Jiang & Wu, 2008), and from the *i*th transmit antenna, is

$$\mathrm{PAPR}(x_i[n]) \triangleq \frac{\max\limits_{0 \leq n \leq N-1} |x_i[n]|^2}{\frac{1}{N} \sum\limits_{n=0}^{N-1} |x_i[n]|^2}. \tag{4.2}$$

Frequently, the performance of a PAPR reduction technique is measured by the complementary cumulative distribution function (CCDF) given by:

$$\mathrm{CCDF} = \Pr\{\mathrm{PAPR} \geq \mathrm{PAPR}_0\}, \tag{4.3}$$

where the CCDF evaluates the probability of the PAPR of a OFDM signal exceeding a given threshold PAPR_0.

Additionally, in MIMO-OFDM systems, the PAPR is defined as the maximum of all N_t PAPR values evaluated in each MIMO path (Manasseh *et al.*, 2012), that is:

$$\mathrm{PAPR}_{\mathrm{MIMO}} = \max_{1 \leq i \leq N_t} \mathrm{PAPR}(x_i[n]). \tag{4.4}$$

4.2.2 Convolutional Code

Convolutional codes (CC) are a type of forward error correction (FEC) codes that contain memory. These codes can thus be implemented simply by using a linear finite state shift register. Convolutional codes are characterized by three parameters (η, k, V), with η denoting the code word length, k the input length, and V the constraint length, defined as the number of bits stored in each shift register, plus the current input bits. The code rate is therefore k/η.

It is clear that choosing different convolutional code parameters results in different bit error rate (BER) performances for the system. However, the PAPR of the system can also change according to the parameters selected for the convolutional code (Frontana & Fair, 2007). PAPR optimization therefore requires an adequate selection of CC parameters.

4.2.3 Successive Suboptimal Cross-Antenna Rotation and Inversion (SS-CARI) Scheme

To simplify the following description, we consider an Alamouti STBC MIMO-OFDM system (Alamouti, 1998) with two transmit antennas, and assume that the channel does not change during at least two OFDM symbol periods. However, the technique can be extended to cover other configurations. In the first symbol period, two data blocks $\mathbf{X}_1 = [X_1[0], X_1[1], \cdots, X_1[N-1]]$ and $\mathbf{X}_2 = [X_2[0], X_2[1], \cdots, X_2[N-1]]$ are transmitted from antennas 1 and 2, respectively, and in the second symbol period, antenna 1 transmits the data block $-\mathbf{X}_2^*$, and antenna 2 transmits $\mathbf{X}_1^*$, where $(\cdot)^*$ represents the elementwise complex conjugate operation.

In the SS-CARI technique proposed by Tan *et al.* (2005), each data block is partitioned into M equal size subblocks given by $\mathbf{X}_i = [\mathbf{X}_{i,1}, \mathbf{X}_{i,2}, \cdots, \mathbf{X}_{i,M}]$, where i is the transmit antenna index. Next, a cross-antenna rotation and inversion (CARI) is performed only on the first subblocks $\mathbf{X}_{1,1}$, $\mathbf{X}_{2,1}$. As a result, we will obtain the four sets of transmit sequences: $\mathbf{X}_1^{(1)} = [\mathbf{X}_{1,1}, \mathbf{X}_{1,2}, \cdots, \mathbf{X}_{1,M}]$ and $\mathbf{X}_2^{(1)} = [\mathbf{X}_{2,1}, \mathbf{X}_{2,2}, \cdots, \mathbf{X}_{2,M}]$, the original set with the first subblock inverted $\mathbf{X}_1^{(2)} = [-\mathbf{X}_{1,1}, \mathbf{X}_{1,2}, \cdots, \mathbf{X}_{1,M}]$ and $\mathbf{X}_2^{(2)} = [-\mathbf{X}_{2,1}, \mathbf{X}_{2,2}, \cdots, \mathbf{X}_{2,M}]$, the original set with the first subblock rotated $\mathbf{X}_1^{(3)} = [\mathbf{X}_{2,1}, \mathbf{X}_{1,2}, \cdots, \mathbf{X}_{1,M}]$ and $\mathbf{X}_2^{(3)} = [\mathbf{X}_{1,1}, \mathbf{X}_{2,2}, \cdots, \mathbf{X}_{2,M}]$, and the original set with the first subblock inverted and rotated $\mathbf{X}_1^{(4)} = [-\mathbf{X}_{2,1}, \mathbf{X}_{1,2}, \cdots, \mathbf{X}_{1,M}]$ and

$\mathbf{X}_2^{(4)} = [-\mathbf{X}_{1,1}, \mathbf{X}_{2,2}, \cdots, \mathbf{X}_{2,M}]$. Next, the PAPR for the four sets obtained are calculated, and the one with the smallest maximum PAPR is retained. This process is repeated with the next subblocks $\mathbf{X}_{1,2}$, $\mathbf{X}_{2,2}$, and successively for all M subblocks. Finally, the set of sequences $\{\tilde{\mathbf{X}}_1, \tilde{\mathbf{X}}_2\}$ is found according to the minimax criterion. This process is summarized in Fig. 4.1.

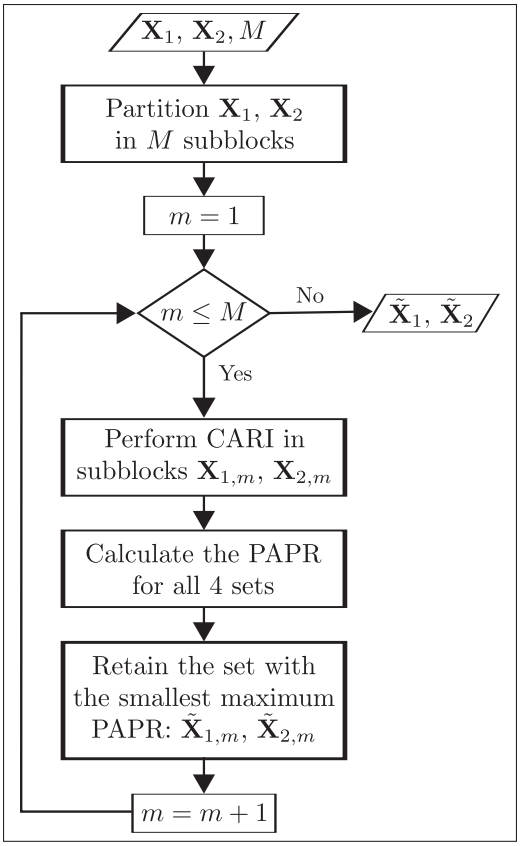

Figure 4.1 SS-CARI algorithm.

Interestingly, when SS-CARI is used to reduce the PAPR over an orthogonal STBC (OSTBC) system, the process needs to be done run in the first symbol period, since $\mathbf{X}_i$ and $\pm\mathbf{X}_i^*$ have the same PAPR properties (Tan *et al.*, 2005). Additionally, when the SS-CARI technique is used, the number of possible permutations is $4M$ (Tan *et al.*, 2005), and the number of side information bits is $S = 2 + \lfloor \log_2(M) \rfloor$, where $\lfloor x \rfloor$ denotes the smallest integer that does not exceed x.

4.2.4 Modified μ-Law Companding

μ-law companding transform (uCT) is a nonlinear nonsymmetrical technique, in which the lower amplitude of the original signal is amplified while the peaks remain unchanged. It thus aims to improve the PAPR by increasing the mean power of the OFDM signal, without changing the signal peaks, unlike other techniques, such as clipping, where the peaks are clipped. The companding process requires compand of the OFDM signal at transmission and of the decompand at the receiver.

Let the peak ratio PR be the relation between the peak amplitude of companding (A) and the peak of the actual signal (x_{peak}). The modified μ-law companding transform (MuCT) introduced by Vallavaraj *et al.* (2004), performs the companding according to the law:

$$y = \text{sgn}(x)\frac{A}{\ln(1+\mu)}\ln\left(1+\frac{\mu}{A}|x|\right), \tag{4.5}$$

where $A = \text{PR}\cdot x_{\text{peak}}$, $\mu > 0$, $|x|$ represents the instantaneous amplitude of the input signal, and $\text{sgn}(\cdot)$ is the sign function. The decompander is the inverse of (4.5).

Thus, selecting $\text{PR} = 1$ results in a classic μ-law companding process. However, with $\text{PR} = 2$, the lower amplitude signals are much higher than in μ-law companding. Additionally, the peaks are affected by a gain greater than unity, which can positively impact the performance of the system (Vallavaraj *et al.*, 2010). Thus, the MuCT parameters μ and PR need to be optimized for a good trade-off between PAPR and BER. In order to optimize the BER versus the PAPR for the new PAPR reduction technique proposed, we use the transform gain (G) concept, defined by Huang *et al.* (2004) as:

$$G = \frac{\text{PAPR}_{\text{w/o}}}{\text{PAPR}_{\text{w}}}, \tag{4.6}$$

where $\text{PAPR}_{\text{w/o}}$ represents the original signal without applying a PAPR reduction scheme, and PAPR_{w} is the PAPR of the signal when a PAPR reduction technique is used.

In this paper, the performance of the companded signal is compared to that of an uncompanded signal of equal power, based on the analyses Mattsson *et al.* (1999) and Wang *et al.* (1999b). It should be recalled that companding the OFDM signal effectively increases its signal strength (Vallavaraj, 2008). Therefore, we include a normalization constant K such that $E_s = E_{s_c}$ (the symbol energy of the uncompanded signal is equal to the symbol energy of the companded signal), and the companding equation at the transmitter is redefined as (Wang *et al.*, 1999b):

$$y = K \cdot \operatorname{sgn}(x) \frac{A}{\ln(1+\mu)} \ln\left(1 + \frac{\mu}{A}|x|\right), \tag{4.7}$$

where K is given by Mattsson *et al.* (1999)

$$K \approx \frac{\ln(1+\mu)}{\mu}. \tag{4.8}$$

At the receiver, to reverse the normalization operation, the signal is multiplied by $1/K$. In the case of MuCT, the normalization constant is redefined as:

$$K \approx \kappa \cdot \frac{\ln(1+\mu)}{\mu}, \tag{4.9}$$

where κ is a constant that is a function of μ and PR, and we find it by simulation.

4.3 Proposed Hybrid PAPR Reduction Technique

A hybrid PAPR reduction technique based on convolutional codes, SS-CARI, and modified companding, identified here for convenience as CSC, is presented in Fig. 4.2. The bit source is processed by a convolutional encoder and a PSK or QAM is used for symbol mapping. Next, the SS-CARI defined in Section 4.2.3 is applied. In the original version of SS-CARI (Tan *et al.*, 2005), side information bits with the set of sequences selected needs to be transmitted to the receiver. The STBC encoder is applied, and at each transmit antenna, the conventional OFDM modulator is employed to generate the OFDM symbol; the input signal is serial-to-parallel (S/P) converted, followed by an inverse fast Fourier transform (IFFT). Each OFDM symbol

is parallel-to-serial (P/S) converted and a cyclic prefix (CP) of length N_{cp} is added. Then, the modified companding, described in Section 4.2.4, is applied, and the output is processed by the digital-to-analog converter (DAC), and by the RF up-converter as a final step, before the transmission.

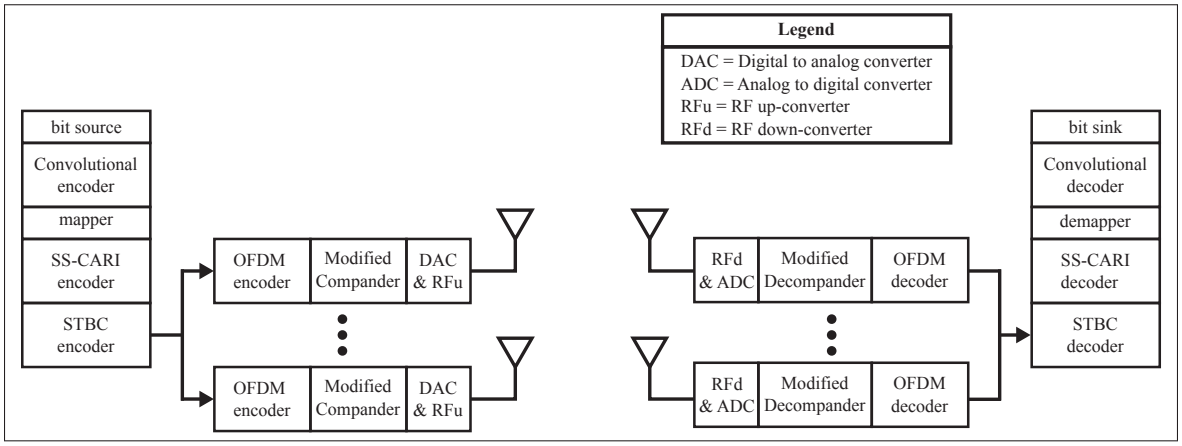

Figure 4.2 Block diagram of the CSC technique.

One limitation of using companding for PAPR reduction is that it produces spectral splatter, as reported by Vallavaraj *et al.* (2004). Therefore, one solution is to use a filter to reduce the out-of-band radiation. In this work, a frequency domain filtering (FDF) (Armstrong, 2001) is implemented, as can be seen in Fig. 4.3, where after the signal is companded on the modified companding block, it is transformed back into a discrete frequency domain by the $N \times L$ FFT block. The out-of-band components of the companded signal, represented by $C_{N/2+1}, \cdots, C_{NL-N/2}$ are replaced by zeros before the second $N \times L$ IFFT, while the in-band components $C_0, \cdots, C_{N/2-1}$ and $C_{NL-N/2+1}, \cdots, C_{NL-1}$ do not change. After the second IFFT block, the signal is serial-to-parallel (P/S) converted, and the cyclic prefix (CP) is added.

However, the use of filtering in the system before the companding block results in "peak regrowing", which considerably increases the PAPR once again. So, we complement the PAPR reduction technique design with an iterative companding and filtering process, as can be seen in Fig. 4.4. This guarantees an optimal PAPR reduction, and controls the spectral splatter. In Fig. 4.4, m represents the number of iterations the process is repeated.

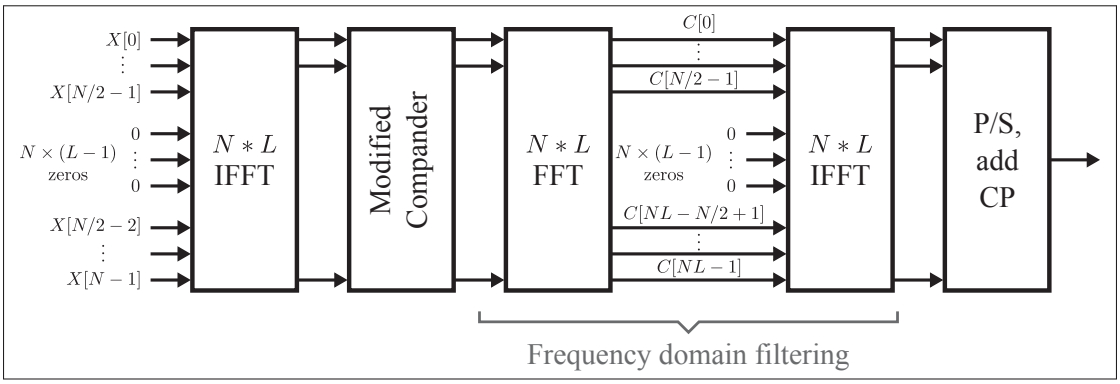

Figure 4.3 Frequency domain filtering based on (Armstrong, 2001).

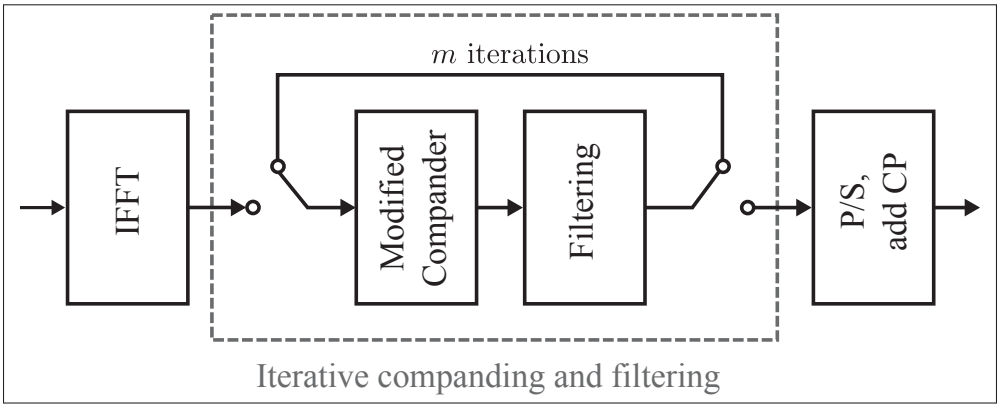

Figure 4.4 Iterative companding and filtering.

In summary, we have presented a hybrid PAPR reduction technique for STBC MIMO-OFDM system based on convolutional code, SS-CARI, and an iterative modified companding and filtering.

4.4 Performance of Hybrid PAPR Reduction Technique

We now present simulation results for a 128 subcarrier OFDM system with quadrature phase-shift keying (QPSK) modulation, 25% guard interval, and oversampling factor, $L = 4$, performed by padding zeros to the baseband modulated signals. An Alamouti space time code is used with 2 transmit antennas and 2 receiver antennas over a Rayleigh channel with Zero Forcing (ZF) equalization. In each case, the algorithm is executed $N_s = 10^5$ times.

The first experiment analyzes the CCDF of PAPR by including a convolutional code (see Fig. 4.5). For this, we take as an example a code rate equal to 1/4. The signal reference, in the figure, is the STBC MIMO-OFDM system without coding, and the polynomials used for each value of the constraint length (V) and its free distance are presented in Table 4.1. It is evident that the selection of the CC can considerably affect the PAPR of the system. For instance, for CCDF $= 10^{-3}$, with $V = 3$ and $V = 7$ the PAPR increase by 4 dB with respect to the reference. For $V = 5$, the PAPR increases by 1 dB. However, with $V = 4$ and $V = 6$, the PAPR is similar to the reference. Based on this, a CC with $R = 1/4$, $V = 4$, and polynomial $[13, 15, 15, 17]$ is chosen for the following experiments.

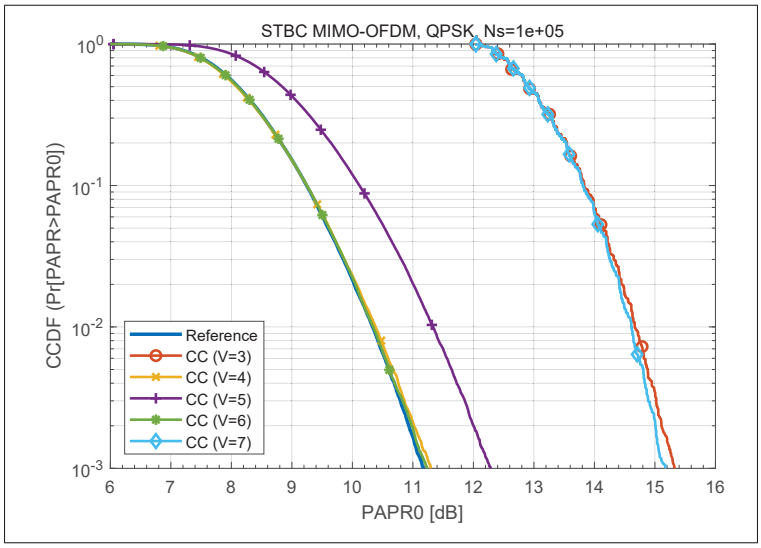

Figure 4.5 Comparison of CCDF in MIMO-OFDM system for different maximum free distance convolutional codes with $R = 1/4$. The reference is the STBC MIMO-OFDM system without coding.

In Fig. 4.6 the reduction of the PAPR obtained by the SS-CARI technique with different numbers of subblocks ($M = 4, 8$ and 16) is evaluated. It can be seen that a reduction of 1.6 dB of the PAPR is achieved, compared to the reference, with a $M = 4$, and a reduction of 1.9 dB with $M = 8$ with slight difference between the cases of $M = 8$ and $M = 16$. Therefore, as the number of subblocks increases, the complexity of the system and the size of the SI increase; however, the PAPR reduction increases at a lower rate each time M increases.

Table 4.1 Rate 1/4 Maximum Free Distance Codes (Proakis & Salehi, 2008).

Constraint Length (V)	Generators in Octal				d_{free}
3	5	7	7	7	10
4	13	15	15	17	13
5	25	27	33	37	16
6	53	67	71	75	18
7	135	135	147	163	20

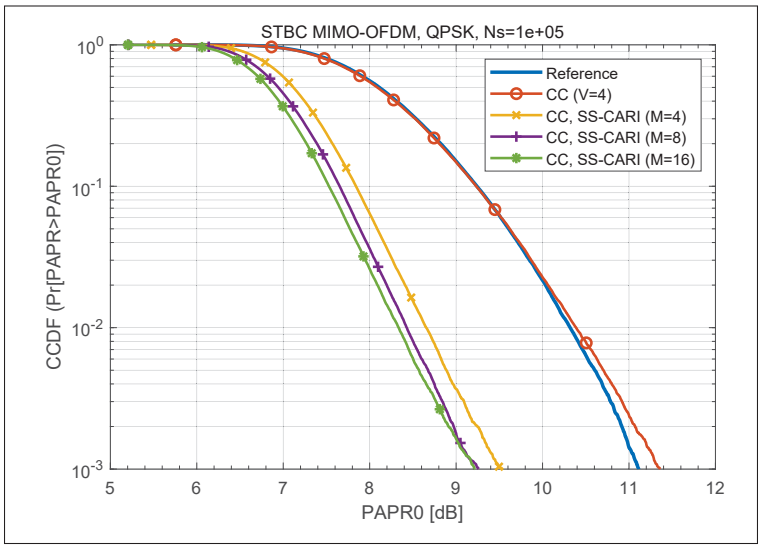

Figure 4.6 Comparison of CCDF in MIMO-OFDM system with SS-CARI technique with different numbers of subblocks. The reference is the STBC MIMO-OFDM system without coding.

Next, we evaluate the modified companding technique alone, i.e., without the influence of CC or the SS-CARI scheme. To this end, the BER for SNR $= 12$ dB versus the gain G in dBs for CCDF $= 10^{-3}$ is plotted for different μ $(1, 5, 10, 20, 50, 100,$ and $255)$ and PR $(1, 1.2, 1.4, 2,$ and $4)$ values (see Fig. 4.7). Some conclusions can be drawn. First, the best BER performance of the system is obtained in the case of small values of the μ parameter. In this region, the use of different values of PR produce only minor differences. However, by increasing the μ value, a significant gain in PAPR can be obtained, and we can see that when

the PR increase, the BER decrees less, as compared to a classic companding method. It is also evident that for PR $= 1$, the highest possible gain of PAPR is obtained, but that the BER degradation is the largest as well.

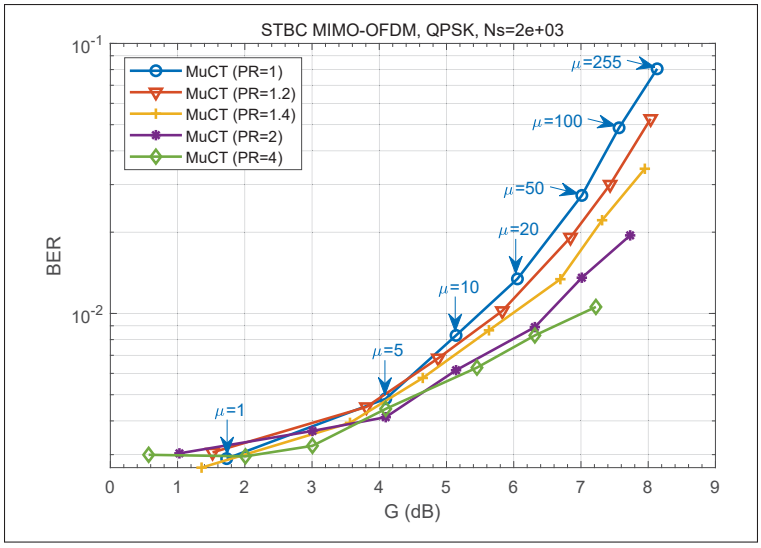

Figure 4.7 BER vs G with modified companding transforms (QPSK, $L = 4$, $N = 128$, CCDF $= 10^{-3}$, and SNR $= 12$ dB).

Based on the previous analysis, we evaluate the hybrid CSC technique that combines CC with $R = 1/4$ and $V = 4$, SS-CARI method with $M = 16$ and MuCT with two versions: $\mu = 10$, PR $= 1.2$ and $\kappa = 2.7$ (case 1), and $\mu = 255$, PR $= 2$ and $\kappa = 15.7$ (case 2). The CCDF of PAPR, the BER performance and the power spectral density (PSD) for a CSC scheme are presented in Fig. 4.8, Fig. 4.9, and Fig. 4.10, respectively. As shown in Fig. 4.8 the use of the SS-CARI scheme allows to obtain a PAPR reduction of 2.5 dB (CCDF $= 10^{-4}$), and with the CSC scheme it is possible to achieve a reduction of 7.3 dB (CCDF $= 10^{-4}$) for case 1, and of 9.5 dB for case 2. As a second reference, the case where only the MuCT is used for $\mu = 10$ and PR $= 1.2$ is also plotted, where a reduction of 5.5 dB is presented.

The BER performance for a CSC technique is plotted in Fig. 4.9, where we can see a gain of 4 dB (BER $= 10^{-3}$) when the CC is added. In addition, degradation due to the inclusion of MuCT is clear; however, it is 0.5 dB for case 1, but 2 dB in case 2, when the BER is compared

to the CC+STBC curve with BER $= 10^{-3}$. Nevertheless, we have a gain when it is compared to the basic reference without coding. It can also be seen that the case of MuCT alone has results in a worse performance.

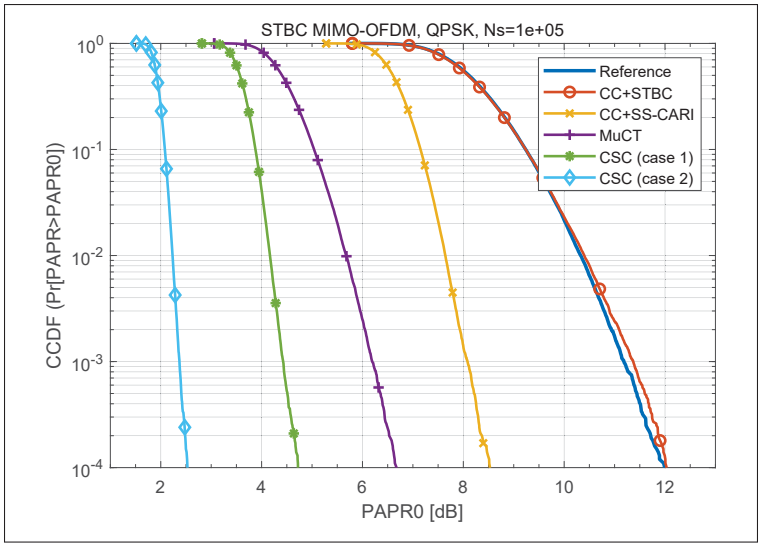

Figure 4.8 CCDF of PAPR curves for CSC hybrid PAPR reduction technique in STBC MIMO-OFDM system with $R = 1/4$, $V = 4$, $M = 16$, and two versions: $\mu = 10$, PR $= 1.2$ and $\kappa = 2.7$ (case 1), and $\mu = 255$, PR $= 2$ and $\kappa = 15.7$ (case 2). The reference is the STBC MIMO-OFDM system without coding.

The results of PSD versus the normalized frequency for the CSC technique are presented in Fig. 4.10. From the graph we can see that due to the MuCT there is out-of-band radiation that is similar to the CSC (case 1), and an increase for the CSC (case 2). The spectral splatter is evident as a limitation when using the MuCT. Because of this, a frequency domain filtering is added to the system.

As shown in Fig. 4.11, a PSD similar to the reference is obtained by the effect of using the filter in the system (see CSC-Filter (m = 1)). However, a problem when using a filter is that it can lead to peak regrowing, which can be seen in the Fig 4.10, where we compare the CCDF for the unfiltered signal (CSC) versus that for the filtered signal (CSC + Filter (m = 1)). We see here that there is an increase in PAPR of 1.8 dB. To tackle this drawback, the iterative system

represented in Fig. 4 is implemented. As a result, the performance of the final proposals of the CSC technique with iterative MuCT and filtering are presented in Fig. 4.11, Fig. 4.12 and Fig. 4.13.

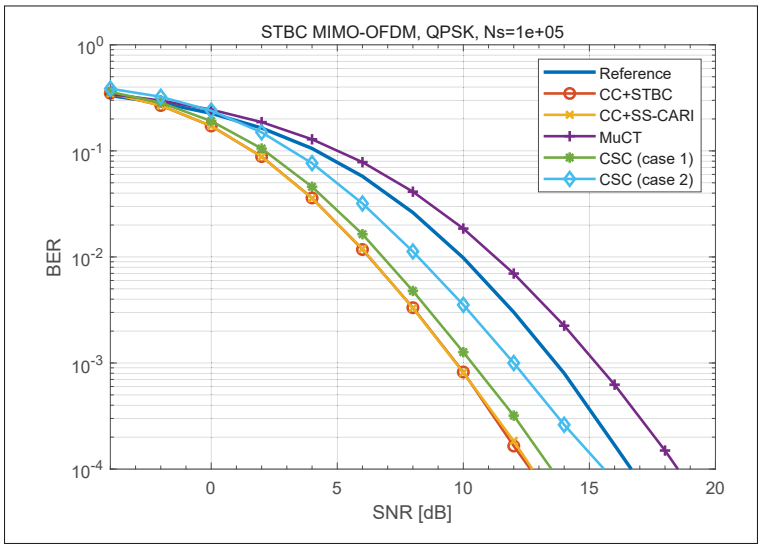

Figure 4.9 BER performance for CSC hybrid PAPR reduction technique in STBC MIMO-OFDM system with $R = 1/4$, $V = 4$, $M = 16$, and two versions: $\mu = 10$, PR $= 1.2$ and $\kappa = 2.7$ (case 1), and $\mu = 255$, PR $= 2$ and $\kappa = 15.7$ (case 2). The reference is the STBC MIMO-OFDM system without coding.

Fig. 4.11 presents the unfiltered signal, the filtered signal without iteration ($m = 1$), the filtered signal with 2 iterations, and the filtered signal with 3 iteration for a $\mu = 1.2$ and PR $= 1.2$. The case with three iterations produces the largest PAPR reduction of 7 dB. However, with two iterations the reduction is 6 dB. For BER performance, we can see that the use of filters and iterations degrades the signal; for example, in the case of $m = 3$, we have a slightly worse value than that of the reference for low SNR, and a slightly better value for high SNR. However, for $m = 2$, the BER is improved in relation to the reference by about 2.5 dBs. Finally, Fig. 4.13 presents the PSD for the CSC iterative filter and MuCT technique. For the cases of $m = 1$ and $m = 2$, a curve similar to the reference is obtained. In the case of $m = 3$, we can see a slight in-band radiation.

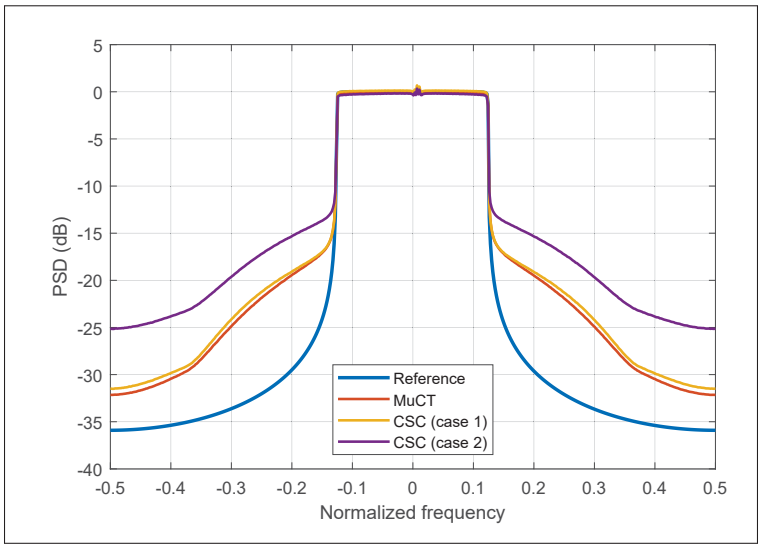

Figure 4.10 PSD curves for CSC hybrid PAPR reduction technique in STBC MIMO-OFDM system with $R = 1/4$, $V = 4$, $M = 16$, and two versions: $\mu = 10$, PR $= 1.2$ and $\kappa = 2.7$ (case 1), and $\mu = 255$, PR $= 2$ and $\kappa = 15.7$ (case 2). The reference is the STBC MIMO-OFDM system without coding.

4.5 Conclusion

STBC MIMO-OFDM is a key method in current wireless communication systems that can improve performance, increase capacity, provide spatial diversity, and achieve ISI mitigation. However, the high peak in the OFDM envelope can impact the non-linear components in the transmitter, and the PAPR increases when the number of transmit antennas increases.

The literature presents a number of techniques for PAPR reduction in OFDM, and more recently, methods have been proposed for MIMO-OFDM systems. However, these techniques may be limited by several factors, such as an increase in complexity, a requirement for side information, BER degradation, in-band or out-of-band radiation, increase in power requirements at the transmitter or limited PAPR reduction capabilities. In this context, a hybrid technique can therefore provide flexibility allowing an optimization of the net gain.

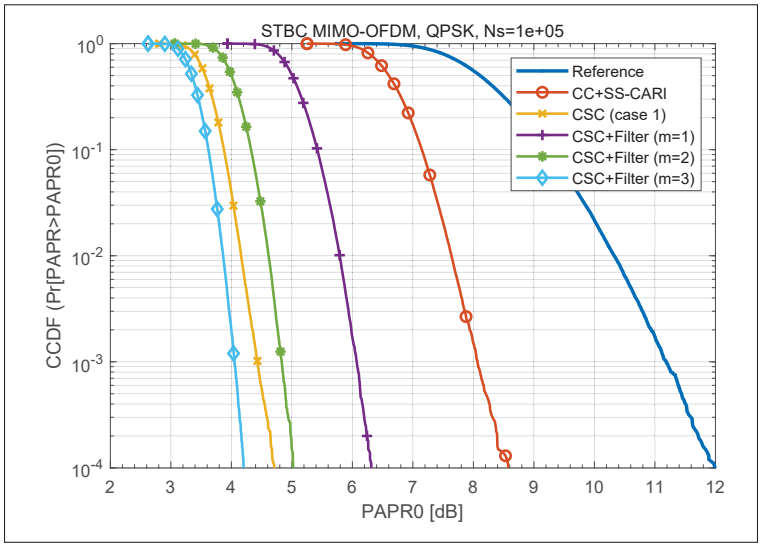

Figure 4.11 CCDF of PAPR curves for CSC hybrid PAPR reduction technique with iterative MuCT and filter in STBC MIMO-OFDM system with $R = 1/4$, $V = 4$, $M = 16$, $\mu = 10$, PR $= 1.2$, and $\kappa = 2.7$ (case 1). The reference is the STBC MIMO-OFDM system without coding.

In this work, we introduced a new hybrid PAPR reduction technique based on convolutional codes and SS-CARI, which takes advantage of the MIMO structure, and a modified companding method. This method, provides a substantial reduction in PAPR while maintaining an adequate performance in comparison with the STBC MIMO-OFDM basic system, and controls out-of-band radiation produced by the companding of the transmitter through the use of iterative companding and filtering. The technique can be optimized by customizing several parameters such as the code rate, the constraint length of CC, the number of subblocks for the SS-CARI process, the μ and PR companding parameters, and the number of companding and filtering iterations, which guarantees flexibility for the method.

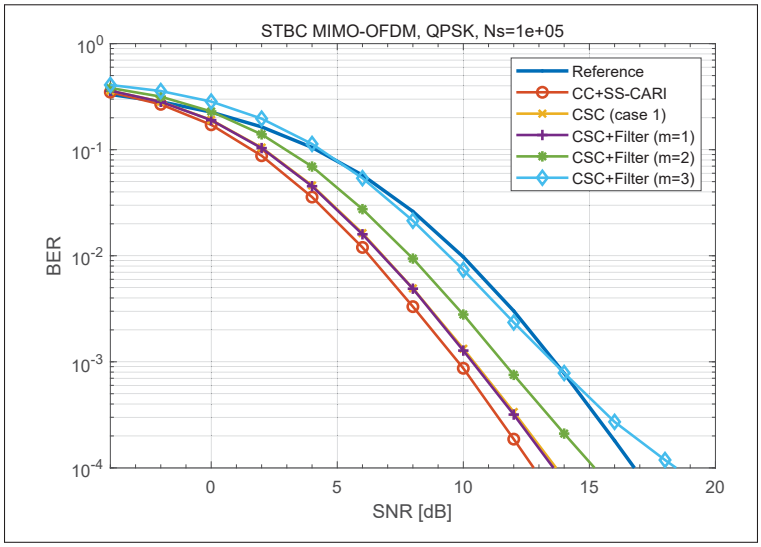

Figure 4.12 BER performance for CSC hybrid PAPR reduction technique with iterative MuCT and filter in STBC MIMO-OFDM system with $R = 1/4$, $V = 4$, $M = 16$, $\mu = 10$, PR $= 1.2$, and $\kappa = 2.7$ (case 1). The reference is the STBC MIMO-OFDM system without coding.

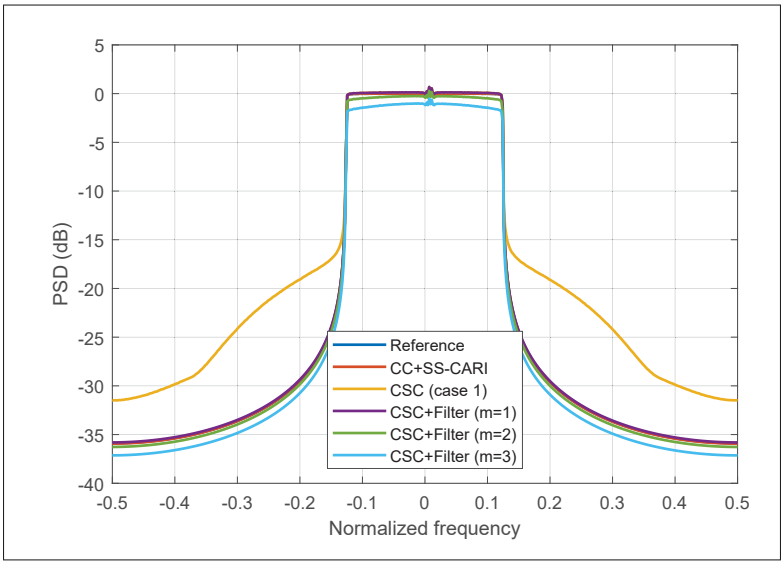

Figure 4.13 PSD curves for CSC hybrid PAPR reduction technique with iterative MuCT and filter in STBC MIMO-OFDM system with $R = 1/4$, $V = 4$, $M = 16$, $\mu = 10$, PR $= 1.2$, and $\kappa = 2.7$ (case 1). The reference is the STBC MIMO-OFDM system without coding.

CONCLUSION AND RECOMMENDATIONS

Summary

In the recent years, MIMO-OFDM has grown to become an essential part of wireless communication systems. It has surfaced in response to the need to meet the challenges imposed by the growing demand for high data rates due to the increased popularity of multimedia services. While MIMO-OFDM represents a high quality method for use in commercial communications, it is nevertheless also widely used in tactical communications and public and safety applications.

Using multi-carrier signals is however accompanied by a high peak-to-average power ratio, which has a significant impact on the performance of non-linear elements at each branch of the transmitter, such as the digital-to-analog converter and high power amplifier. Besides, optimizing the OFDM envelope by reducing the PAPR reduces the system cost by operating the amplifiers more efficiently. Moreover, the PAPR improvement can be converted into range, coverage gain or energy save. For instance, increasing the range is important in tactical communications since it is key to maximize the network coverage.

It is therefore clearly obvious, how crucial it is to include PAPR reduction techniques in current MIMO-OFDM systems.

Recent decades have seen, an extensive study of options to reduce the PAPR, taking into account relevant considerations that may condition the choice of the best technique, such as the PAPR reduction capacity, the BER degradation, the computational complexity, the spectral degradation, additional power requirements at the transmitter, and the need for side information. As a result, numerous methods are available in the literature covering, OFDM signals, which attempt to exploit different characteristics of the multicarrier envelope to produce peak reductions or increase the average power. Thus, according to the taxonomy adopted in this

thesis, these techniques are classified into four categories, namely: coding, multiple signaling and probabilistic, signal distortion, and hybrid.

The study of hybrid techniques has attracted a lot of interest, and it was indeed one of the objectives of this thesis, since such techniques can take advantage of the good results obtained with different methods. For example, we know that distortion techniques are the simplest, and they provide good results in terms of PAPR reduction; however, the distortion scheme can degrade the BER significantly. On the other hand, multiple-signal or probabilistic techniques generally achieve a lower reduction than distortion methods, in addition to increasing the system complexity. Although the former does not degrade the BER, some schemes may require side information, which can make the performance conditional to the excellent reception of side information. Meanwhile, coding techniques have not been widely used in the literature because they can present poor PAPR reduction results in several situations. However, they have the advantage of improving the BER performance. An exciting idea is therefore to combine techniques from each category in a bid to arrive at a hybrid flexible method that can be configured for different conditions according to the net gain required or the need to optimize a given parameter, such as the PAPR, the BER, or the spectral efficiency.

The research developed in this thesis therefore proceeds according to several essential steps:

1. The PAPR reduction techniques in OFDM systems were extensively studied, allowing to classify, compare and analyze existing techniques. Also, we highlighted the advantages and disadvantages of each scheme, as well as the benefits of combining them.
2. We analyzed how to optimize forward error correction codes to reduce the PAPR. To that end, we studied the structure of the codes, their mathematical construction and their relationship with the PAPR.
3. The PAPR problem was analyzed in MIMO-OFDM systems; we started with a review of the techniques proposed in the literature. Although some methods are an extension of

those existing in OFDM, others are new, and adapted to the structure of MIMO trying to take advantage of the multiple antennas system.

4. Working from previous studies, we were able to achieve the main objective of the thesis, that is, to propose a hybrid technique that combines coding techniques with methods that utilize additional degrees of freedom provided by MIMO; we proposed a method in which convolutional codes are optimized to avoid PAPR increases, and we combine the SS-CARI technique, and an iterative companding and filtering scheme to obtain a higher PAPR reduction method.

Thesis Results

After the bibliographic review, multiple techniques that aim to decrease the PAPR in OFDM and MIMO-OFDM systems were found. We concluded that hybrid techniques are a good option for the current requirements of the systems due to the possibility of obtaining high PAPR reduction rates without affecting system performance.

An illustrative comparison between hybrid and individual techniques was presented in Chapter 3. In the simulation, we consider an OFDM system with 512 subcarriers over white Gaussian noise channel, a cyclic prefix length of 128, a binary phase shift keying modulation, and oversampling rate equal to one. One technique of each category was selected: a modified code repetition with majority logic detection plus interleaving and a code rate 1/4, the selected mapping with 4 or 8 phase sequences rotation factor defined by $P_v^u \in [\pm 1, \pm j]$, and the clipping with clipping level equal to 70% and 50%. After analyzing the results, it is clear that the hybrid technique MCR+SLM ($U = 8$) + CP 50% provides a greater reduction of the CCDF of the PAPR, about 8.78 dB, as compared to the conventional OFDM for CCDF, equal to 10^{-4}. Although, clipping technique causes distortion and therefore degradation of the performance, when combining clipping with an error correction technique, the hybrid technique improves

the performance. For example, we can see a gain of 2.16 dB (BER $= 10^{-3}$) when the hybrid technique (MCR + SLM ($U = 8$) + CP 50 %) is added.

The impact of forward error correction on the PAPR for the coded OFDM system was studied based on a relationship that depends only on the data sequence between the autocorrelation function of the IFFT input and the maximum PAPR of the OFDM signal given by an upper bound on the peak factor. The autocorrelation of the coded OFDM was modeled by the Markov Chain Model, and an extensive simulation was done with linear block codes and convolutional codes.

In the case of linear block codes, the simulation examples comprised of codes with colored and white autocorrelations, such as repetition codes, repetition codes plus interleaver and modified repetition codes plus interleaver. As expected, OFDM signals with a large autocorrelation values, such as repetition codes, have a significant PAPR value. We showed that in the repetition codes, the autocorrelation depends directly on the code rate, and an increase in the autocorrelation can produce an increase in the PAPR of the COFDM signal.

The impact of convolutional codes on the PAPR of the OFDM signal was examined based on four parameters, namely, the code rate, the code structure, the free distance, and the constraint length. We showed that a reduction of the code rate could increase the PAPR because such a reduction can increase the generation of all-equal bit sequences in the output of the encoder for two or more states. For the analysis of the code structure, we defined the structure number as the number of consecutive generators exiting in the generation of the convolutional code. We showed that, for most cases, there is a relationship such that for codes with a higher structure number value, a greater autocorrelation is obtained, which can produce an increase in the PAPR. This was fulfilled for the cases presented with code rate $R = 1/2$, $R = 1/8$, and with an exception for the case $R = 1/4$. The free distance was examined as an important parameter that defines the BER performance that reaches the code, and therefore impacts the net system

gain. In this case, we calculated the net gain concerning to the reduction of the PAPR and the BER performance of the system. For the constraint length, it could be concluded that the PAPR performance experiences degradation when the constraint length is low, which is evident for lower values of the code rate. Finally, we calculated the net gain, and showed a strategy for choosing the convolutional code that has the optimal net gain for a specific requirement of PAPR and BER performance.

Several PAPR reduction methods were analyzed for use in a hybrid technique, and in the end, we chose three, namely: convolutional codes, SS-CARI, and companding. The convolutional codes are widely used in current communication systems, both commercial and tactical. Then, it is interesting to optimize these codes according to the reduction of PAPR. Meanwhile, SS-CARI has been considered as a technique that fully optimized the degree of freedom provided by MIMO; it has reduced complexity and does not change the BER. On the other hand, companding was selected because it provides a high PAPR reduction rate, and under a proper configuration of its parameters, the BER degradation can be controlled. Additionally, unlike other distortion techniques, where the peaks of the envelope are cut or reduced, companding modified the average power of the signal, which permits efficient use of an operational amplifier, which in turns considerably impacts the system performance.

The hybrid technique proposed was validated by simulation, and significant results regarding PAPR reduction, BER performance, spectral efficiency, and low complexity were found. Additionally, it was shown to be a flexible technique. The simulation was implemented on an Alamouti STBC MIMO-OFDM system with two transmit, and two receive antennas, 128 subcarriers, a 25% guard interval, QPSK modulation, and an oversampling factor equal to 4, performed by padding zeros to the baseband modulated signals over a Rayleigh channel with Zero Forcing equalization and the algorithm executed $N_s = 10^5$ times.

As a result, we can see a considerable PAPR reduction of ~ 6.6 dB (CCDF $= 10^{-4}$) when using convolutional codes with a code rate equal to $1/4$, a constraint length equal to 4 and the generator polynomial $[13, 15, 15, 17]$, the SS-CARI technique with $M = 16$ subblocks and an iterative companding and filtering with $\mu = 10$, a peak ratio equal to 1.2, $\kappa = 2.7$ and a frequency domain filtering ($m = 2$). Additionally, a BER rate reduction of 2 dB and similar power spectral density as with the basic STBC MIMO-OFDM is obtained with two iterations of companding and filtering blocks. Note that the method is the reduced complexity, and although it requires side information, the SI can be avoided by inserting pilot tones as in a blind cross-antenna successive suboptimal CARI. Also, it is clarified that although the results have been presented for the Alamouti 2x2 case to reduce the computational complexity of the simulation, and this hybrid technique can be extended to another antenna's configuration.

Recommendations for future work

The work presented in this thesis provides interesting methods and results for optimizing the PAPR of the MIMO-OFDM system, but also it can be extended in the following research directions.

1. The work proposed in the manuscript entitled "*Optimizing forward error correction codes for COFDM with reduced PAPR*" (Sandoval *et al.*, 2019a) can be extended by including the comparative analysis with other codes that have been suggested in the literature for PAPR reduction, such as: simple odd parity code (SOPC), complement block coding (CBC), sub-block complementary coding (SBCC), and Golay codes. In addition, codes that are currently being studied for future systems, for example: turbo codes, concatenate codes, low-density parity-check (LDPC) codes, and polar codes.
2. The analyses about the impact of FEC on the PAPR to OFDM systems, presented in Chapter 3, can be extended to single-carrier frequency-division multiple access (SC-FDMA) systems, also known as discrete Fourier transform-spread-OFDM (DFT-s-OFDM). In mo-

bile communications, SC-FDMA has been considered, from the fourth generation (4G), as an attractive alternative to OFDMA, especially for the up-link communications because it presents lower PAPR. Additionally, DFT-s-OFDM was ratified by the 3rd Generation Partnership Project (3GPP) Release 15[1] and it will be also supported on 5G new radio (NR) and used for an enhanced mobile broadband (eMBB) uplink up to at least 40 GHz.

3. According to the 3GPP Release 15, the cyclic prefix OFDM waveform will be supported for both 5G NR download and upload. However, 5G NR introduce scalable OFDM numerology to support diverse spectrum band/types and deployment models (Qualcomm, 2016). An interesting study involves evaluate the PAPR performance for a system with the 5G waveform characteristics in order to optimize the new hybrid PAPR reduction technique for 5G mobile communications.
4. The hybrid technique proposed for MIMO-OFDM system considers a MIMO system with spatial diversity where the STBC structure is used. New studies could analyze the reduction of PAPR in MIMO-OFDM systems with spatial multiplexing. Additionally, hybrid techniques for PAPR reduction can be proposed for massive MIMO system, which is a key technique for 5G communications.
5. A next step in this research may be the implementation of the hybrid technique presented in this work in hardware to verify their performance. For instance, it can be implemented in software defined radio (SDR) systems to verify the performance, the reduction of the PAPR, and the complexity of its implementation. In addition, tests can be performed to verify the gain in range and coverage when the PAPR is reduced under the parameters of tactical communications systems.

[1] https://www.3gpp.org/release-15

APPENDIX I

SYSTEMATIC LITERATURE REVIEW RESULTS

Table-A I-1 Articles per PAPR reduction technique

Category	Technique	Reference
Coding	Coding	Al-akaidi *et al.* (2006); Venkataraman *et al.* (2006); Fischer & Siegl (2009); Jinlong & Yuehong (2009)
Multiple Signal and Probabilistic	Active constellation extension	Woo & Jones (2005); Naeiny & Marvasti (2011); Krongold *et al.* (2005); Tsiligkaridis & Jones (2010)
	CARI or CFPI	Ouyang (2009); Huang & Li (2007); Su *et al.* (2011); Chang *et al.* (2014); Tan *et al.* (2005); Li *et al.* (2007)
	Precoding	Cha *et al.* (2014); Nandi *et al.* (2009); Zhu *et al.* (2009); Aggarwal *et al.* (2006); Beko *et al.* (2015); Cha & Kim (2017); Ayaz *et al.* (2013); Kim *et al.* (2008); Elavarasan *et al.* (2012); Chen & Ansari (2007); Baig *et al.* (2011); Malkin *et al.* (2008); Cha & Kim (2016); Gao *et al.* (2009); Sujatha & Dananjayan (2014); Ahirwar & Rajan (2005); Jiang *et al.* (2004a); Wu *et al.* (2011); Hao *et al.* (2011); Kim & Jung (2017)
	PTS	Schenk *et al.* (2006); Ishida *et al.* (2007); WANG & feng TAO (2007); Wang *et al.* (2007); Guo-fang *et al.* (2008); Yan *et al.* (2009b); Mata *et al.* (2009); Zhang *et al.* (2010); Phetsomphou *et al.* (2010); Wang & Liu (2011); Mouhib *et al.* (2011); Li *et al.* (2012); Rani & Saini (2012); Hassaneen *et al.* (2013a,b); MANJITH & SUGANTHI (2013); Li *et al.* (2013); Inoue *et al.* (2013); Jiang *et al.* (2014); Ku (2014); Manjith & Suganthi (2014); Bouaziz & Rekkal (2015); Vidya *et al.* (2015); Amhaimar *et al.* (2016); Lahcen *et al.* (2017)
	SLM	Sghaier *et al.* (2015); Hassan *et al.* (2009); Alharbi & Chambers (2008b); Asseri *et al.* (2008); Gao *et al.* (2008); Fischer & Hoch (2007); Lee *et al.* (2003); Tsai *et al.* (2008); Jeon *et al.* (2011); Li *et al.* (2010a); Wang *et al.* (2011); Alharbi & Chambers (2008a); Joo *et al.* (2010); Park *et al.* (2013); Lee & de Figueiredo (2010); Ouyang & Ding (2015); Hsueh *et al.* (2012); Fischer & Hoch (2006); Jiang *et al.* (2013); Taşpınar & Yıldırım (2015); Bassem *et al.* (2007); Hu *et al.* (2013); Sghaier *et al.* (2013); Baek *et al.* (2005); Siegl & Fischer (2008); Chanpokapaiboon *et al.* (2011); Gao *et al.* (2007); Suyama *et al.* (2006); Umeda *et al.* (2010); Abdullah *et al.* (2017)
	SLM and PTS	Somasekhar & Mallikarjunaprasad (2014); Trang *et al.* (2005); Baek *et al.* (2004); Moon *et al.* (2003); Suyama *et al.* (2009); Khan *et al.* (2010)
	Tone reservation	Manasseh *et al.* (2013); Rihawi *et al.* (2007); Deng *et al.* (2014); Ni *et al.* (2016); Henkel *et al.* (2012); Zhang & Goeckel (2007)
	Wavelet entropy algorithm	Damati *et al.* (2014); Hamarsheh *et al.* (2014)
	Others	Vijayalaxmi & Narayana Reddy (2016); Bao *et al.* (2016b); Hung & Tsai (2014); Wakeel & Henkel (2014a); Studer & Larsson (2013); Jiang & Li (2012); Jaganathan & Narasimhan (2008); Ryu (2008); Li & Xia (2007); Latinovic & Bar-Ness (2006); Wang & Li (2009); Khademi *et al.* (2012); Khademi & van der Veen (2013); Li *et al.* (2010b); Luo *et al.* (2015); Karimi *et al.* (2014); Zhu *et al.* (2011); Wang & Bar-Ness (2006); Ouyang *et al.* (2013); Yao & Hu (2013); Wu *et al.* (2008); SHIN & SEO (2014); Gong & Shao (2010); Wang & Wang (2007); Pérez & Jiménez (2017); Wakeel & Henkel (2014b); Fischer & Siegl (2010); Sghaier *et al.* (2016); Kota *et al.* (2016); Bao *et al.* (2016a); Arvola *et al.* (2016); Wang *et al.* (2010); Li & Xia (2008); Lee *et al.* (2005); Yan *et al.* (2009a); Ramaswamy & Reddy (2016)
Signal Distortion	Clipping	Xia *et al.* (2005); Kwon *et al.* (2007); Zhu (2012); Bittner *et al.* (2008); Kwon *et al.* (2009); Kim & Daneshrad (2009); Singh & Kumar (2016)
	Peak cancellation	Braz *et al.* (2010); Kageyama *et al.* (2015)
Hybrid	Hybrid	Verma & Tharani (2016); Tiwari *et al.* (2014); Sheikh *et al.* (2013); Manasseh *et al.* (2012); Siegl & Fiserch (2007); Mukunthan & Dananjayan (2013); Yue & Wang (2006); Pachori & Mishra (2016b); He *et al.* (2011); Pachori & Mishra (2016a); Kimura *et al.* (2011); Daoud & Damati (2010); Pandurangan & Perumal (2011); Ezri & Tsodik (2012)

Table-A I-2 Precoding techniques

Technique	Reference
Redundant spatial resources at the transmitter through a singular-value-decomposition-based generalized inverse	Cha *et al.* (2014)
Nonredundant linear precoding with pseudo-noise (PN) sequence	Nandi *et al.* (2009)
Multi-layer precoding: outer-layer (trellis exploration algorithm) reduce PAPR, inner-layer (optimal power allocation)	Zhu *et al.* (2009)
Convex optimization technique subject to a constraint on constellation error vector magnitude (EVM)	Aggarwal *et al.* (2006)
Iterative sphere-geodesic descent method (GDM)	Beko *et al.* (2015)
Convex problem formulation	Cha & Kim (2017)
Discrete-cosine transform matrix (DCTM)	Ayaz *et al.* (2013)
Hidden pilot scheme, based on orthogonal polyphase sequences	Kim *et al.* (2008)
Square Root Raised Cosine Function and Trapezoidal function	Elavarasan *et al.* (2012)
Frame precoding: Erasure Pattern Selection (EPS)	Chen & Ansari (2007)
Zadoff-Chu matrix transform (ZCMT)	Baig *et al.* (2011)
Solving the optimization problem using an interior-point method (IPM) based on the conjugate-gradient (CG) algorithm	Malkin *et al.* (2008)
Block diagonalization (BD) precoding scheme	Cha & Kim (2016)
Non-redundant linear precoding, PN sequences	Gao *et al.* (2009)
Inverse Discrete Cosine Transform (IDCT) along with constant modulus algorithm	Sujatha & Dananjayan (2014)
Inverse Discrete Fourier Transform (IDFT) and Hadamard transform	Ahirwar & Rajan (2005)
Nonlinear spatial precoder	Jiang *et al.* (2004a)
DFT-precoding combined with spatial precoding	Wu *et al.* (2011)
Minimum error probability based precoding matrix	Hao *et al.* (2011)
Hidden training sequence-aided precoding scheme	Kim & Jung (2017)

Table-A I-3 Selected mapping techniques

Technique	Comments	w/wo SI	Complexity	Reference
directed SLM (dSLM)	Modified receiver based on Zero-Forcing (ZF)	without	low	Asseri *et al.* (2008)
directed SLM (dSLM)	Summarize: oSLM, sSLM, and dSLM	without	low	Fischer & Hoch (2007)
directed SLM (dSLM)	Original directed SLM	with	low	Fischer & Hoch (2006)
concurrent SLM (cSLM)	Original concurrent SLM	with	moderate	Lee *et al.* (2003)
concurrent SLM (cSLM)	"Only embed the SI in the first/second symbols of the first antenna and use SI power allocation technique to protect SI"Lee & de Figueiredo (2010)	with		Lee & de Figueiredo (2010)
concurrent SLM (cSLM)	"Exploits the associated antenna diversity gain to mitigate errors in the transmission of the SI" Alharbi & Chambers (2008b)	with		Alharbi & Chambers (2008b)
concurrent SLM (cSLM)	"Reduce complexity by the conjugate symbols on two antennas have the same PAPR property with STBC" Gao *et al.* (2007)	with	low	Gao *et al.* (2007)
cSLM, low complexity	"Large number of candidate signal sets in the time domain without performing an extra IFFT calculation" Wang *et al.* (2011)		low	Wang *et al.* (2011)
low complexity	"Generates alternative signal sequences by simply adding mapping signal sequences to an OFDM signal"Jeon *et al.* (2011)		low	Jeon *et al.* (2011)
low complexity	Time-domain circular shift (TDCS) scheme		low	Tsai *et al.* (2008)
low-complexity	low-complexity transmitter architecture	without	low	Li *et al.* (2010a)
Blind SLM (BSLM)	For STBC	without		Sghaier *et al.* (2015)
Blind SLM (BSLM)	Blind SLM using cyclic shift (BSLM-CS)			Joo *et al.* (2010)
Blind SLM (BSLM)	Pilot-assisted blind selected mapping (PB-SLM)	without		Park *et al.* (2013)
Combined SLM-Alamouti		without		Sghaier *et al.* (2013)
SLM	Based on STBC/SFBC			Ouyang & Ding (2015)
modified SLM (mSLM)	"Rotating two symbols in the OFDM frame in place of sending useful information in combination with the SLM" Alharbi & Chambers (2008a)	with		Alharbi & Chambers (2008a)
small overhead SLM (s-SLM)	Reduce the SI	with		Hassan *et al.* (2009)
decomposed iSLM (D-iSLM), and decomposed cSLM (D-cSLM)	"Reduce the SI. The real and imaginary part of the transmitted signals are treated separately"Gao *et al.* (2008)			Gao *et al.* (2008)
iSLM and cSLM		with	high	Baek *et al.* (2005)
enhanced SLM (ESLM)	Subcarrier phase hopping for space division multiplexing (SPH-SDM) with an enhanced selected mapping (ESLM)			Suyama *et al.* (2006)
SLM	SLM in combination with Subband Permutation			Bassem *et al.* (2007)
directed SLM (dSLM)	Temporal directed and spatial simplified SLM (dsSLM) in a broascast	without	low	Siegl & Fischer (2008)
block diagonalization SLM (BD-SLM)				Umeda *et al.* (2010)
iSLM	SLM Technique with Centering Phase Sequence Matrix			Chanpokapaiboon *et al.* (2011)
cross-modified SLM	Combine cross-individual SLM with modified-individual SLM			Hsueh *et al.* (2012)
phase offset SLM (P-SLM)	Maintains the structure of the Alamouti SFBC	without		Jiang *et al.* (2013)
extended SLM (eSLM)		without		Hu *et al.* (2013)
SLM	based on parallel artificial bee colony (P-ABC) algorithm1. Proposed ABC Based SLM Algorithm2. Proposed ABC/best/1 and MABC/best/1 Based SLMAlgorithms			Taşpınar & Yıldırım (2015)
SCS-SLM	Selective Codeword Shift (SCS)			Abdullah *et al.* (2017)

Table-A I-4 Partial transmit sequence techniques

Technique	Reference
Spatial shifting (SS) of PTS	Schenk *et al.* (2006)
Subcarrier-Block Phase Hopping: Combining subcarrier phase hopping for space division multiplexing (SPH-SDM) and PTS	Ishida *et al.* (2007)
One optimal inter-subblock shifting and inversion (IASSI) and two simple suboptimal	WANG & feng TAO (2007)
Optimal inter-antenna and subblock shifting and inversion (IASSI) and two suboptimal IASSI schemes	Wang *et al.* (2007)
Dynamic PTS with guided scrambling	Guo-fang *et al.* (2008)
PTS with the multi-antenna cooperative working	Yan *et al.* (2009b)
Concurrent algorithm with Improved-PTS method (NCI-PTS)	Mata *et al.* (2009)
Optimum Combination of PTS	Zhang *et al.* (2010)
Based on oPTS	Phetsomphou *et al.* (2010)
Cooperative PTS (co-PTS)	Wang & Liu (2011)
Boolean Particle Swarm intelligence Optimization (BPSO) applied to PTS (BPSO/PTS)	Mouhib *et al.* (2011)
Cooperative and alternate PTS (C-A-PTS)	Li *et al.* (2012)
Cooperative PTS (Co-PTS)	Rani & Saini (2012)
Modified PTS with circular shifting	Hassaneen *et al.* (2013a)
Modified PTS with circular shifting	Hassaneen *et al.* (2013b)
PTS based Bacterial Foraging Optimization Algorithm (BFOA-PTS)	MANJITH & SUGANTHI (2013)
Improved PTS algorithm	Li *et al.* (2013)
Coded PTS	Inoue *et al.* (2013)
Phase offset-based PTS (P-PTS)	Jiang *et al.* (2014)
Low complexity PTS: Method of joint sample-selection between antennas	Ku (2014)
Bacterial Foraging Optimization (BFO) and Modified Cuckoo Search algorithm (MCS) (HBFOMCS-PTS)	Manjith & Suganthi (2014)
Based on cooperative and alternate PTS (C-A-PTS)	Bouaziz & Rekkal (2015)
Adjacent partitioning technique of PTS	Vidya *et al.* (2015)
Based on individual PTS (iPTS)	Amhaimar *et al.* (2016)
Low complexity PTS based on iPTS	Lahcen *et al.* (2017)

Table-A I-5 Tone reservation techniques

Technique	Reference
Constrained adaptive Markov chain Monte Carlo (CAMCMC) technique to select peak reduction tones (PRT)	Manasseh *et al.* (2013)
Formulated as second order cone programming problem (SOCP)	Rihawi *et al.* (2007)
It scheme takes signals on both antennas into account when designing the peak reduction symbols.	Deng *et al.* (2014)
Adaptive tone reservation (ATR)	Ni *et al.* (2016)
Multi-user TR and others techniques	Henkel *et al.* (2012)
Interior-point method (IPM) and gradient descent method	Zhang & Goeckel (2007)

Table-A I-6 Clipping techniques

Technique	Number of articles	Reference
Clipping	2	Zhu (2012); Kim & Daneshrad (2009)
Clipping and filtering	1	Bittner *et al.* (2008)
Clipping and iterative reconstruction	3	Xia *et al.* (2005); Kwon *et al.* (2007, 2009)
Adaptive Clipping	1	Singh & Kumar (2016)

Table-A I-7 Hybrid PAPR reduction techniques

Hybrid			Reference
Technique 1	**Technique 2**	**Technique 3**	
Clipping and filtering	PTS		Verma & Tharani (2016)
PTS	SLM		Tiwari *et al.* (2014)
Orthogonal space time block code (OS-TBC)	SLM	Spreading code	Sheikh *et al.* (2013)
Phase information of the pilot symbols	Tone reservation		Manasseh *et al.* (2012)
Interleaving	Modified PTS	Pulse shaping	Mukunthan & Dananjayan (2013)
Coding	SLM	Clipping	Yue & Wang (2006)
Neural network based trained module of approximate gradient project scheme (AGP-NN)	PTS		Pachori & Mishra (2016b)
Simplified tone reservation	cross antenna rotation and inversion (CARI)		He *et al.* (2011)
Active gradient project (AGP)	PTS		Pachori & Mishra (2016a)
linear coding	PTS	Genetic alhorithm (GA)	Daoud & Damati (2010)
FECs	PTS		Pandurangan & Perumal (2011)
Precoding	Clipping and filtering		Kimura *et al.* (2011)
Precoding	SLM		Ezri & Tsodik (2012)
Precoding	SLM		Siegl & Fiserch (2007)

BIBLIOGRAPHY

Abdullah, E., Idris, A. & Saparon, A. (2017). PAPR REDUCTION USING SCS-SLM TECHNIQUE IN STFBC MIMO-OFDM. *ARPN Journal of Engineering and Applied Sciencies*, 12(10), 3218-3221.

Abouda, A. A. (2004, June). PAPR reduction of OFDM signal using turbo coding and selective mapping. *Proceedings of the 6th Nordic Signal Processing Symposium, 2004. NORSIG 2004.*, pp. 248-251.

Aggarwal, A., Stauffer, E. R. & Meng, T. H. (2006, June). Optimal Peak-to-Average Power Ratio Reduction in MIMO-OFDM Systems. *2006 IEEE International Conference on Communications*, 7, 3094-3099. doi: 10.1109/ICC.2006.255280.

Ahirwar, V. & Rajan, B. S. (2005, Nov). Low PAPR full-diversity space-frequency codes for MIMO-OFDM systems. *GLOBECOM '05. IEEE Global Telecommunications Conference, 2005.*, 3, 5 pp.-. doi: 10.1109/GLOCOM.2005.1577896.

Al-akaidi, M. M., Daoud, O. R. & Gow, J. A. (2006). MIMO-OFDM-based DVB-H systems: a hardware design for a PAPR reduction technique. *IEEE Transactions on Consumer Electronics*, 52(4), 1201-1206. doi: 10.1109/TCE.2006.273134.

Alamouti, S. M. (1998). A simple transmit diversity technique for wireless communications. *IEEE Journal on Selected Areas in Communications*, 16(8), 1451-1458. doi: 10.1109/49.730453.

Alharbi, F. S. & Chambers, J. A. (2008a, Aug). A combined SLM and closed-loop QO-STBC for PAPR mitigation in MIMO-OFDM transmission. *2008 16th European Signal Processing Conference*, pp. 1-4.

Alharbi, F. S. & Chambers, J. A. (2008b, March). Peak-to-average power ratio mitigation in quasi-orthogonal space time block coded MIMO-OFDM systems using selective mapping. *2008 Loughborough Antennas and Propagation Conference*, pp. 157-160. doi: 10.1109/LAPC.2008.4516890.

Amhaimar, L., Ahyoud, S., Asselman, A. & Said, E. (2016). Peak-to-Average Power ratio reduction based varied Phase for MIMO-OFDM Systems. *International Journal of Advanced Computer Science and Applications*, 7(9), 432–437.

Anoh, K., Tanriover, C. & Adebisi, B. (2017). On the Optimization of Iterative Clipping and Filtering for PAPR Reduction in OFDM Systems. *IEEE Access*, 5, 12004-12013. doi: 10.1109/ACCESS.2017.2711533. DOI: 10.1109/ACCESS.2017.2711533.

Armstrong, J. (2001). New OFDM peak-to-average power reduction scheme. *IEEE VTS 53rd Vehicular Technology Conference, Spring 2001. Proceedings (Cat. No.01CH37202)*, 1, 756-760 vol.1. doi: 10.1109/VETECS.2001.944945.

Armstrong, J. (2002). Peak-to-average power reduction for OFDM by repeated clipping and frequency domain filtering. *Electronics Letters*, 38(5), 246-247. DOI: 10.1049/el: 20020175.

Arvola, A., Tölli, A. & Gesbert, D. (2016, Nov). A user cooperative beamforming approach to PAPR reduction in MIMO-OFDM uplink. *2016 50th Asilomar Conference on Signals, Systems and Computers*, pp. 691-695. doi: 10.1109/ACSSC.2016.7869133.

Asseri, M. I., Sharif, B. S., Goff, S. Y. L. & Tsimenidis, C. C. (2008, Nov). Reduced complexity dSLM recovery in MIMO-OFDM without side information. *2008 1st IFIP Wireless Days*, pp. 1-5. doi: 10.1109/WD.2008.4812835.

Ayaz, M., Baig, I., Ahmad, I. & Alelaiwi, A. A. (2013). PAPR Reduction in Underwater Acoustic Sensor Networks: A Discrete Cosine Transform Matrix Precoding Based MIMO-OFDM System. *International Information Institute (Tokyo).Information*, 16(5), 2977-2985. Consulted at https://search.proquest.com/docview/1406224947?accountid= 27231. Copyright - Copyright International Information Institute May 2013; Document feature - Diagrams; Equations; Graphs; ; Last updated - 2016-07-30.

Baek, M.-S., Kim, M.-J., You, Y.-H. & Song, H.-K. (2004). Semi-blind channel estimation and PAR reduction for MIMO-OFDM system with multiple antennas. *IEEE Transactions on Broadcasting*, 50(4), 414-424. doi: 10.1109/TBC.2004.837885.

Baek, M.-S., Yeo, S.-Y., Kim, M.-J., You, Y.-H. & Song, H.-K. (2005, Jan). PAR reduction scheme for next generation wireless LAN system with multiple antennas. *2005 Digest of Technical Papers. International Conference on Consumer Electronics, 2005. ICCE.*, pp. 319-320. doi: 10.1109/ICCE.2005.1429846.

Baig, I., Jeoti, V. & Drieberg, M. (2011, Sept). A ZCMT precoding based STBC MIMO-OFDM system with reduced PAPR. *2011 National Postgraduate Conference*, pp. 1-5. doi: 10.1109/NatPC.2011.6136332.

Bao, H., Fang, J., Chen, Z., Li, H. & Li, S. (2016a). An Efficient Bayesian PAPR Reduction Method for OFDM-Based Massive MIMO Systems. *IEEE Transactions on Wireless Communications*, 15(6), 4183-4195. doi: 10.1109/TWC.2016.2536662.

Bao, H., Fang, J., Chen, Z. & Jiang, T. (2016b). Perturbation-Assisted PAPR Reduction for Large-Scale MIMO-OFDM Systems via ADMM. *CoRR*, abs/1607.02681. Consulted at http://arxiv.org/abs/1607.02681.

Bassem, B. J. A., Slaheddine, J. & Ammar, B. (2007, March). A PAPR Reduction Method for STBC MIMO-OFDM Systems Using SLM in Combination with Subband Permutation. *Wireless and Mobile Communications, 2007. ICWMC '07. Third International Conference on*, pp. 88-88. doi: 10.1109/ICWMC.2007.5.

Bauml, R. W., Fischer, R. F. H. & Huber, J. B. (1996). Reducing the peak-to-average power ratio of multicarrier modulation by selected mapping. *Electronics Letters*, 32(22), 2056-2057. DOI: 10.1049/el:19961384.

Bäuml, R. W., Fischer, R. F. & Huber, J. B. (1996). Reducing the peak-to-average power ratio of multicarrier modulation by selected mapping. *Electronics Letters*, 32(22), 2056–2057.

Baxley, R. J. & Zhou, G. T. (2004). Power savings analysis of peak-to-average power ratio in OFDM. *IEEE Transactions on Consumer Electronics*, 50(3), 792-798. DOI: 10.1109/TCE.2004.1341681.

Beko, M., Dinis, R., Dimić, G., Tuba, M. & Montezuma, P. (2015, Nov). A geodesic descent technique for PAPR reduction in MIMO-OFDM. *2015 23rd Telecommunications Forum Telfor (TELFOR)*, pp. 492-495. doi: 10.1109/TELFOR.2015.7377514.

Benchimol, I. B., Pimentel, C., Souza, R. D. & Uchôa-Filho, B. F. (2014). A new computational decoding complexity measure of convolutional codes. *EURASIP Journal on Advances in Signal Processing*, 2014(1), 173. doi: 10.1186/1687-6180-2014-173.

Bilardi, G., Padovani, R. & Pierobon, G. (1983). Spectral Analysis of Functions of Markov Chains with Applications. *IEEE Transactions on Communications*, 31(7), 853-861. doi: 10.1109/TCOM.1983.1095910. DOI: 10.1109/TCOM.1983.1095910.

Bittner, S., Zillmann, P. & Fettweis, G. (2008, May). Equalisation of MIMO-OFDM Signals Affected by Phase Noise and Clipping and Filtering. *2008 IEEE International Conference on Communications*, pp. 609-614. doi: 10.1109/ICC.2008.120.

Bouaziz, S. & Rekkal, K. (2015, Nov). A PAPR reduction for STBC MIMO-OFDM systems in 4G wireless communications using PTS scheme. *2015 First International Conference on New Technologies of Information and Communication (NTIC)*, pp. 1-5. doi: 10.1109/NTIC.2015.7368744.

Braz, I., Guan, L., Zhu, A. & Brazil, T. J. (2010, Sept). PAPR reduction technique using unused subcarriers for SFBC-based MIMO-OFDM systems. *The 3rd European Wireless Technology Conference*, pp. 141-144.

Breiling, H., Muller-Weinfurtner, S. H. & Huber, J. B. (2001). SLM peak-power reduction without explicit side information. *IEEE Communications Letters*, 5(6), 239-241. DOI: 10.1109/4234.929598.

Breiling, M., Miiller-Weinfurtner, S. H. & Huber, J. B. (2000). Distortionless reduction of peak power without explicit side information. *Global Telecommunications Conference, 2000. GLOBECOM '00. IEEE*, 3, 1494-1498.

Britto, R. & Usman, M. (2015, Oct). Bloom's taxonomy in software engineering education: A systematic mapping study. *2015 IEEE Frontiers in Education Conference (FIE)*, pp. 1-8. doi: 10.1109/FIE.2015.7344084.

Bruninghaus, K. & Rohling, H. (1998, May). Multi-carrier spread spectrum and its relationship to single-carrier transmission. *Vehicular Technology Conference, 1998. VTC 98. 48th IEEE*, 3, 2329-2332.

Budisin, S. (1992, Sep). Golay complementary sequences are superior to PN sequences. *[Proceedings 1992] IEEE International Conference on Systems Engineering*, pp. 101-104.

c. Tsai, Y., k. Deng, S., c. Chen, K. & c. Lin, M. (2008). Turbo Coded OFDM for Reducing PAPR and Error Rates. *IEEE Transactions on Wireless Communications*, 7(1), 84-89. DOI: 10.1109/TWC.2008.060610.

Carson, N. & Gulliver, T. A. (2002). PAPR reduction of OFDM using selected mapping, modified RA codes and clipping. *Proceedings IEEE 56th Vehicular Technology Conference*, 2, 1070-1073.

Cha, H. S. & Kim, D. K. (2017). A Desired PAR-Achieving Precoder Design for Multiuser MIMO OFDM Based on Concentration of Measure. *IEEE Signal Processing Letters*, 24(3), 284-288. doi: 10.1109/LSP.2016.2635978.

Cha, H. S., Chae, H., Kim, K., Jang, J., Yang, J. & Kim, D. K. (2014). Generalized Inverse Aided PAPR-Aware Linear Precoder Design for MIMO-OFDM System. *IEEE Communications Letters*, 18(8), 1363-1366. doi: 10.1109/LCOMM.2014.2328177.

Cha, H.-S. & Kim, D. K. (2016). PAR-Constrained Multiuser MIMO OFDM based on Convex Optimization and Concentration of Measure. *arXiv preprint arXiv:1603.01991*.

Chang, B., Li, H. & Gao, W. T. (2014, Sept). A low-complexity scheme for PAPR reduction without side information in STBC-OFDM systems. *2014 IEEE 10th International Conference on Intelligent Computer Communication and Processing (ICCP)*, pp. 305-310. doi: 10.1109/ICCP.2014.6937013.

Chanpokapaiboon, T., Puttawanchai, P. & Suksompong, P. (2011, May). Enhancing PAPR performance of MIMO-OFDM systems using SLM technique with centering phase sequence matrix. *The 8th Electrical Engineering/ Electronics, Computer, Telecommunications and Information Technology (ECTI) Association of Thailand - Conference 2011*, pp. 405-408. doi: 10.1109/ECTICON.2011.5947860.

Chen, G. & Ansari, R. (2007, Oct). Frame Expansion Based Peak to Average Power Ratio Reduction in MIMO OFDM Systems. *2007 IEEE Workshop on Signal Processing Systems*, pp. 61-66. doi: 10.1109/SIPS.2007.4387518.

Chen, H. & Liang, H. (2007a). Combined Selective Mapping and Binary Cyclic Codes for PAPR Reduction in OFDM Systems. *IEEE Transactions on Wireless Communications*, 6(10), 3524-3528. DOI: 10.1109/TWC.2007.060145.

Chen, H. & Liang, H. (2007b, March). A Modified Selective Mapping with PAPR Reduction and Error Correction in OFDM Systems. *2007 IEEE Wireless Communications and Networking Conference*, pp. 1329-1333.

Chen, H. & Haimovich, A. M. (2003). Iterative estimation and cancellation of clipping noise for OFDM signals. *IEEE Communications Letters*, 7(7), 305-307. DOI: 10.1109/LCOMM.2003.814720.

Cho, Y. S., Kim, J., Yang, W. Y. & Kang, C. G. (2010a). MIMO-OFDM Wireless Communications with MATLAB (ch. 7, pp. 209-250). Wiley-IEEE Press.

Cho, Y. S., Kim, J., Yang, W. Y. & Kang, C. G. (2010b). MIMO-OFDM Wireless Communications with MATLAB (ch. 10, pp. 281-318). Wiley-IEEE Press.

Choubey, K. & HOD, P. J. (2014). PAPR Reduction using Clipping with FEC Coding in OFDM System. *International Journal of Engineering Research and Technology*, 3(1 (January-2014)).

Choubey, K. & Jain, P. (2014). PAPR Reduction using Companding and FEC Coding in OFDM System. *International Journal of Scientific & Engineering Research*, 5(1), 2150.

Cimini, L. J. & Sollenberger, N. R. (2000). Peak-to-average power ratio reduction of an OFDM signal using partial transmit sequences. *Communications Letters, IEEE*, 4(3), 86–88.

Cuteanu, E.-V. & Isar, A. (2012). PAPR Reduction of OFDM Signals using Partial Transmit Sequence and Clipping Hybrid Scheme. *The Eight Advanced International Conference on Telecommunications*, pp. 164–171.

Damati, A., Daoud, O. & Hamarsheh, Q. (2014, Feb). Wavelet transform basis to detect the odd peaks in wireless systems. *2014 IEEE 11th International Multi-Conference on Systems, Signals Devices (SSD14)*, pp. 1-5. doi: 10.1109/SSD.2014.6808766.

Daoud, O. & Damati, A. (2010, June). Improving the MIMO-OFDM systems performance-based GA. *The IEEE symposium on Computers and Communications*, pp. 1012-1016. doi: 10.1109/ISCC.2010.5546598.

Davis, J. A. & Jedwab, J. (1999). Peak-to-mean power control in OFDM, Golay complementary sequences, and Reed-Muller codes. *IEEE Transactions on Information Theory*, 45(7), 2397-2417. DOI: 10.1109/18.796380.

Deng, X., Jiang, T., Zhou, Y., Ye, C. & Qi, Q. (2014). Peak-to-average power ratio reduction in space frequency block coding multi-input multi-output orthogonal frequency division multiplexing systems by tone reservation. *International Journal of Communication Systems*, 27(12), 3874–3883. doi: 10.1002/dac.2582.

Dyba, T., Dingsoyr, T. & Hanssen, G. K. (2007, Sept). Applying Systematic Reviews to Diverse Study Types: An Experience Report. *First International Symposium on Empirical Software Engineering and Measurement (ESEM 2007)*, pp. 225-234. doi: 10.1109/ESEM.2007.59.

Elavarasan, P., Nagarajan, G. & Narayanan, A. (2012, Aug). PAPR reduction in MIMO-OFDM systems using joint channel estimation and Precoding. *2012 IEEE International Conference on Advanced Communication Control and Computing Technologies (ICACCCT)*, pp. 327-331. doi: 10.1109/ICACCCT.2012.6320796.

Elmasry, G. F. (2010). A comparative review of commercial vs. tactical wireless networks. *IEEE Communications Magazine*, 48(10), 54-59. DOI: 10.1109/MCOM.2010.5594677.

Ermolova, N. Y. & Vainikainen, P. (2003). On the relationship between peak factor of a multicarrier signal and aperiodic autocorrelation of the generating sequence. *IEEE Communications Letters*, 7(3), 107-108. doi: 10.1109/LCOMM.2003.809996. DOI: 10.1109/LCOMM.2003.809996.

Ezri, D. & Tsodik, G. (2012, April). PAPR reduction in MIMO OFDM using unitary matrix precoding. *European Wireless 2012; 18th European Wireless Conference 2012*, pp. 1-3.

Fischer, R. F. H. & Hoch, M. (2007, June). Peak-to-Average Power Ratio Reduction in MIMO OFDM. *2007 IEEE International Conference on Communications*, pp. 762-767. doi: 10.1109/ICC.2007.130.

Fischer, R. F. H. & Siegl, C. (2009, June). Successive PAR Reduction in (MIMO) OFDM. *2009 IEEE International Conference on Communications*, pp. 1-5. doi: 10.1109/ICC.2009.5199497.

Fischer, R. & Hoch, M. (2006). Directed selected mapping for peak-to-average power ratio reduction in MIMO OFDM. *Electronics Letters*, 42, 1289-1290(1). Consulted at http://digital-library.theiet.org/content/journals/10.1049/el_20062668.

Fischer, R. F. H. & Siegl, C. (2010). Probabilistic signal shaping in MIMO OFDM via successive candidate generation. *European Transactions on Telecommunications*, 21(7), 648–654. doi: 10.1002/ett.1416.

Foschini, G. J. (1996). Layered space-time architecture for wireless communication in a fading environment when using multi-element antennas. *Bell labs technical journal*, 1(2), 41–59.

Frontana, E. & Fair, I. (2007, Aug). Avoiding PAPR degradation in Convolutional Coded OFDM Signals. *2007 IEEE Pacific Rim Conference on Communications, Computers and Signal Processing*, pp. 312-315. doi: 10.1109/PACRIM.2007.4313237.

Galda, D. & Rohling, H. (2002). A low complexity transmitter structure for OFDM-FDMA uplink systems. *Vehicular Technology Conference. IEEE 55th Vehicular Technology Conference. VTC Spring 2002 (Cat. No.02CH37367)*, 4, 1737-1741.

Gao, J., Wang, J. & Wang, Y. (2007, Sept). A Low Complexity PAPR Reduction Technique for STBC MIMO-OFDM System. *2007 International Conference on Wireless Communications, Networking and Mobile Computing*, pp. 109-112. doi: 10.1109/WICOM.2007.34.

Gao, J., Wang, J. & Xie, Z. (2008, Oct). Decomposed selected mapping for peak-to-average power ratio reduction in MIMO-OFDM systems. *2008 9th International Conference on Signal Processing*, pp. 1900-1903. doi: 10.1109/ICOSP.2008.4697513.

Gao, J., Zhu, X. & Nandi, A. K. (2009). Non-redundant precoding and PAPR reduction in MIMO OFDM systems with ICA based blind equalization. *IEEE Transactions on Wireless Communications*, 8(6), 3038-3049. doi: 10.1109/TWC.2009.080541.

Gesbert, D., Shafi, M., Shiu, D.-s., Smith, P. J. & Naguib, A. (2003). From theory to practice: an overview of MIMO space-time coded wireless systems. *Selected Areas in Communications, IEEE Journal on*, 21(3), 281–302.

Ghassemi, A. & Gulliver, T. A. (2008). Partial Selective Mapping OFDM with Low Complexity IFFTs. *IEEE Communications Letters*, 12(1), 4-6. DOI: 10.1109/LCOMM.2008.071397.

Ghassemi, A. & Gulliver, T. A. (2010). PAPR reduction of OFDM using PTS and error-correcting code subblocking - Transactions Papers. *IEEE Transactions on Wireless Communications*, 9(3), 980-989. DOI: 10.1109/TWC.2010.03.061099.

Goff, S. Y. L., Al-Samahi, S. S., Khoo, B. K., Tsimenidis, C. C. & Sharif, B. S. (2009). Selected mapping without side information for PAPR reduction in OFDM. *IEEE Transactions on Wireless Communications*, 8(7), 3320-3325. DOI: 10.1109/TWC.2009.070463.

Goldsmith, A. (2004). Wireless communications. United States of America: Cambridge University Press.

Gong, P. & Shao, Z. (2010, Dec). PAPR reduction scheme in SFBC MIMO-OFDM based on transformation. *International Conference on Computational Problem-Solving*, pp. 108-110.

Guo-fang, D., Fei, G., Fan, J. & Zi-bin, Z. (2008, July). Enhancement of PAPR reduction using dynamic PTS algorithm in multiple antennas system. *2008 8th IEEE International Conference on Computer and Information Technology*, pp. 613-617. doi: 10.1109/CIT.2008.4594745.

Hamarsheh, Q., Daoud, O. & Saraireh, S. (2014). Wavelet Entropy Algorithm to Allocate the Extreme Power Peaks in WiMax Systems. *International Journal of Interactive Mobile Technologies*, 8(4), 14 - 19. Consulted at http://search.ebscohost.com/login.aspx?direct=true&db=egs&AN=99147915&site=ehost-live.

Hampton, J. R. (2013). *Introduction to MIMO communications*. Cambridge university press.

Han, S. H. & Lee, J. H. (2005). An overview of peak-to-average power ratio reduction techniques for multicarrier transmission. *IEEE Wireless Communications*, 12(2), 56-65. DOI: 10.1109/MWC.2005.1421929.

Hao, M. J., Tsai, Y.-C. & Lee, M.-H. (2011, Dec). Joint estimation of frequency offset and channel parameters for MIMO-OFDM systems with PAPR reduction precoder. *2011 International Symposium on Intelligent Signal Processing and Communications Systems (ISPACS)*, pp. 1-6. doi: 10.1109/ISPACS.2011.6146063.

Hassan, E. S., El-Khamy, S. E., Dessouky, M. I., El-Dolil, S. A. & El-samie, F. E. A. (2009). Peak-to-average power ratio reduction in space-time block coded multi-input multi-output orthogonal frequency division multiplexing systems using a small overhead selective mapping scheme. *IET Communications*, 3(10), 1667-1674. doi: 10.1049/iet-com.2008.0565.

Hassaneen, S. S., Soliman, H. Y., Elbarbary, K. A. & Elhennawy, A. E. (2013a, Dec). Modified PTS with circular shifting for PAPR reduction in MIMO OFDM systems. *2013 Second International Japan-Egypt Conference on Electronics, Communications and Computers (JEC-ECC)*, pp. 1-6. doi: 10.1109/JEC-ECC.2013.6766375.

Hassaneen, S. S., Soliman, H. Y., k. A. Elbarbary & Elhennawy, A. E. (2013b, Dec). Reducing the peak to average power ratio in MIMO OFDM systems. *2013 9th International Computer Engineering Conference (ICENCO)*, pp. 128-133. doi: 10.1109/ICENCO.2013.6736488.

He, X., Jiang, T. & Zhu, G. (2011). A novel simplified tone reservation combined with cross antenna rotation and inversion to reduce PAPR for MIMO-OFDM system. *Wireless Communications and Mobile Computing*, 11(10), 1406–1414. doi: 10.1002/wcm.937.

Henkel, W., Wakeel, A. & Taseska, M. (2012, Aug). Peak-to-average ratio reduction with Tone Reservation in multi-user and MIMO OFDM. *2012 1st IEEE International Conference on Communications in China (ICCC)*, pp. 372-376. doi: 10.1109/ICCChina.2012.6356910.

Heo, S. J., Noh, H. S., No, J. S. & Shin, D. J. (2007). A Modified SLM Scheme with Low Complexity for PAPR Reduction of OFDM Systems. *2007 IEEE 18th International Symposium on Personal, Indoor and Mobile Radio Communications*, pp. 1-5.

Hsueh, T. C., Lin, P. Y. & Lin, J. S. (2012, Aug). PAPR reduction techniques with cross SLM schemes for MIMO-OFDM systems. *2012 IEEE International Conference on Signal Processing, Communication and Computing (ICSPCC 2012)*, pp. 197-202. doi: 10.1109/ICSPCC.2012.6335625.

Hu, W. W., Ciou, Y. C., Li, C. P. & Huang, W. J. (2013, June). PAPR reduction scheme in SFBC MIMO-OFDM systems without side information. *2013 IEEE International Conference on Communications (ICC)*, pp. 4708-4712. doi: 10.1109/ICC.2013.6655316.

Huang, H. & Li, S. (2007, Sept). A Novel PAPR Reduction Method in MIMO-OFDM Systems by Frequency Block Exploitations. *2007 IEEE 18th International Symposium on Personal, Indoor and Mobile Radio Communications*, pp. 1-5. doi: 10.1109/PIMRC.2007.4394473.

Huang, X., Lu, J., Zheng, J., Letaief, K. B. & Gu, J. (2004). Companding transform for reduction in peak-to-average power ratio of OFDM signals. *IEEE Transactions on Wireless Communications*, 3(6), 2030-2039. doi: 10.1109/TWC.2004.837619.

Hung, Y. C. & Tsai, S. H. L. (2014). PAPR Analysis and Mitigation Algorithms for Beamforming MIMO OFDM Systems. *IEEE Transactions on Wireless Communications*, 13(5), 2588-2600. doi: 10.1109/TWC.2014.031914.130347.

Huo, Y., Dong, X. & Xu, W. (2017). 5G Cellular User Equipment: From Theory to Practical Hardware Design. *IEEE Access*, 5, 13992-14010. doi: 10.1109/ACCESS.2017.2727550. DOI: 10.1109/ACCESS.2017.2727550.

Hwang, T., Yang, C., Wu, G., Li, S. & Li, G. Y. (2009). OFDM and Its Wireless Applications: A Survey. *IEEE Transactions on Vehicular Technology*, 58(4), 1673-1694. DOI: 10.1109/TVT.2008.2004555.

Inoue, Y., Tsutsui, H. & Miyanaga, Y. (2013, Nov). Study of PAPR reduction using coded PTS in MIMO-OFDM systems. *2013 International Symposium on Intelligent Signal Processing and Communication Systems*, pp. 363-368. doi: 10.1109/ISPACS.2013.6704577.

Ishida, Y., Suyama, S., Suzuki, H. & Fukawa, K. (2007, April). MIMO-OFDM Transmission Employing Subcarrier-Block Phase Hopping for PAPR Reduction. *2007 IEEE 65th Vehicular Technology Conference - VTC2007-Spring*, pp. 2470-2474. doi: 10.1109/VETECS.2007.509.

Jaganathan, M. & Narasimhan, R. (2008, March). Peak-to-Average Power Reduction in MIMO OFDM by Spatial Nulling. *2008 IEEE Wireless Communications and Networking Conference*, pp. 1178-1182. doi: 10.1109/WCNC.2008.212.

Jayalath, A. D. S. & Tellambura, C. (2000). The use of interleaving to reduce the peak-to-average power ratio of an OFDM signal. *Global Telecommunications Conference, 2000. GLOBECOM '00. IEEE*, 1, 82-86.

Jayalath, A. D. S. & Tellambura, C. (2002). A blind SLM receiver for PAR-reduced OFDM. *Proceedings IEEE 56th Vehicular Technology Conference*, 1, 219-222.

Jayalath, A. D. S. & Tellambura, C. (2005). SLM and PTS peak-power reduction of OFDM signals without side information. *IEEE Transactions on Wireless Communications*, 4(5), 2006-2013. DOI: 10.1109/TWC.2005.853916.

Jeon, H. B., No, J. S. & Shin, D. J. (2011). A Low-Complexity SLM Scheme Using Additive Mapping Sequences for PAPR Reduction of OFDM Signals. *IEEE Transactions on Broadcasting*, 57(4), 866-875. DOI: 10.1109/TBC.2011.2151570.

Jeruchim, M. (1984). Techniques for Estimating the Bit Error Rate in the Simulation of Digital Communication Systems. *IEEE Journal on Selected Areas in Communications*, 2(1), 153-170. doi: 10.1109/JSAC.1984.1146031.

Jiang, J., Buchrer, R. M. & Tranter, W. H. (2004a, Nov). Peak to average power ratio reduction for MIMO-OFDM wireless system using nonlinear precoding. *Global Telecommunications Conference, 2004. GLOBECOM '04. IEEE*, 6, 3989-3993 Vol.6. doi: 10.1109/GLOCOM.2004.1379116.

Jiang, T. & Li, C. (2012). Simple Alternative Multisequences for PAPR Reduction Without Side Information in SFBC MIMO-OFDM Systems. *IEEE Transactions on Vehicular Technology*, 61(7), 3311-3315. doi: 10.1109/TVT.2012.2201970.

Jiang, T. & Wu, Y. (2008). An Overview: Peak-to-Average Power Ratio Reduction Techniques for OFDM Signals. *IEEE Transactions on Broadcasting*, 54(2), 257-268. DOI: 10.1109/TBC.2008.915770.

Jiang, T., Guizani, M., Chen, H., Xiang, W. & Wu, Y. (2008). Derivation of PAPR Distribution for OFDM Wireless Systems Based on Extreme Value Theory. *IEEE Transactions on Wireless Communications*, 7(4), 1298-1305. doi: 10.1109/TWC.2008.060862.

Jiang, T., Ni, C. & Guan, L. (2013). A Novel Phase Offset SLM Scheme for PAPR Reduction in Alamouti MIMO-OFDM Systems Without Side Information. *IEEE Signal Processing Letters*, 20(4), 383-386. doi: 10.1109/LSP.2013.2245119.

Jiang, T., Ni, C., Guan, L. & Qi, Q. (2014). Peak-to-average power ratio reduction in alamouti multi-input-multi-output orthogonal frequency division multiplexing systems without side information using phase offset based-partial transmit sequence scheme. *IET Communications*, 8(5), 564-570. doi: 10.1049/iet-com.2013.0812.

Jiang, T. & Zhu, G. (2004a). Nonlinear companding transform for reducing peak-to-average power ratio of OFDM signals. *IEEE Transactions on Broadcasting*, 50(3), 342-346. DOI: 10.1109/TBC.2004.834030.

Jiang, T. & Zhu, G. (2004b, Sept). OFDM peak-to-average power ratio, reduction by complement block coding scheme and its modified version. *IEEE 60th Vehicular Technology Conference, 2004. VTC2004-Fall. 2004*, 1, 448-451.

Jiang, T. & Zhu, G. (2005). Complement block coding for reduction in peak-to-average power ratio of OFDM signals. *IEEE Communications Magazine*, 43(9), S17-S22.

Jiang, T., Zhu, G. & Zheng, J. (2004b). Block coding scheme for reducing PAPR in OFDM systems with large number of subcarriers. *Journal of Electronics*, 21(6), 482–489.

Jiang, T., Yang, Y. & Song, Y.-H. (2005). Exponential companding technique for PAPR reduction in OFDM systems. *IEEE Transactions on Broadcasting*, 51(2), 244-248. DOI: 10.1109/TBC.2005.847626.

Jiang, Y. (2010). A practical guide to error-control coding using MATLAB (ch. 1, pp. 1-17). 685 Canton Street, Norwood, MA 02062: Artech House.

Jinlong, X. & Yuehong, G. (2009, April). Reduction of Peak-to-Average Power Ratio in MIMO-OFDM System Based on the Copy Theory. *2009 International Conference on Networks Security, Wireless Communications and Trusted Computing*, 2, 751-754. doi: 10.1109/NSWCTC.2009.164.

Johansson, T. & Fritzin, J. (2014). A Review of Watt-Level CMOS RF Power Amplifiers. *IEEE Transactions on Microwave Theory and Techniques*, 62(1), 111-124. doi: 10.1109/TMTT.2013.2292608. DOI: 10.1109/TMTT.2013.2292608.

Joo, H.-S., No, J.-S. & Shin, D.-J. (2010, Nov). A blind SLM PAPR reduction scheme using cyclic shift in STBC MIMO-OFDM system. *2010 International Conference on Information and Communication Technology Convergence (ICTC)*, pp. 272-273. doi: 10.1109/ICTC.2010.5674679.

Joshi, A. & Saini, D. S. (2015, March). Performance analysis and peak-to-average power ratio reduction of concatenated LDPC coded OFDM system using low complexity PTS. *2015 International Conference on Signal Processing and Communication (ICSC)*, pp. 195-200.

Ju, S. M. & Leung, S. H. (2003). Clipping on COFDM with phase on demand. *IEEE Communications Letters*, 7(2), 49-51. DOI: 10.1109/LCOMM.2002.808399.

Kageyama, T., Muta, O. & Gacanin, H. (2015, Aug). An adaptive peak cancellation method for linear-precoded MIMO-OFDM signals. *2015 IEEE 26th Annual International Symposium on Personal, Indoor, and Mobile Radio Communications (PIMRC)*, pp. 271-275. doi: 10.1109/PIMRC.2015.7343308.

Karimi, B. R., Beheshti, M. & Omidi, M. J. (2014). PAPR Reduction in MIMO-OFDM Systems: Spatial and Temporal Processing. *Wireless Personal Communications*, 79(3), 1925–1940. doi: 10.1007/s11277-014-1965-y.

Khademi, S. & van der Veen, A. J. (2013). Constant Modulus Algorithm for Peak-to-Average Power Ratio (PAPR) Reduction in MIMO OFDM/A. *IEEE Signal Processing Letters*, 20(5), 531-534. doi: 10.1109/LSP.2013.2254114.

Khademi, S., der Veen, A. J. V. & Svantesson, T. (2012, March). Precoding technique for peak-to-average-power-ratio (PAPR) reduction in MIMO OFDM/A systems. *2012 IEEE International Conference on Acoustics, Speech and Signal Processing (ICASSP)*, pp. 3005-3008. doi: 10.1109/ICASSP.2012.6288547.

Khan, F. (2009). LTE for 4G Mobile Broadband: Air Interface Technologies and Performance (ch. 5, pp. 88-108). Cambridge University Press.

Khan, Y. A., Matin, M. A. & Ferdous, S. I. (2010). PAPR Reduction in MIMO-OFDM Systems using Modified PTS and SLM without Side Information. *International Journal of Communication Networks and Information Security*, 2(3), 240-247. Consulted at https://search.proquest.com/docview/813372486?accountid=27231. Copyright - Copyright

Kohat University of Science and Technology (KUST) Dec 2010; Document feature - Equations; Tables; Graphs; ; Last updated - 2011-05-26.

Kim, B. W., Jung, S. Y. & Park, D. J. (2008, May). New Transmit Precoding for a Hidden Pilot Design in MIMO-OFDM Systems. *2008 IEEE International Conference on Communications*, pp. 678-682. doi: 10.1109/ICC.2008.133.

Kim, B. W. & Jung, S.-Y. (2017). Peak-to-average power ratio reduction of a hidden training sequence-aided precoding scheme for MIMO-OFDM. *International Journal of Communication Systems*, 30(1), e2910–n/a. doi: 10.1002/dac.2910. e2910.

Kim, H. S. & Daneshrad, B. (2009, Nov). A Theoretical Treatment of PA Power Optimization in Clipped MIMO-OFDM Systems. *GLOBECOM 2009 - 2009 IEEE Global Telecommunications Conference*, pp. 1-6. doi: 10.1109/GLOCOM.2009.5426131.

Kimura, R., Tajika, Y. & Higuchi, K. (2011, May). CF-Based Adaptive PAPR Reduction Method for Block Diagonalization-Based Multiuser MIMO-OFDM Signals. *2011 IEEE 73rd Vehicular Technology Conference (VTC Spring)*, pp. 1-5. doi: 10.1109/VETECS.2011.5956759.

Kojima, T., Shida, Y. & Fujino, T. (2010). A study of SLM PAPR reduction of OFDM signals without side information. *The 2010 International Conference on Advanced Technologies for Communications*, pp. 168-171.

Kota, P., Gaikwad, A. & Patil, B. (2016). TRELLIS CODED MAPPING FOR PEAK TO AVERAGE POWER REDUCTION IN SFBC MIMO OFDM SYSTEMS. *ICTACT Journal on Communication Technology*, 7(3).

Krongold, B. S., Woo, G. R. & Jones, D. L. (2005, October). Fast Active Constellation Extension for MIMO-OFDM PAR Reduction. *Conference Record of the Thirty-Ninth Asilomar Conference onSignals, Systems and Computers, 2005.*, pp. 1476-1479. doi: 10.1109/ACSSC.2005.1600011.

Ku, S. J. (2014). Low-Complexity PTS-Based Schemes for PAPR Reduction in SFBC MIMO-OFDM Systems. *IEEE Transactions on Broadcasting*, 60(4), 650-658. doi: 10.1109/TBC.2014.2364966.

Kwon, U. K., Kim, D., Kim, K. & Im, G. H. (2007). Amplitude Clipping and Iterative Reconstruction of STBC/SFBC-OFDM Signals. *IEEE Signal Processing Letters*, 14(11), 808-811. doi: 10.1109/LSP.2007.900034.

Kwon, U. K., Kim, D. & Im, G. H. (2009). Amplitude clipping and iterative reconstruction of MIMO-OFDM signals with optimum equalization. *IEEE Transactions on Wireless Communications*, 8(1), 268-277. doi: 10.1109/T-WC.2009.071034.

Lahcen, A., Saida, A. & Adel, A. (2017). Low Computational Complexity PTS Scheme for PAPR Reduction of MIMO-OFDM Systems. *Procedia Engineering*, 181(Supplement

C), 876 - 883. doi: https://doi.org/10.1016/j.proeng.2017.02.480. 10th International Conference Interdisciplinarity in Engineering, INTER-ENG 2016, 6-7 October 2016, Tirgu Mures, Romania.

Latinovic, Z. & Bar-Ness, Y. (2006). SFBC MIMO-OFDM peak-to-average power ratio reduction by polyphase interleaving and inversion. *IEEE Communications Letters*, 10(4), 266-268. doi: 10.1109/LCOMM.2006.1613742.

Lee, B. M. & de Figueiredo, R. J. (2010). MIMO-OFDM PAPR reduction by selected mapping using side information power allocation. *Digital Signal Processing*, 20(2), 462 - 471. doi: http://dx.doi.org/10.1016/j.dsp.2009.06.025.

Lee, H., Liu, D. N., Zhu, W. & Fitz, M. P. (2005, May). Peak power reduction using a unitary rotation in multiple transmit antennas. *IEEE International Conference on Communications, 2005. ICC 2005. 2005*, 4, 2407-2411 Vol. 4. doi: 10.1109/ICC.2005.1494767.

Lee, Y.-L., You, Y.-H., Jeon, W.-G., Paik, J.-H. & Song, H.-K. (2003). Peak-to-average power ratio in MIMO-OFDM systems using selective mapping. *IEEE Communications Letters*, 7(12), 575-577. doi: 10.1109/LCOMM.2003.821329.

Li, C. P., Wang, S. H. & Tsai, K. H. (2010a, May). A Low Complexity Transmitter Architecture and Its Application to PAPR Reduction in SFBC MIMO-OFDM Systems. *2010 IEEE International Conference on Communications*, pp. 1-5. doi: 10.1109/ICC.2010.5502740.

Li, G., Yang, S., Mu, X. & Qi, L. (2007, Nov). A new method for peak-to-average power ratio reduction in MIMO-OFDM system. *2007 International Symposium on Intelligent Signal Processing and Communication Systems*, pp. 614-617. doi: 10.1109/ISPACS.2007.4445962.

Li, S., Wang, K. & HOU, S. (2010b). PAPR Reduction Algorithm for MIMO-OFDM Based on Conjugate Symmetry Character. *Proceedings of Annual Conference of China Institute of Communications*, 494–497.

Li, X. & Cimini, L. J. (1997, May). Effects of clipping and filtering on the performance of OFDM. *1997 IEEE 47th Vehicular Technology Conference. Technology in Motion*, 3, 1634-1638.

Li, Y. Z., Wang, Y. J. & Huang, L. Q. (2013, 10). An Improved Algorithm Based on Optimized PTS in MIMO-OFDM System. *Advanced Information and Computer Technology in Engineering and Manufacturing, Environmental Engineering*, 765(Advanced Materials Research), 2801–2804. doi: 10.4028/www.scientific.net/AMR.765-767.2801.

Li, Y., Gao, M. & Yi, Z. (2012, Nov). A cooperative and alternate PTS scheme for PAPR reduction in STBC MIMO-OFDM system. *2012 IEEE 14th International Conference on Communication Technology*, pp. 268-272. doi: 10.1109/ICCT.2012.6511227.

Li, Z. & Xia, X. G. (2007, Nov). PAPR Reduction for Space-Time-Frequency Coded MIMO-OFDM Systems. *IEEE GLOBECOM 2007 - IEEE Global Telecommunications Conference*, pp. 2796-2800. doi: 10.1109/GLOCOM.2007.529.

Li, Z. & Xia, X. G. (2008). PAPR Reduction for Repetition Space-Time-Frequency Coded MIMO-OFDM Systems Using Chu Sequences. *IEEE Transactions on Wireless Communications*, 7(4), 1195-1202. doi: 10.1109/TWC.2008.061024.

Lim, D. W., Heo, S. J. & No, J. S. (2009). An overview of peak-to-average power ratio reduction schemes for OFDM signals. *Journal of Communications and Networks*, 11(3), 229-239. DOI: 10.1109/JCN.2009.6391327.

Lim, D.-W., No, J.-S., Lim, C.-W. & Chung, H. (2005). A new SLM OFDM scheme with low complexity for PAPR reduction. *IEEE Signal Processing Letters*, 12(2), 93-96. DOI: 10.1109/LSP.2004.840915.

Lin, S. & Costello, D. J. (2004). Error control coding: Fundamentals and Applications (ed. 2nd, ch. 11, pp. 453-513). Upper Saddle River, NJ, USA: Prentice-Hall, Inc.

Liu, F., Pan, Z. & Chen, L. *(2010)*.

Luo, R., Niu, N., Zheng, M., Li, R. & Yang, J. (2015). An Optimized Iterative Scheme for PAPR Reduction with Low Complexity. *Wireless Personal Communications*, 80(1), 321–333. doi: 10.1007/s11277-014-2011-9.

Ma, T.-M., Shi, Y.-S. & Wang, Y.-G. (2011). A Novel SLM Scheme for PAPR Reduction in OFDM Systems. *Journal of Computer Networks and Communications*, 2011. DOI: 10.1155/2011/195740.

Mahajan, K. A. & Mukhare, S. V. (2012). Comparison of Signal Scrambling PAPR Reduction Techniques with Signal Distortion Techniques in OFDM Signal. *IJCA Proceedings on International Conference on Recent Trends in Information Technology and Computer Science (ICRTITCS-2011)*, (1).

Malkin, M., Zou, H., Malek, A., Cioffi, J. M. & Krongold, B. (2008, Oct). Optimal constellation distortion for PAR reduction in MIMO-OFDM systems. *2008 42nd Asilomar Conference on Signals, Systems and Computers*, pp. 943-947. doi: 10.1109/ACSSC.2008.5074550.

Manasseh, E., Ohno, S., Yamamoto, T. & Nakamoto, M. (2013, Nov). Efficient PAPR reduction techniques for MIMO-OFDM based cognitive radio networks. *2013 International Symposium on Intelligent Signal Processing and Communication Systems*, pp. 357-362. doi: 10.1109/ISPACS.2013.6704576.

Manasseh, E., Ohno, S. & Nakamoto, M. (2012). Combined channel estimation and PAPR reduction technique for MIMO–OFDM systems with null subcarriers. *EURASIP Journal on Wireless Communications and Networking*, 2012(1), 201. doi: 10.1186/1687-1499-2012-201.

MANJITH, R. & SUGANTHI, M. (2013). A SUB-OPTIMAL PTS ALGORITHM BASED ON BACTERIAL FORAGING OPTIMIZATION TECHNIQUE FOR PAPR REDUCTION IN MIMO-OFDM SYSTEM. *Journal of Theoretical & Applied Information Technology*, 57(2), 261 - 268. Consulted at http://search.ebscohost.com/login.aspx?direct=true&db=egs&AN=93654138&site=ehost-live.

Manjith, R. & Suganthi, M. (2014). Peak to Average Power Ratio Reduction using a Hybrid of Bacterial Foraging and Modified Cuckoo Search Algorithm in MIMO-OFDM System. *Research Journal of Applied Sciences, Engineering and Technology*, 7(21), 4423-4433.

Mannerkoski, J. & Koivunen, V. (2000). Autocorrelation properties of channel encoded sequences-applicability to blind equalization. *IEEE Transactions on Signal Processing*, 48(12), 3501-3507. DOI: 10.1109/78.887043.

Mata, T., Boonsrimuang, P., Boonsrimuang, P. & Kobayashi, H. (2009, Dec). A new weighting factor with concurrent PAPR reduction algorithm for STBC MIMO-OFDM. *2009 IEEE 9th Malaysia International Conference on Communications (MICC)*, pp. 136-140. doi: 10.1109/MICC.2009.5431481.

Mattsson, A., Mendenhall, G. & Dittmer, T. (1999). Comments on: "Reduction of peak-to-average power ratio of OFDM system using a companding technique". *IEEE Transactions on Broadcasting*, 45(4), 418-419. doi: 10.1109/11.825537.

McEliece, R. J. & Lin, W. (1996). The trellis complexity of convolutional codes. *IEEE Transactions on Information Theory*, 42(6), 1855-1864. doi: 10.1109/18.556680.

Moision, B. (2008, Jan). A truncation depth rule of thumb for convolutional codes. *2008 Information Theory and Applications Workshop*, pp. 555-557. doi: 10.1109/ITA.2008.4601052.

Moon, J.-H., You, Y.-H., Jeon, W.-G., Kwon, K.-W. & Song, H.-K. (2003). Peak-to-average power control for multiple-antenna HIPERLAN/2 and IEEE802.11a systems. *IEEE Transactions on Consumer Electronics*, 49(4), 1078-1083. doi: 10.1109/TCE.2003.1261199.

Mouhib, K. E., Oquour, A., Jabrane, Y., Said, B. A. & Ouahman, A. A. (2011). PAPR Reduction Using BPSO/PTS and STBC in MIMO OFDM System. *Journal of Computer Science*, 7(4), 454.

Mukunthan, P. & Dananjayan, P. (2013). A modified PTS combined with interleaving and pulse shaping method based on PAPR reduction for STBC MIMO-OFDM system. *WSEAS transactions on communications*, 12(3), 121–131.

Muller, S. H. & Huber, J. B. (1997a). A novel peak power reduction scheme for OFDM. *The 8th IEEE International Symposium on Personal, Indoor and Mobile Radio Communications, 1997. Waves of the Year 2000. PIMRC '97.*, 3, 1090-1094.

Muller, S. H. & Huber, J. B. (1997b). OFDM with reduced peak-to-average power ratio by optimum combination of partial transmit sequences. *Electronics Letters*, 33(5), 368-369. DOI: 10.1049/el:19970266.

Muller, S. H. & Huber, J. B. (1997c). A comparison of peak power reduction schemes for OFDM. *Global Telecommunications Conference, 1997. GLOBECOM'97., IEEE*, 1, 1–5.

Myung, H. G., Lim, J. & Goodman, D. J. (2006a, Sept). Peak-To-Average Power Ratio of Single Carrier FDMA Signals with Pulse Shaping. *2006 IEEE 17th International Symposium on Personal, Indoor and Mobile Radio Communications*, pp. 1-5.

Myung, H. G., Lim, J. & Goodman, D. J. (2006b). Single carrier FDMA for uplink wireless transmission. *IEEE Vehicular Technology Magazine*, 1(3), 30-38. DOI: 10.1109/MVT.2006.307304.

Naeiny, M. F. & Marvasti, F. (2011). PAPR reduction of space-frequency coded OFDM systems using Active Constellation Extension. *AEU - International Journal of Electronics and Communications*, 65(10), 873 - 878. doi: http://dx.doi.org/10.1016/j.aeue.2011.02.006.

Nandi, A. K., Gao, J. & Zhu, X. (2009, Dec). Independent component analysis - an innovative technique for wireless MIMO OFDM systems. *2009 4th International Conference on Computers and Devices for Communication (CODEC)*, pp. 1-8.

Nee, R. D. J. V. (1996, Nov). OFDM codes for peak-to-average power reduction and error correction. *Global Telecommunications Conference, 1996. GLOBECOM '96. 'Communications: The Key to Global Prosperity*, 1, 740-744.

Nee, R. V. & de Wild, A. (1998, May). Reducing the peak-to-average power ratio of OFDM. *Vehicular Technology Conference, 1998. VTC 98. 48th IEEE*, 3, 2072-2076.

Ngajikin, N., Fisal, N. & Yusof, S. K. (2003, Aug). PAPR reduction in WLAN-OFDM system using code repetition technique. *Proceedings. Student Conference on Research and Development, 2003. SCORED 2003.*, pp. 85-89.

Ni, C., Ma, Y. & Jiang, T. (2016). A Novel Adaptive Tone Reservation Scheme for PAPR Reduction in Large-Scale Multi-User MIMO-OFDM Systems. *IEEE Wireless Communications Letters*, 5(5), 480-483. doi: 10.1109/LWC.2016.2588489.

Ochiai, H. & Imai, H. (2000). Performance of the deliberate clipping with adaptive symbol selection for strictly band-limited OFDM systems. *IEEE Journal on Selected Areas in Communications*, 18(11), 2270-2277. doi: 10.1109/49.895032. DOI: 10.1109/49.895032.

Ochiai, H. & Imai, H. (2001). On the distribution of the peak-to-average power ratio in OFDM signals. *IEEE Transactions on Communications*, 49(2), 282-289. DOI: 10.1109/26.905885.

Oguntade, A. O. (2010). *Range estimation for tactical radio waveforms using link budget analysis*. (Ph.D. thesis, University of Toledo).

O'Neill, R. & Lopes, L. B. (1995, Sep). Envelope variations and spectral splatter in clipped multicarrier signals. *Proceedings of 6th International Symposium on Personal, Indoor and Mobile Radio Communications*, 1, 71-75.

Ouyang, X., Jin, J., Jin, G. & Wang, Z. (2013, April). Partial shift mapping with inter-antenna switch for PAPR reduction in MIMO-OFDM systems. *2013 IEEE Wireless Communications and Networking Conference (WCNC)*, pp. 2750-2753. doi: 10.1109/WCNC.2013.6554997.

Ouyang, Y. (2009, April). Peak-to-Average Power Ratio Reduction by Cross-Antenna Translation for SFBC MIMO-OFDM Systems. *VTC Spring 2009 - IEEE 69th Vehicular Technology Conference*, pp. 1-4. doi: 10.1109/VETECS.2009.5073770.

Ouyang, Y. & Ding, H. (2015, Oct). Peak-to-average power ratio reduction techniques for MIMO-OFDM systems with STBC/SFBC. *2015 IEEE International Conference on Communication Problem-Solving (ICCP)*, pp. 540-543. doi: 10.1109/ICCPS.2015.7454224.

Oza, M., Kim, J. & Kim, S. (2012, June). Range estimation of turbo coded waveforms over vegetative mountain blockage using link budget analysis. *IEEE international Symposium on Broadband Multimedia Systems and Broadcasting*, pp. 1-5.

Pachori, K. & Mishra, A. (2016a). An efficient combinational approach for PAPR reduction in MIMO–OFDM system. *Wireless Networks*, 22(2), 417–425. doi: 10.1007/s11276-015-0974-4.

Pachori, K. & Mishra, A. (2016b). A hybrid envelope fluctuations reduction approach using multilayer neural network for MIMO-OFDM signals. *Wireless Networks*, 22(8), 2705–2712. doi: 10.1007/s11276-015-1126-6.

Pandurangan, M. & Perumal, D. (2011). Modified PTS with FECs for PAPR reduction in MIMO-OFDM system with different subblocks and subcarriers. *IJCSI International Journal of Computer Science Issues*, 8(4), 444–452.

Park, J., Hong, E., Kim, H., Kim, K. & Har, D. (2013). Pilot-assisted data recovery for OFDM systems with blind selected mapping scheme and space-frequency block coding. *Digital Signal Processing*, 23(5), 1704 - 1711. doi: http://dx.doi.org/10.1016/j.dsp.2013.07.002.

Petersen, K., Vakkalanka, S. & Kuzniarz, L. (2015). Guidelines for conducting systematic mapping studies in software engineering: An update. *Information and Software Technology*, 64(Supplement C), 1 - 18. doi: https://doi.org/10.1016/j.infsof.2015.03.007.

Phetsomphou, D., Yoshizawa, S. & Miyanaga, Y. (2010, Oct). A partial transmit sequence technique for PAPR reduction in MIMO-OFDM systems. *2010 10th International Symposium on Communications and Information Technologies*, pp. 672-676. doi: 10.1109/ISCIT.2010.5665073.

Prabhu, H., Edfors, O., Rodrigues, J., Liu, L. & Rusek, F. (2014). A low-complex peak-to-average power reduction scheme for OFDM based massive MIMO systems. *Communications, Control and Signal Processing (ISCCSP), 2014 6th International Symposium on*, pp. 114–117.

Pérez, R. P. & Jiménez, V. P. G. (2017, June). Power envelope reduction in MIMO-OFDM with block diagonalization by using fuzzy inference systems. *2017 13th International Wireless Communications and Mobile Computing Conference (IWCMC)*, pp. 2187-2191. doi: 10.1109/IWCMC.2017.7986622.

Proakis, J. G. & Salehi, M. (2008). Digital Communications (ed. 5th, ch. 7-8, pp. 400-589). New York, NY, USA: McGraw-Hill.

Puspitaningayu, P. & Hendrantoro, G. (2014, Oct). Performance of anti-jamming techniques with bit interleaving in OFDM-based tactical communications. *2014 6th International Conference on Information Technology and Electrical Engineering (ICITEE)*, pp. 1-5.

Qualcomm. (2016). Making 5G NR a reality: leading the technology inventions for a unified, more capable 5G air interface. *White paper*.

Rahmatallah, Y. & Mohan, S. (2013). Peak-To-Average Power Ratio Reduction in OFDM Systems: A Survey And Taxonomy. *IEEE Communications Surveys Tutorials*, 15(4), 1567-1592. DOI: 10.1109/SURV.2013.021313.00164.

Rajbanshi, R. (2007). *OFDM-based cognitive radio for DSA networks*. (Ph.D. thesis, Information & Telecommuncation Technology Center, University of Kansas, Lawrence, KS, USA).

Ramaswamy, T. & Reddy, K. C. (2016). Low Complexity Iterative Piece-Wise Companding Transform for Reduction of PAPR in MIMO OFDM Systems. *Indian Journal of Science and Technology*, 9(38). Consulted at http://52.172.159.94/index.php/indjst/article/view/92441.

Ramezani, H. (2007). OFDM High Power Amplifier Effects. MATLAB Central File Exchange. Consulted at https://www.mathworks.com/matlabcentral/fileexchange/15331.

Rani, B. & Saini, G. (2012, Dec). PAPR reduction using Cooperative PTS for space frequency block code MIMO-OFDM signal. *2012 2nd IEEE International Conference on Parallel, Distributed and Grid Computing*, pp. 132-134. doi: 10.1109/PDGC.2012.6449804.

Rappaport, T. S., Sun, S., Mayzus, R., Zhao, H., Azar, Y., Wang, K., Wong, G. N., Schulz, J. K., Samimi, M. & Gutierrez, F. (2013). Millimeter Wave Mobile Communications for 5G

Cellular: It Will Work! *IEEE Access*, 1, 335-349. doi: 10.1109/ACCESS.2013.2260813. DOI: 10.1109/ACCESS.2013.2260813.

Ren, G., Zhang, H. & Chang, Y. (2003). A complementary clipping transform technique for the reduction of peak-to-average power ratio of OFDM system. *IEEE Transactions on Consumer Electronics*, 49(4), 922-926. DOI: 10.1109/TCE.2003.1261175.

Richardson, A. (2005). WCDMA design handbook (ch. 1, pp. 7). United Kingdom: Cambridge University Press.

Rihawi, B., Louet, Y. & Zabre, S. (2007, Sept). PAPR Reduction Scheme with SOCP for MIMO-OFDM. *2007 International Conference on Wireless Communications, Networking and Mobile Computing*, pp. 271-274. doi: 10.1109/WICOM.2007.74.

Ryu, H. G. (2008). System design and analysis of MIMO SFBC CI-OFDM system against the nonlinear distortion and narrowband interference. *IEEE Transactions on Consumer Electronics*, 54(2), 368-375. doi: 10.1109/TCE.2008.4560101.

Ryu, H.-G., Lee, J.-E. & Park, J.-S. (2004). Dummy sequence insertion (DSI) for PAPR reduction in the OFDM communication system. *IEEE Transactions on Consumer Electronics*, 50(1), 89-94. DOI: 10.1109/TCE.2004.1277845.

Sakran, H., Shokair, M. & Elazm, A. A. (2008, Oct). An efficient technique for reducing PAPR of OFDM system in the presence of nonlinear high power amplifier. *2008 9th International Conference on Signal Processing*, pp. 1749-1752.

Sakran, H. Y., Shokair, M. M. & Elazm, A. A. (2009). Combined interleaving and companding for PAPR reduction in OFDM systems. *Progress in Electromagnetics Research C*, 6, 67–78.

Sandoval, F., Poitau, G. & Gagnon, F. (2017). Hybrid Peak-to-Average Power Ratio Reduction Techniques: Review and Performance Comparison. *IEEE Access*, 5, 27145-27161. doi: 10.1109/ACCESS.2017.2775859.

Sandoval, F., Poitau, G. & Gagnon, F. (2019a). Optimizing Forward Error Correction Codes for COFDM with Reduced PAPR. *IEEE Transactions on Communications*, 1-1. doi: 10.1109/TCOMM.2019.2910811.

Sandoval, F., Poitau, G. & Gagnon, F. (2019b). On Optimizing the PAPR of OFDM Signals With Coding, Companding, and MIMO. *IEEE Access*, 7, 24132-24139. doi: 10.1109/ACCESS.2019.2899965.

Schenk, T. C. W., Smulders, P. F. M. & Fledderus, E. R. (2006, May). The Application of Spatial Shifting for Peak-to-Average Power Ratio Reduction in MIMO OFDM Systems. *2006 IEEE 63rd Vehicular Technology Conference*, 4, 1859-1863. doi: 10.1109/VETECS.2006.1683169.

Sghaier, M., Abdelkefi, F. & Siala, M. (2013, April). Efficient embedded signaling through Alamouti STBC precoders in MIMO-OFDM systems. *2013 IEEE Wireless Communications and Networking Conference (WCNC)*, pp. 4053-4058. doi: 10.1109/WCNC.2013.6555226.

Sghaier, M., Abdelkefi, F., Omri, A. & Siala, M. (2016, April). An efficient reduced complexity PAPR reduction approach for 3GPP LTE system. *2016 IEEE Wireless Communications and Networking Conference*, pp. 1-6. doi: 10.1109/WCNC.2016.7564947.

Sghaier, M., Abdelkefi, F. & Siala, M. (2015). PAPR reduction scheme with efficient embedded signaling in MIMO-OFDM systems. *EURASIP Journal on Wireless Communications and Networking*, 2015(1), 240. doi: 10.1186/s13638-015-0443-x.

Sharma, P. & Verma, S. (2011). Reducing PAPR of OFDM based wireless systems using companding with convolutional codes. *International Journal of Distributed and Parallel Systems*, 2(6), 99-105.

Sheikh, J. A., Parah, S. A., Bhat, G. M. & ul Amin, M. (2013, Nov). PAPR reduction in MIMO-OFDM system using combination of OSTBC Encoder and Spreading code sequence. *IMPACT-2013*, pp. 11-15. doi: 10.1109/MSPCT.2013.6782078.

SHIN, J. & SEO, B. (2014). PAPR Reduction Scheme for MISO and MIMO OFDM Systems with Limited Feedback. *WSEAS Transactions on Communications*, 13, 355-362.

Siegl, C. & Fischer, R. F. H. (2008, Jan). Joint Spatial and Temporal PAR Reduction in MIMO OFDM. *7th International ITG Conference on Source and Channel Coding*, pp. 1-6.

Siegl, C. & Fiserch, R. F. H. (2007, June). Peak-to-Average Power Ratio Reduction in Multi-User OFDM. *2007 IEEE International Symposium on Information Theory*, pp. 2746-2750. doi: 10.1109/ISIT.2007.4557634.

Singh, S. & Kumar, A. (2016). Performance Analysis of Adaptive Clipping Technique for Reduction of PAPR in Alamouti Coded MIMO-OFDM Systems. *Procedia Computer Science*, 93(Supplement C), 609 - 616. doi: https://doi.org/10.1016/j.procs.2016.07.246. Proceedings of the 6th International Conference on Advances in Computing and Communications.

Sklar, B. (2001). Digital Communications, Fundamentals and Applications (ed. 2nd, ch. 7, pp. 381-429). New Jersey, NJ, USA: Prentice Hall P T R.

Somasekhar, B. & Mallikarjunaprasad, A. (2014, Nov). Modified SLM and PTS approach to reduce PAPR in MIMO OFDM. *2014 International Conference on Electronics, Communication and Computational Engineering (ICECCE)*, pp. 245-253. doi: 10.1109/ICECCE.2014.7086621.

Studer, C. & Larsson, E. G. (2013). PAR-Aware Large-Scale Multi-User MIMO-OFDM Downlink. *IEEE Journal on Selected Areas in Communications*, 31(2), 303-313. doi: 10.1109/JSAC.2013.130217.

Su, Y. S., Wu, T. C., Wang, C. H. & Chang, M. K. (2011, June). A low-complexity cross-antenna rotation and inversion scheme for PAPR reduction of STBC MIMO-OFDM systems. *2011 IEEE 16th International Workshop on Computer Aided Modeling and Design of Communication Links and Networks (CAMAD)*, pp. 31-35. doi: 10.1109/CAMAD.2011.5941112.

Sujatha, S. & Dananjayan, P. (2014, Dec). PAPR Reduction Using Constant Modulus Algorithm and IDCT in MIMO-OFDM Networks. *2014 3rd International Conference on Eco-friendly Computing and Communication Systems*, pp. 238-241. doi: 10.1109/Ecofriendly.2014.55.

Suyama, S., Nomura, N., Suzuki, H. & Fukawa, K. (2006, Sept). Subcarrier Phase Hopping MIMO-OFDM Transmission Employing Enhanced Selected Mapping for PAPR Reduction. *2006 IEEE 17th International Symposium on Personal, Indoor and Mobile Radio Communications*, pp. 1-5. doi: 10.1109/PIMRC.2006.254355.

Suyama, S., Adachi, H., Suzuki, H. & Fukawa, K. (2009, April). PAPR Reduction Methods for Eigenmode MIMO-OFDM Transmission. *VTC Spring 2009 - IEEE 69th Vehicular Technology Conference*, pp. 1-5. doi: 10.1109/VETECS.2009.5073767.

Tan, M., Latinovic, Z. & Bar-Ness, Y. (2005). STBC MIMO-OFDM peak-to-average power ratio reduction by cross-antenna rotation and inversion. *IEEE Communications Letters*, 9(7), 592-594. doi: 10.1109/LCOMM.2005.1461674.

Taşpınar, N. & Yıldırım, M. (2015). A Novel Parallel Artificial Bee Colony Algorithm and Its PAPR Reduction Performance Using SLM Scheme in OFDM and MIMO-OFDM Systems. *IEEE Communications Letters*, 19(10), 1830-1833. doi: 10.1109/LCOMM.2015.2465967.

Tellado-Mourelo, J. (1999). *Peak to average power reduction for multicarrier modulation*. (Ph.D. thesis, Department of Electrical Engineering, Stanford University).

Tellambura, C. (1997). Upper bound on peak factor of N-multiple carriers. *Electronics Letters*, 33(19), 1608-1609. doi: 10.1049/el:19971069. DOI: 10.1049/el:19971069.

Tiwari, H., Roshan, R. & Singh, R. K. (2014, Dec). PAPR reduction in MIMO-OFDM using combined methodology of selected mapping (SLM) and partial transmit sequence (PTS). *2014 9th International Conference on Industrial and Information Systems (ICIIS)*, pp. 1-5. doi: 10.1109/ICIINFS.2014.7036495.

Trang, N. T. T., Han, T. & Kim, N. (2005). Power efficiency improvement by PAPR reduction and predistorter in MIMO-OFDM system. *The 7th International Conference on Advanced Communication Technology, 2005, ICACT 2005.*, 2, 1381-1386. doi: 10.1109/ICACT.2005.246228.

Tsai, Y.-C., Chen, T.-H., Lo, Y.-H. & Lin, M.-C. (2008, Dec). A low-complexity selective mapping PAPR reduction scheme for coded MIMO-OFDM. *2008 International Symposium on Information Theory and Its Applications*, pp. 1-4. doi: 10.1109/ISITA.2008.4895428.

Tsiligkaridis, T. & Jones, D. L. (2010). PAPR Reduction Performance by Active Constellation Extension for Diversity MIMO-OFDM Systems. *JECE*, 2010, 13:1–13:7. doi: 10.1155/2010/930368.

Umeda, S., Suyama, S., Suzuki, H. & Fukawa, K. (2010, May). PAPR Reduction Method for Block Diagonalization in Multiuser MIMO-OFDM Systems. *2010 IEEE 71st Vehicular Technology Conference*, pp. 1-5. doi: 10.1109/VETECS.2010.5493834.

Vallavaraj, A., Stewart, B. G., Harrison, D. K. & McIntosh, F. G. (2004, Sept). Reduction of peak to average power ration of OFDM signals using companding. *The Ninth International Conference onCommunications Systems, 2004. ICCS 2004.*, pp. 160-164. doi: 10.1109/ICCS.2004.1359359.

Vallavaraj, A., Stewart, B. G., Harrison, D. K. & McIntosh, F. G. (2008). Reducing the PAPR of OFDM Using a Simplified Scrambling SLM Technique with No Explicit Side Information. *2008 14th IEEE International Conference on Parallel and Distributed Systems*, pp. 902-907.

Vallavaraj, A. (2008). *An investigation into the application of companding to wireless OFDM systems*. (Ph.D. thesis, Glasgow Caledonian University).

Vallavaraj, A., Stewart, B. G. & Harrison, D. K. (2010). An evaluation of modified μ-Law companding to reduce the PAPR of OFDM systems. *AEU - International Journal of Electronics and Communications*, 64(9), 844 - 857. doi: https://doi.org/10.1016/j.aeue.2009.07.013.

Venkataraman, A., Reddy, H. & Duman, T. M. (2006). Space-Time Coded OFDM with Low PAPR. *EURASIP Journal on Advances in Signal Processing*, 2006(1), 087125. doi: 10.1155/ASP/2006/87125.

Verma, R. & Tharani, L. (2016, Sept). Constant Modulus Algorithm for PAPR Reduction Using PTS and Clipping Hybrid Scheme in MIMO OFDM/A. *2016 International Conference on Micro-Electronics and Telecommunication Engineering (ICMETE)*, pp. 337-342. doi: 10.1109/ICMETE.2016.87.

Vidya, M., Vijayalakshmi, M. & Ramalingareddy, K. (2015, Dec). Performance enhancement of efficient partitioning technique for PAPR reduction in MIMO-OFDM system using PTS. *2015 Conference on Power, Control, Communication and Computational Technologies for Sustainable Growth (PCCCTSG)*, pp. 247-253. doi: 10.1109/PCCCTSG.2015.7503942.

Vijayalaxmi, M. & Narayana Reddy, S. (2016). PAPR Reduction in SFBC OFDM System-MCMA Approach. In Satapathy, S. C., Rao, N. B., Kumar, S. S., Raj, C. D., Rao, V. M. & Sarma, G. V. K. (Eds.), *Microelectronics, Electromagnetics and Telecommunications: Proceedings of ICMEET 2015* (pp. 327–338). New Delhi: Springer India. doi: 10.1007/978-81-322-2728-1_29.

Vijayarangan, V. & Sukanesh, R. (2009). An overview of techniques for reducing peak to average power ratio and its selection criteria for orthogonal frequency division multiplexing radio systems. *Journal of theoretical and applied information technology*, 5(1), 25–36.

Wakeel, A. & Henkel, W. (2014a, June). Least-squares iterative PAR reduction for point-to-point large-scale MIMO-OFDM systems. *2014 IEEE International Conference on Communications (ICC)*, pp. 4638-4643. doi: 10.1109/ICC.2014.6884053.

Wakeel, A. & Henkel, W. (2014b, Dec). Least-squares iterative peak-to-average ratio reduction for MIMO-OFDM systems. *2014 IEEE Global Communications Conference*, pp. 3934-3939. doi: 10.1109/GLOCOM.2014.7037422.

Wang, C. L., Wang, S. S. & Chang, H. L. (2011, March). A low-complexity SLM based PAPR reduction scheme for SFBC MIMO-OFDM systems. *2011 IEEE Wireless Communications and Networking Conference*, pp. 1449-1453. doi: 10.1109/WCNC.2011.5779373.

Wang, J. S., Hwang, S. H., Song, I. & Kim, Y. H. (2010). Reduction of PAPR without Side Information for Frequency Switched Transmit Diversity-Based MIMO-OFDM Systems. *IEEE Communications Letters*, 14(12), 1116-1118. doi: 10.1109/LCOMM.2010.101810.101359.

Wang, L. & Liu, J. (2011). Cooperative PTS for PAPR reduction in MIMO-OFDM. *Electronics Letters*, 47(5), 351-352. doi: 10.1049/el.2010.3099.

Wang, L. & Wang, Y. (2007). MIMO-OFDM peak-to-average power ratio reduction by two-dimensional permutation. *Electronics Letters*, 43(10), 579-580. doi: 10.1049/el:20070781.

Wang, S. H. & Li, C. P. (2009). A Low-Complexity PAPR Reduction Scheme for SFBC MIMO-OFDM Systems. *IEEE Signal Processing Letters*, 16(11), 941-944. doi: 10.1109/LSP.2009.2027205.

Wang, X., Tjhung, T. T. & Ng, C. S. (1999a). Reduction of peak-to-average power ratio of OFDM system using a companding technique. *IEEE Transactions on Broadcasting*, 45(3), 303-307. DOI: 10.1109/11.796272.

Wang, X., Tjhung, T. T. & Ng, C. S. (1999b). Reply to the comments on "Reduction of peak-to-average power ratio of OFDM system using a companding technique". *IEEE Transactions on Broadcasting*, 45(4), 420-422. doi: 10.1109/11.825538.

Wang, Y., Tao, X., Zhang, P., Xu, J., Wang, X. & Suzuki, T. (2007, Sept). MIMO-OFDM PAPR Reduction by Combining Shifting and Inversion with Matrix Transform. *2007 IEEE 18th International Symposium on Personal, Indoor and Mobile Radio Communications*, pp. 1-5. doi: 10.1109/PIMRC.2007.4394510.

Wang, Y., Xu, J. & Jiang, L. (2014). Challenges of System-Level Simulations and Performance Evaluation for 5G Wireless Networks. *IEEE Access*, 2, 1553-1561. DOI: 10.1109/ACCESS.2014.2383833.

WANG, Y. & feng TAO, X. (2007). Inter-antenna and subblock shifting and inversion for peak-to-average power ratio reduction in MIMO-OFDM systems. *The Journal of China Universities of Posts and Telecommunications*, 14(4), 41 - 45. doi: http://dx.doi.org/10.1016/S1005-8885(08)60036-9.

Wang, Z. & Bar-Ness, Y. (2006, March). Peak-to-Average Power Ratio Reduction by Polyphase Interleaving and Inversion for SFBC MIMO-OFDM with Generalized Complex Orthogonal Code. *2006 40th Annual Conference on Information Sciences and Systems*, pp. 317-320. doi: 10.1109/CISS.2006.286485.

Wei, S., Goeckel, D. L. & Kelly, P. E. (2002). A modern extreme value theory approach to calculating the distribution of the peak-to-average power ratio in OFDM systems. *2002 IEEE International Conference on Communications. Conference Proceedings. ICC 2002 (Cat. No.02CH37333)*, 3, 1686-1690.

Wilkinson, T. A. & Jones, A. E. (1995, Jul). Minimisation of the peak to mean envelope power ratio of multicarrier transmission schemes by block coding. *1995 IEEE 45th Vehicular Technology Conference. Countdown to the Wireless Twenty-First Century*, 2, 825-829.

Wilson, S. G. (1995). Digital modulation and coding (ch. 5, pp. 527). New Jersey, NJ, USA: Prentice-Hall, Inc.

Wohlin, C., Runeson, P., Höst, M., Ohlsson, M. C., Regnell, B. & Wesslén, A. (2012). *Experimentation in software engineering*. Springer Science & Business Media.

Woo, G. R. & Jones, D. L. (2005, May). Peak power reduction in MIMO OFDM via active channel extension. *IEEE International Conference on Communications, 2005. ICC 2005. 2005*, 4, 2636-2639 Vol. 4. doi: 10.1109/ICC.2005.1494827.

Wu, H., Haustein, T., Jorswieck, E. A. & Hoeher, P. A. (2011). Sum Rate Optimization by Spatial Precoding for a Multiuser MIMO DFT-Precoded OFDM Uplink. *EURASIP Journal on Advances in Signal Processing*, 2011(1), 927936. doi: 10.1155/2011/927936.

Wu, Z., Qiu, R. & Zhu, S. (2008, Oct). MIMO-OFDM PAPR Reduction by Space-Frequency Permutation and Inversion. *2008 4th International Conference on Wireless Communications, Networking and Mobile Computing*, pp. 1-4. doi: 10.1109/WiCom.2008.149.

Xia, L., Ying, Z., Youxi, T. & Shaoqian, L. (2005, May). Iterative estimation and cancellation of clipping distortion for turbo receiver in MIMO-OFDM system. *Proceedings. 2005 International Conference on Communications, Circuits and Systems, 2005.*, 1, 185-188 Vol. 1. doi: 10.1109/ICCCAS.2005.1493389.

Xin, Y. & Fair, I. J. (2004, Sept). Error-control selective mapping coding for PAPR reduction in OFDM systems. *IEEE 60th Vehicular Technology Conference, 2004. VTC2004-Fall. 2004*, 1, 583-587.

Yan, B., Zhang, H., Yang, Y., Hu, Q. & Qiu, M. (2009a, Nov). An improved algorithm for peak-to-average power ratio reduction in MIMO-OFDM systems. *2009 International Conference on Wireless Communications Signal Processing*, pp. 1-4. doi: 10.1109/WCSP.2009.5371667.

Yan, X., Chunli, W. & Qi, W. (2009b, March). Research of Peak-to-Average Power Ratio Reduction Improved Algorithm for MIMO-OFDM System. *2009 WRI World Congress on Computer Science and Information Engineering*, 1, 171-175. doi: 10.1109/CSIE.2009.71.

Yang, H. (2005). A road to future broadband wireless access: MIMO-OFDM-Based air interface. *IEEE Communications Magazine*, 43(1), 53-60. doi: 10.1109/MCOM.2005.1381875.

Yao, Y. & Hu, J. (2013, Oct). MIMO-OFDM PAPR reduction by residue number system. *2013 International Conference on Computational Problem-Solving (ICCP)*, pp. 441-444. doi: 10.1109/ICCPS.2013.6893506.

Yi, W. & Linfeng, G. (2009). *An Investigation of Peak-to-Average Power Reduction in MIMO-OFDM Systems*. (Ph.D. thesis, Blekinge Institute of Technology, Blekinge, Sweden).

Yue, G. & Wang, X. (2006). A hybrid PAPR reduction scheme for coded OFDM. *IEEE Transactions on Wireless Communications*, 5(10), 2712-2722. DOI: 10.1109/TWC.2006.04136.

Zhang, H. & Goeckel, D. L. (2007). Peak Power Reduction in Closed-Loop MIMO-OFDM Systems via Mode Reservation. *IEEE Communications Letters*, 11(7), 583-585. doi: 10.1109/LCOMM.2007.070275.

Zhang, X., Duan, Y. & Tao, G. (2010, Oct). The research of peak-to-average power ratio performance by optimum combination of partial transmit sequences in MIMO-OFDM system. *2010 3rd International Congress on Image and Signal Processing*, 9, 4476-4479. doi: 10.1109/CISP.2010.5646770.

Zhu, D., Natarajan, B. & Dyer, J. S. (2009, Aug). Peak-to-Average Power Ratio Reduction in MIMO-OFDM with Trellis Exploration Algorithm. *2009 Proceedings of 18th International Conference on Computer Communications and Networks*, pp. 1-6. doi: 10.1109/ICCCN.2009.5235316.

Zhu, D., Natarajan, B. & Dyer, J. S. (2011). Peak-to-average power ratio reduction in space–time coded MIMO-OFDM via preprocessing. *Wireless Communications and Mobile Computing*, 11(1), 108–120. doi: 10.1002/wcm.918.

Zhu, X. (2012). A Low-BER Clipping Scheme for PAPR Reduction in STBC MIMO-OFDM Systems. *Wireless Personal Communications*, 65(2), 335–346. doi: 10.1007/s11277-011-0259-x.